INFORMATION TO USERS

This manuscript has been reproduced from the microfilm master. UMI films the text directly from the original or copy submitted. Thus, some thesis and dissertation copies are in typewriter face, while others may be from any type of computer printer.

The quality of this reproduction is dependent upon the quality of the copy submitted. Broken or indistinct print, colored or poor quality illustrations and photographs, print bleedthrough, substandard margins, and improper alignment can adversely affect reproduction.

In the unlikely event that the author did not send UMI a complete manuscript and there are missing pages, these will be noted. Also, if unauthorized copyright material had to be removed, a note will indicate the deletion.

Oversize materials (e.g., maps, drawings, charts) are reproduced by sectioning the original, beginning at the upper left-hand corner and continuing from left to right in equal sections with small overlaps. Each original is also photographed in one exposure and is included in reduced form at the back of the book.

Photographs included in the original manuscript have been reproduced xerographically in this copy. Higher quality 6" x 9" black and white photographic prints are available for any photographs or illustrations appearing in this copy for an additional charge. Contact UMI directly to order.

UMI

A Bell & Howell Information Company
300 North Zeeb Road, Ann Arbor MI 48106-1346 USA
313/761-4700 800/521-0600

Accurate and Stable Reduction of RLC Networks Using Split Congruence Transformations

by

Kevin J. Kerns

A dissertation submitted in partial fulfillment

of the requirements for the degree of

Doctor of Philosophy

University of Washington

1996

Approved by 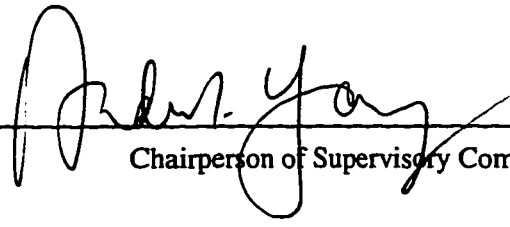

Chairperson of Supervisory Committee

Program Authorized to Offer Degree Electrical Engineering

Date 9-26-96

In presenting this dissertation in partial fulfillment of the requirements for the Doctoral degree at the University of Washington, I agree that the Library shall make its copies freely available for inspection. I further agree that extensive copying of this dissertation is allowable only for scholarly purposes, consistent with "fair use" as prescribed in the U.S. Copyright Law. Requests for copying or reproduction of this dissertation may be referred to University Microfilms, 1490 Eisenhower Place, P. O. Box 975, Ann Arbor, MI 48106, to whom the author has granted "the right to reproduce and sell (a) copies of the manuscript in microform and/or (b) printed copies of the manuscript made from microform."

Signature Kevin J Kerns

Date Sept. 26, 1996

University of Washington

Abstract

Accurate and Stable Reduction of RLC Networks Using Split Congruence Transformations

by Kevin J. Kerns

Chairperson of the Supervisory Committee: Professor Andrew T. Yang
Department of Electrical Engineering

RLC (resistor, inductor, capacitor) network reduction refers to the formulation of small networks whose port behavior is similar to that of large RLC networks. The motivation for this research is that circuits are switching faster so that layout and package parasitics associated with very large scale integrated (VLSI) circuits become more important and require simulation before fabrication. Parasitic effects are often modeled using lumped linear RLC networks which are extracted from the geometry of the layout and package, but these networks are so large that subsequent simulation is impractical or impossible. As a result, it is necessary to reduce these networks after extraction and before simulation. Several network reduction algorithms have been developed in the last few years, but none exist which guarantee both accuracy and passivity (most guarantee only accuracy). If the reduced networks are not accurate then the results of the simulation will probably be wrong, but if the reduced networks are not passive then the subsequent simulation may not work at all. This thesis presents a set of transformations called Split Congruence Transformations (SCT's) which can be used to accurately reduce a network while preserving passivity. Several examples, including a prototype SPICE-in SPICE-out network reduction tool are given which show the utility of SCT's.

Table of Contents

List of Figures

List of Tables

Acknowledgments

I would like to thank Ivan Wemple, whose research on extracting huge RC substrate networks, led to my own research on network reduction, and Andrew Yang for providing invaluable guidance and direction — and for saying "that's not good enough" — several times. Steve Corey provided a lot of insight to my research during our many conversations, and without him, some of this thesis would not be written. Steve Corey and Ryan Welch spent a lot of their time proof reading this thesis, and they saved me from many minor mistakes as well as a few major embarrassments. Finally, I wish to thank the Catalyst Foundation, which funded my research, and Dr. Al Ruehli for providing me with the PEEC model I used to demonstrate network reduction.

Chapter 1
Introduction

RLC (resistor, inductor, capacitor) network reduction refers to the formulation of small networks whose port behavior is similar to that of large RLC networks. Several reduction algorithms currently exist, but none of these preserve both passivity and accuracy for general RLC networks. This thesis presents a set of transformations called Split Congruence Transformations (SCT's) which can be used to reduce RLC networks accurately while preserving passivity. The following sections provide motivation for this research, the basic requirements for network reduction algorithms, and an overview of the proposal.

1.1 Motivation for Network Reduction

Very large scale integrated (VLSI) circuits are being designed to run faster and to use less power. To do this, designs are more aggressive, device sizes are shrinking, and power supplies are lower voltage. In conservative digital designs, it is simple to ensure that a circuit will work without considering the impact of the actual layout by using a clock which is sufficiently slow that signals have plenty of slack, or time to reach their destination, before they are required. More aggressive designs reduce the amount of the slack so that the circuit will run faster, but less slack makes signal delays caused by physical layout of the circuit more significant. Because the chip dimensions are typically smaller than the wavelength of a signal, on-chip RLC parasitics tend to behave like thermal diffusion, while off-chip parasitics, which correspond to dimensions that are large compared to signal wavelengths, tend to exhibit wavelike behavior, e.g. reflection and ringing. In order to ensure that the layout of an aggressive design will work, parasitic effects must be included in simulations of the circuit.

In addition to more aggressive designs, shrinking device sizes make on-chip and off-chip parasitics more significant. Smaller devices have output impedances similar to those of larger devices, but they have smaller loading and self capacitance. These devices are faster since the time required

for a digital circuit to transition is on the order of the output impedance times the total capacitance. As device sizes decrease, so do wire widths, but average wire lengths, which scale with chip size, remain the same, and the result is that the resistance of signal and power paths is increasing. Smaller devices require that supply voltages be lowered to ensure that electric fields do not cause breakdown, but lower voltages make circuits more sensitive to fluctuations in the supply which become proportionally larger. These fluctuations, known as "ground bounce," occur because digital devices do not smoothly draw current. Instead, peak current is drawn during signal transitions, and little current is drawn at other times. The resistance of the line causes a voltage drop proportional to the magnitude of the current, and the inductance of the line causes a drop proportional to the change in current. Therefore, high currents or sudden changes cause voltage spikes in the supply. In summary, not only do shrinking device sizes increase the sensitivity to parasitics, but they can actually make the parasitics worse.

The majority of the power consumed by a digital VLSI circuit occurs during transitions of the logic gates. In reality, these gates do not always transition smoothly during a clock cycle, but may fluctuate rapidly as different inputs independently change state. Although these glitches have a minor effect on circuit performance (provided they stabilize by the time the signal is needed), they can have a dramatic effect on the power consumed by the circuit. Glitches can be very sensitive to minor changes in signal delay, so that the individual line delays must be accurately modeled for analysis of the effect of layout on power consumption.

In mixed signal designs, more integration of analog and digital devices are being made on the same chip. Here, the rapid transition of digital circuits can couple to the analog devices through several means. First, ground bounce can cause fluctuations in the power supply. Second, current is injected into the chip substrate during transitions in the digital devices. This current causes fluctuations in the substrate voltage which can couple to the analog devices through changes in the threshold voltage.

All of these effects have encouraged research to model on-chip and off-chip parasitics, and many of these models can be expressed as lumped RLC networks, (e.g. [1][2][3][4][5]). These networks form macromodels which are included in circuit simulations in order to assess the effect of the parasitics. Unfortunately, these models are so large that subsequent simulations become impractical or impossible, so the models must be reduced before the circuits can be simulated. In the next section, the requirements for a useful reduction algorithm are presented.

1.2 Requirements for Network Reduction

To ensure the veracity of subsequent circuit simulations, reduced networks must be *accurate*. The user of the reduction tool must have confidence that the behavior at the ports of a derived netlist accurately approximates that of the original netlist. In addition the user should be able to specify the error tolerance and frequency range for which accuracy is maintained. This allows the user to make a trade off between simulation speed and accuracy, and increases the flexibility of the tool. Specification of the size of the reduced networks is not an adequate means of expressing accuracy since one part of a network may require only a few terms to fit behavior while others may require many.

Reduced networks must be *passive*. A passive network is one which cannot generate more energy than it absorbs, and thus is absolutely stable. If a reduced network is not passive, simulations which use it may exhibit artificial oscillations or exponential growth which render them useless. One way to ensure passivity is to synthesize an RLC network with the same behavior as the reduced network and then drop all negative elements — this technique can cause an unacceptable loss of accuracy and should not be used. Asymptotic stability implies that the real part of the poles of the transfer function are less than or equal to zero. Such a network is stable provided nothing is hooked to the ports, but if it is not passive, a passive linear termination to the ports exists which will make the system unstable. Examples of this are provided in Chapters 2 and 7.

Most commercial circuit simulators model networks using a modified admittance formulation [6], and the majority of the state variables represent network nodal voltage. In order to make the reduced models *compatible* with these simulators, the behavior of the reduced networks must be specified as admittance. RLC elements are extracted from a netlist, and the voltage nodes of the netlist which are shared by both RLC and non-RLC elements become the ports. Admittance parameters allow the reduced netlist to be added to the non-RLC element netlist for simulation without the use of a transformer.

The reduced networks must be *efficient* —they should be as small as possible so that subsequent circuit simulations require minimal time and memory. In general, network reduction takes much less time than does simulation of the reduced networks so more emphasis should be placed on making the networks small, rather than on speeding the reduction process.

1.3 Overview

This thesis is organized as follows. First, previous work on network reduction is reviewed in Chapter 2. Here, a common formulation is used which highlights the key features of the different algorithms, and it is shown that the algorithms do not preserve passivity. Chapter 3 derives the formulation of the matrices which represent the network using modified nodal analysis, and Chapter 4 presents congruence transforms which can be used to reduced the size of these matrices via direct admittance-to-admittance transformations which preserve selected network behavior. Chapter 5 shows how the transforms presented in the previous chapter are used to reduce RC networks while preserving network passivity and bounding accuracy in an algorithm called Pole Analysis via Congruence Transformations (PACT). Chapter 6 shows why the PACT formulation cannot be applied to general RLC networks, and it shows that SCT's preserve passivity by preserving the "passive form" of the network. Chapter 7 presents several examples of network reduction using SCT's, and concluding remarks are made in Chapter 8.

Math conventions are used in this thesis which are consistent with Golub and Van Loan [7]. Unless otherwise stated, all variables are real with the exception of $\{i...n, r, p, q\}$ which are integers, and s which is complex frequency. Using this convention, x is a scalar, $\mathbf{x}$ is a vector, $\mathbf{X}$ is a matrix, $\mathbf{X}^{\mathbf{T}}$ is the transpose of $\mathbf{X}$, $\mathbf{X}^{-\mathbf{T}}$ is the inverse transpose of $\mathbf{X}$, and x_{ij} is the element in the ith row and jth column of $\mathbf{X}$. All vectors are column vectors except where noted, and the identity and zero matrices are represented as $\mathbf{I}$ and $\mathbf{0}$ respectively.

Chapter 2
Related Work

This chapter reviews the well known network reduction algorithms. Here, the different techniques are derived such that they all extend from a common formulation in order to simplify comparisons of the methods. The key point of this chapter is that the techniques are nonsymmetric and can be applied to any voltage transfer function, and that none presented here preserves the passivity of general RLC networks.

The first well know network reduction technique was applied to signal delay and was presented by Elmore in 1948 [8]. The voltage transfer function between an input signal and an output signal is derived for a network, and the delay is approximated as

$$\tau_d = \frac{h_1}{h_0} \tag{2.1}$$

where h_0 and h_1 are the first two moments (offset and slope) of the voltage transfer function in the Laplace domain at $s = 0$. This technique requires that the source impedance and load capacitance be approximated with linear elements so that the voltage transfer function can be expressed as a linear equation. The next section presents the common formulation that is used in the derivation of the more advanced techniques which reduce not only voltage transfer functions, but admittance, impedance, and any other input-output relationship.

2.1 Common Formulation

The formulation here is used by all of the techniques in the following sections of this chapter, and is used to simplify comparisons of the methods presented in these sections. Given a linear network with n independent voltages and currents, the Laplace domain relationship between the voltages of the voltage nodes (currents of the current nodes) versus the current injected into the voltage nodes (voltage applied to the current nodes) can be expressed as

$$(\mathbf{G}+s\mathbf{C})\,\mathbf{x} = \mathbf{b}. \tag{2.2}$$

The $n \times n$ matrices **G** and **C** represent the frequency independent and frequency dependent parts of the network respectively, the vector **x** represents the n values of the voltage and current nodes, and the vector **b** represents the n currents and voltages injected into these nodes. The transfer function of this network in the Laplace domain, which relates the m inputs contained in the vector **u** to the p outputs contained in the vector **l**, can be expressed as

$$\mathbf{l}(s) = \mathbf{H}(s)\,\mathbf{u}(s). \tag{2.3}$$

The transfer function is related to the network as

$$\mathbf{H}(s) = \mathbf{L}^{\mathrm{T}}(\mathbf{G}+s\mathbf{C})^{-1}\mathbf{B}. \tag{2.4}$$

Here, the excitation matrix **B** contains m columns, each of which corresponds to excitation of one of the input ports, and the observation matrix **L** contains p columns, each of which corresponds to observation of one of the output ports. If $p = m$, all input elements are port voltages, and all output elements are current flowing into the corresponding ports, then $\mathbf{H}(s)$ describes the multiport admittance, $\mathbf{Y}(s)$.

A simplifying transformation can be made to (2.4) without changing the behavior at the ports.

$$\mathbf{H}(s+s_0) = \mathbf{L}^{\mathrm{T}}(\mathbf{I}-s\mathbf{A})^{-1}\mathbf{R}, \tag{2.5}$$

where

$$\begin{aligned} \mathbf{A} &= -(\mathbf{G}+s_0\mathbf{C})^{-1}\mathbf{C} \\ \mathbf{R} &= (\mathbf{G}+s_0\mathbf{C})^{-1}\mathbf{B} \end{aligned}. \tag{2.6}$$

Here s_0 is a constant, and the Taylor series expansion of (2.5) about s_0 is

$$\mathbf{H}(s+s_0) = \mathbf{L}^{\mathrm{T}}\left(\mathbf{I}+s\mathbf{A}+s^2\mathbf{A}^2+\ldots\right)\mathbf{R}. \tag{2.7}$$

This constant is often set to zero since, for most networks, the low frequency behavior is more important than that at high frequencies. Equations (2.4)...(2.7) are used as a starting point for the derivations in each of the following sections. Because **A** is nonsymmetric and $\mathbf{R} \neq \mathbf{L}$, the algorithms using this formulation do not generally preserves symmetry so that the reduced networks are nonsymmetric.

2.2 Asymptotic Waveform Evaluation (AWE)

The simplest general technique for network reduction, called "Asymptotic Waveform Evaluation" (AWE), was developed in the late 1980's by Pillage and Rohrer [9]. Here, the size of the network is reduced by approximating (2.4) with a Taylor series expanded about $s = s_0$ as shown in (2.7). A recursive method of calculating the moments of the transfer function is revealed by writing (2.7) as

$$\mathbf{H}(s+s_0) = \mathbf{L}^{\mathbf{T}}\left(\mathbf{X}_{(0)} + s\mathbf{X}_{(1)} + s^2\mathbf{X}_{(2)} + \ldots\right) \tag{2.8}$$

where

$$\begin{aligned} \mathbf{X}_{(0)} &= \mathbf{R} \\ \mathbf{X}_{(i)} &= \mathbf{A}\mathbf{X}_{(i-1)} \end{aligned} \tag{2.9}$$

The individual terms of $\mathbf{H}(s)$ are represented as the Taylor series

$$h_{kl}(s+s_0) = h_{kl(0)} + sh_{kl(1)} + s^2 h_{kl(2)} + \ldots, \tag{2.10}$$

and

$$h_{kl(i)} = \mathbf{l}_k^{\mathbf{T}}\mathbf{x}_{l(i)} \tag{2.11}$$

where $\mathbf{l}_k$ and $\mathbf{x}_l$ are the kth and lth columns of $\mathbf{L}$ and $\mathbf{X}$ respectively.

Equation (2.10) is not a useful representation of the transfer function since the Taylor series will not converge for $|s-s_0| \geq \rho$ where ρ is the absolute distance between s_0 and its closest pole. The poles occur at values of s for which $(\mathbf{G} + s\mathbf{C})$ of (2.4) is singular. Because all transfer functions of linear networks containing discrete elements can be completely described by rational polynomials, it is appropriate to fit (2.10) to an equation of the form

$$h_{kl}(s+s_0) \approx \frac{a_0 + sa_1 + \ldots + s^q a_q}{1 + sb_1 + \ldots + s^r b_r} \tag{2.12}$$

via the Padé approximation. The integers r and q are less than or equal to n, and $q = r - 1$ (usually). The values of the coefficients in (2.12) are selected such that the first $q+r+1$ moments expanded about $s = s_0$ of the rational polynomial are equal to those given by (2.11).

In perfect math, (2.12) exactly represents the behavior of the transfer function when $r = n$. Unfortunately, solving for the values of the coefficients in the denominator becomes ill conditioned as r becomes large, and only the poles closest to s_0 are correctly identified. As a result, cal-

culation of more moments does not guarantee a better fit to the data. Furthermore, poles of the reduced network (i.e. values of s for which the denominator of (2.12) is zero) may occur for $\mathrm{Re}(s) > 0$ so that the network is unstable. While asymptotic stability can be ensured by dropping such poles, passivity is not easily ensured.

2.3 Complex Frequency Hopping (CFH)

An extension to AWE was proposed by Huang in 1990 by which stiff systems could be more accurately approximated by including a second moment expansion point on the real axis (i.e. the first s_0 is zero and the second is real and negative) [10]. This analysis was refined by Chiprout and Nakhla in 1995 who developed a method called "Complex Frequency Hopping" (CFH) [11]. In this technique, the moment expansions presented for AWE are carried out at several locations on the imaginary axis (i.e. $\mathrm{Re}(s_0) = 0$). It is shown that, when r is fixed and q grows large in the Padé approximation for (2.12), the r roots of the denominator converge to the r poles closest to s_0. CFH uses this property to identify all of the poles which are close to the imaginary axis in a specified frequency range. The numerator of (2.12) is then determined using a selected set of low-order moments generated at the various expansion points which are referred to as "hops".

Of the r poles found from a hop, those which are furthest from the expansion point may not be accurately identified. In order to verify the accuracy of a pole, overlap of poles found from two adjacent hops is evaluated. If overlap occurs (i.e. they have approximately the same value), all poles found within the radius of the overlapped pole are assumed to be accurate and poles outside of this radius are rejected. Fig. 2.1 illustrates the selection of poles for two hops. Four poles are identified in the first hop, and three in the second. The radius of accuracy is estimated by using the largest radius for which common poles are found, and poles outside of that radius are rejected. Enough hops are used that accuracy of all of the poles in the region of interest can be verified, and poles in the lower half of the s-plane are automatically identified since all poles occur as complex pairs.

The advantage of CFH is that it is more accurate than AWE. It is not a Padé approximation because it preserves the poles rather than the moments of the transfer function. The major disadvantage of CFH is that multiple expansion points must be used, each of which requires its own (expensive) LU factorization. Furthermore, CFH must factorize complex matrices whereas AWE uses real matrices.

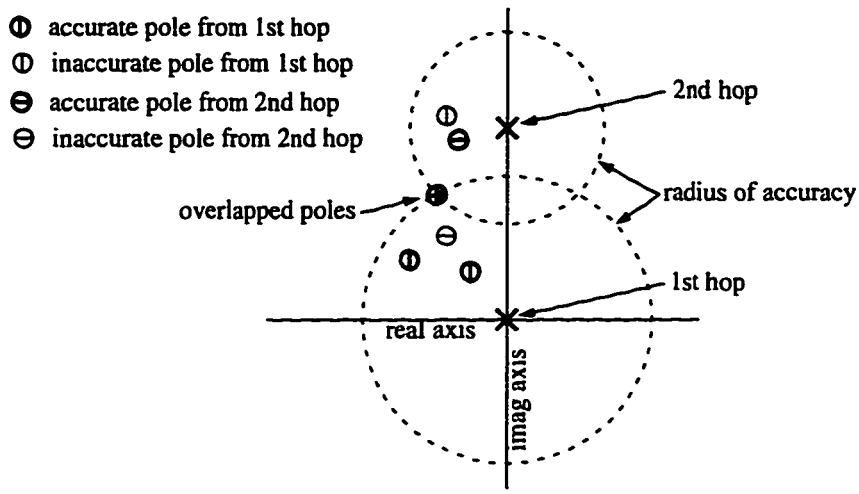

Figure 2.1. Illustration of CFH pole selection in the complex s plane (adapted from [11]).

It can be shown that the poles of the transfer function are the eigenvalues of the generalized eigenvalue problem

$$\det(\mathbf{G} + \lambda\mathbf{C}) = 0, \tag{2.13}$$

and that the CFH pole analysis is simply a form of shifted inverse iteration (with a block size of r) to identify selected eigenvalues of (2.13) (e.g. see Section 7.3 of [7] and references therein). Because CFH identifies the actual poles, all poles in the reduced network will be on the left hand side of the complex plane ($\mathrm{Re}(s) < 0$) and asymptotic stability will be ensured. Unfortunately, asymptotic stability does not imply that the reduced network is passive, and active networks may still be created.

2.4 Matrix Padé Via a Lanczos-type Process (MPVL)

The form of (2.4) is similar to that used to model flexible structures in control theory. Here, it was demonstrated in the mid-1980's that Krylov subspace techniques, which include the Lanczos [12] and Arnoldi [13] processes, can be applied to the problem of linear model reduction in order to obtain models in a well-conditioned manner (e.g. [14] and [15]). A Krylov subspace of the matrix $\mathbf{A}$ and the column vectors contained in $\mathbf{V}$ is defined as

$$\mathbf{K}_q(\mathbf{A}, \mathbf{V}) = \mathrm{span}\{\mathbf{V}, \mathbf{AV}, \ldots, \mathbf{A}^{q-1}\mathbf{V}\}. \tag{2.14}$$

In 1994, Gallivan *et. al* [16] pointed out that the Lanczos process could be applied to the problem of network reduction, and at nearly the same time, Feldmann and Freund [17][18] published an

algorithm called "Padé via Lanczos" (PVL) which did so. PVL could only be applied to one-port networks, but the following year a multiport version called "Matrix Padé via a Lanczos-type Process" (MPVL) was introduced by the same authors [19]. This algorithm was shown to implicitly find an efficient Padé approximation of linear networks in a well-conditioned manner. The following derivation of MPVL has been simplified in order to show how moments are implicitly matched in a well-conditioned manner without delving into the details of the algorithm or the Lanczos process.

Given two nonsingular square biorthonormal matrices $\mathbf{V}$ and $\mathbf{W}$ (biorthonormal means that $\mathbf{W}^{\mathbf{T}}\mathbf{V} = \mathbf{I}$), insertion of $\mathbf{V}\mathbf{V}^{-1}$ on the left side of the denominator in (2.5) and $\mathbf{W}^{-\mathbf{T}}\mathbf{W}^{\mathbf{T}}$ on the right transforms the network without changing the port behavior,

$$\mathbf{H}(s+s_0) = \mathbf{L}^{\mathbf{T}}\mathbf{V}\left(\mathbf{I} - s\mathbf{W}^{\mathbf{T}}\mathbf{A}\mathbf{V}\right)^{-1}\mathbf{W}^{\mathbf{T}}\mathbf{R}. \tag{2.15}$$

If $\mathbf{V}$ and $\mathbf{W}$ are $n \times k$ matrices with $k < n$, then the size of the network will be reduced because $\mathbf{W}^{\mathbf{T}}\mathbf{A}\mathbf{V}$ is a $k \times k$ matrix. However, $\mathbf{H}(s + s_0)$ will not be preserved since the products of $\mathbf{V}$ and $\mathbf{W}$ with their generalized inverses do not equal the identity matrix. Fortunately, Theorem 2.1 shows that it is possible to formulate these matrices such that the moments of the transfer function found from (2.7) and given by

$$\begin{aligned} \mathbf{H}(s+s_0) &= \mathbf{H}_0 + s\mathbf{H}_1 + s^2\mathbf{H}_2 + \ldots \\ \mathbf{H}_i &= \mathbf{L}^{\mathbf{T}}\mathbf{A}^i\mathbf{R} \end{aligned} \tag{2.16}$$

are preserved.

Theorem 2.1. Given $\mathbf{A} \in \Re^{n\times n}$, $\mathbf{L} \in \Re^{n\times p}$, $\mathbf{R} \in \Re^{n\times m}$, $\mathbf{V} \in \Re^{n\times k}$, $\mathbf{W} \in \Re^{n\times k}$, $\mathbf{W}^T\mathbf{V} = \mathbf{I}$, $k \le n$, $m \le n$, $p \le n$,

$$\operatorname{span}\left(\mathbf{A}^i\mathbf{R}\right) \subseteq \operatorname{span}(\mathbf{V}),\ (i \in \{0, 1, \ldots, m'-1\}), \tag{2.17}$$

and

$$\operatorname{span}\left(\left(\mathbf{A}^{\mathbf{T}}\right)^i\mathbf{L}\right) \subseteq \operatorname{span}(\mathbf{W}),\ (i \in \{0, 1, \ldots, p'-1\}), \tag{2.18}$$

then

$$\mathbf{L}^{\mathbf{T}}\mathbf{A}^i\mathbf{R} = \mathbf{L}^{\mathbf{T}}\mathbf{V}\left(\mathbf{W}^{\mathbf{T}}\mathbf{A}\mathbf{V}\right)^i\mathbf{W}^{\mathbf{T}}\mathbf{R},\ (i \in \{0, 1, \ldots, p'+m'-1\}). \tag{2.19}$$

Proof: Equation (2.17) and (2.18) imply

$$\text{there exists } \left(\alpha_i \in \Re^{k\times m}\right) \text{ such that } \mathbf{A}^i\mathbf{R} = \mathbf{V}\alpha_i,\ (i \in \{0, 1, \ldots, m'-1\}) \tag{2.20}$$

and

$$\text{there exists } \left(\beta_i \in \Re^{k\times p}\right) \text{ such that } \left(\left(\mathbf{A}^{\mathbf{T}}\right)^i\mathbf{L}\right) = \mathbf{W}\beta_i,\ (i \in \{0, 1, \ldots, p'-1\}) \tag{2.21}$$

respectively. From (2.20) and (2.21) and because $\mathbf{W}^{\mathbf{T}}\mathbf{V} = \mathbf{I}$,

$$\mathbf{V}\mathbf{W}^{\mathbf{T}}\mathbf{A}^i\mathbf{R} = \mathbf{V}\mathbf{W}^{\mathbf{T}}\mathbf{V}\alpha_i = \mathbf{V}\alpha_i = \mathbf{A}^i\mathbf{R},\ (i \in \{0, 1, \ldots, m'-1\}), \tag{2.22}$$

and

$$\mathbf{L}^{\mathbf{T}}\mathbf{A}^i\mathbf{V}\mathbf{W}^{\mathbf{T}} = \beta_i^{\mathbf{T}}\mathbf{W}^{\mathbf{T}}\mathbf{V}\mathbf{W}^{\mathbf{T}} = \beta_i^{\mathbf{T}}\mathbf{W}^{\mathbf{T}} = \mathbf{L}^{\mathbf{T}}\mathbf{A}^i,\ (i \in \{0, 1, \ldots, p'-1\}). \tag{2.23}$$

Finally, it is easy to show by recursively using the equalities given in (2.22) and (2.23) that (2.19) is true.

QED.

The nonsymmetric "look-ahead" Lanczos algorithm [20] has been designed to derive $\mathbf{V}$ and $\mathbf{W}$ which meet the requirements of Theorem 2.1 in a well-conditioned manner. This algorithm derives these two sets of vectors such that $\mathbf{T} = \mathbf{W}^{\mathbf{T}}\mathbf{A}\mathbf{V}$ in (2.15) is banded with p superdiagonals and m subdiagonals. In actual implementations, $\mathbf{W}^{\mathbf{T}}\mathbf{V}$ forms a block diagonal matrix instead of the identity matrix so that breakdown can be avoided. Breakdown results when corresponding vectors in $\mathbf{V}$ and $\mathbf{W}$ are nearly orthogonal. Since this algorithm provides $\mathbf{W}^{\mathbf{T}}\mathbf{V} \neq \mathbf{I}$, the actual formulation of MPVL is somewhat more complex than is presented here.

The advantage of MPVL over AWE is that by implicitly matching moments via the Lanczos process, MPVL is well conditioned. But, like AWE, MPVL does not ensure that reduced RLC networks are passive or even asymptotically stable. An example of this is illustrated by the network in Fig. 2.2 which shows the termination of the one-port RLC network listed in Appendix A by a

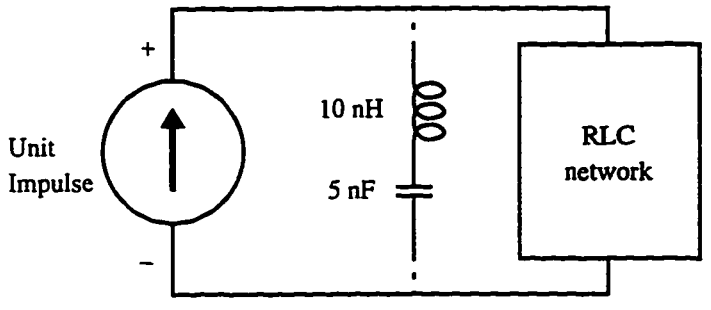

Figure 2.2. A one-port RLC network is probed by a unit impulse. The simulation is conducted with and without termination by an LC shunt.

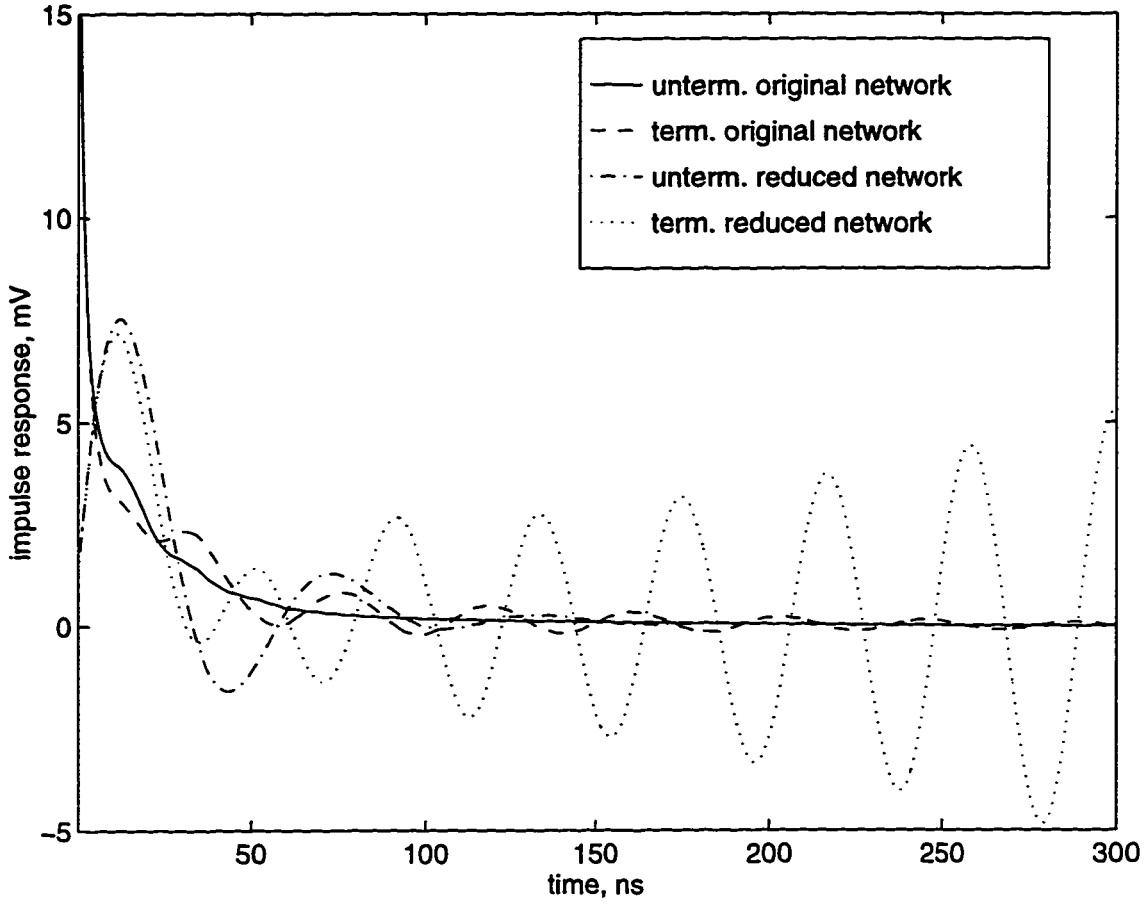

Figure 2.3. Example showing 8th-order MPVL approximation of the network in Fig. 2.2. Although the reduced network is asymptotically stable, it is not passive, and in this case, the terminated reduced system is unstable.

series LC shunt. This network is reduced using an 8th-order MPVL reduction (16 moments matched), and Fig. 2.3 shows a transient simulation, using backward Euler integration, of the terminated and unterminated original and reduced networks. The vertical axis is the port voltage response to a unit impulse current. Both the admittance and impedance of the reduced network are asymptotically stable (no poles with positive real values), but the network is not passive. The unterminated reduced network is stable because there are no impedance poles with positive real components. As can be seen in Fig. 2.3, termination of the network by the LC shunt has a small effect on the original network, but it causes the system which includes the reduced network to become unstable.

2.5 Arnoldi's Method

Arnoldi's algorithm [13] provides an alternative to the look-ahead Lanczos algorithm for a well-conditioned solution to the span requirement of (2.20). This technique was presented for the reduction of RL networks by Silveira *et. al.* in 1995 [21], but it is easily extended to RLC networks. Instead of using two separate sets of biorthonormal projection vectors, **V** and **W**, as does MPVL, this technique uses a single set of vectors, **V**, which are orthonormal ($\mathbf{V}^T\mathbf{V} = \mathbf{I}$). The formulation corresponding to (2.15) is

$$\mathbf{H}(s+s_0) = \mathbf{L}^T\mathbf{V}\left(\mathbf{I} - s\mathbf{V}^T\mathbf{A}\mathbf{V}\right)^{-1}\mathbf{V}^T\mathbf{R}, \tag{2.24}$$

and the span requirement for **V** is

$$\text{span}\left(\mathbf{A}^i\mathbf{R}\right) \subseteq \text{span}(\mathbf{V}),\ (i \in \{0, 1, \ldots, m'-1\})\ . \tag{2.25}$$

The constant p' is equal to zero in (2.18) so that only m' moments are matched instead of $m'+p'$ moments which are matched by MPVL because span(**L**) $\not\subset$ span(**R**) implies that span(**L**) $\not\subset$ span(**V**). It is interesting to note that since this technique was proposed for the reduction of RL networks, the matrix **G** in (2.4) is definite and **R** = **L** (ignoring negative signs). As a result, the Cholesky factorization, $\mathbf{D}^T\mathbf{D} = \mathbf{G}$, exists. An alternate formulation of (2.5) for $s_0 = 0$ as

$$\mathbf{H}(s) = \mathbf{P}^T(\mathbf{I} + s\mathbf{E})^{-1}\mathbf{P} \tag{2.26}$$

where

$$\begin{aligned} \mathbf{E} &= -\mathbf{D}^{-T}\mathbf{C}\mathbf{D}^{-1} \\ \mathbf{P} &= \mathbf{D}^{-T}\mathbf{B} \end{aligned}, \tag{2.27}$$

allows as many moments to be matched as does MPVL while using Arnoldi's method. The reason is that matching the span requirement of **V** for the left hand side of (2.26) also matches it for the right hand side. Unfortunately, this formulation breaks down for general RLC networks because **G** is indefinite. In Chapter 3, a symmetric formulation is presented which allows both the Arnoldi- and Lanczos- derived transforms to fit two moments per iteration for general RLC networks.

In summary, MPVL and the Arnoldi-based technique solve the ill conditioning problem of AWE, but do not ensure passivity or even asymptotic stability. CFH does preserve asymptotic stability by preserving the poles of the network, but it does not ensure that passivity is preserved. Finally, none of the techniques preserve symmetry, or provide a direct admittance-to-admittance conversion of the network.

Chapter 3
Formulation of Multiport Admittance Using Modified Nodal Analysis

The algorithms presented in Chapter 2 are general algorithms which are useful for any transfer function between voltage and current (e.g. admittance, impedance, voltage gain, etc.), and this is why the generic transfer function "$\mathbf{H}(s)$" is used in (2.4). Using these algorithms, an admittance formulation of the reduced networks requires that the inputs to the corresponding nodes of the original network be voltage. Therefore, these techniques require that one voltage source corresponding to each port be included in the original network. In other words, to probe the admittance of a network, the voltages of the ports are set using voltage sources and the resulting currents into the ports are equal to the currents flowing through these sources.

Since it is desired that both the original and reduced networks be represented as admittance, an alternative formulation based on partitioning Modified Nodal Analysis (MNA) [6] network matrices is used which allows a direct admittance-to-admittance conversion via congruence transformations of the network matrices. Section 3.1 reviews how MNA network matrices are formulated for RLC networks, and Section 3.2 derives the multiport admittance, $\mathbf{Y}(s)$, by using a partitioning of these networks. Transforms are derived in the next chapter to reduce the size of the network matrices presented in Section 3.1 while preserving properties of $\mathbf{Y}(s)$ derived in Section 3.2.

3.1 Modified Nodal Analysis

MNA is used to formulate symmetric matrices which relate network voltages and currents to the inputs in the frequency domain as

$$(\mathbf{G} + s\mathbf{C})\,\mathbf{x} = \mathbf{b}. \tag{3.1}$$

The time independent elements are represented by $\mathbf{G}$ and the time dependent elements are represented by $\mathbf{C}$. MNA uses two types of variables to represent the state of the network — type 1 and type 2 state variables are nodal voltages and branch currents respectively. Corresponding to this definition, type 1 branch elements are those which can be represented as admittances (i.e. branch

currents can be related to branch voltages) such as nonzero resistors (conductors) and capacitors. Type 2 elements are those which can be represented as impedances (i.e. branch voltages can be related to branch currents) such as resistors and inductors. Each type 2 element requires one state variable to represent branch current, and as a result, resistors are usually stamped as type 1 in order to minimize the number of unknowns.

Equation (3.1) can be partitioned into type 1 and type 2 components as

$$\left(\begin{bmatrix} \mathbf{G}_1 & \mathbf{G}_3^T \\ \mathbf{G}_3 & \mathbf{G}_2 \end{bmatrix} + s \begin{bmatrix} \mathbf{C}_1 & \mathbf{0} \\ \mathbf{0} & \mathbf{C}_2 \end{bmatrix} \right) \begin{bmatrix} \mathbf{x}_1 \\ \mathbf{x}_2 \end{bmatrix} = \begin{bmatrix} \mathbf{b}_1 \\ \mathbf{0} \end{bmatrix} \tag{3.2}$$

by ordering the nodal voltages (type 1) before the branch currents (type 2). The subscript 1 represents type 1 matrices, 2 represents type 2 matrices, and 3 represents the connecting matrices between the type 1 and type 2 components. The vector $\mathbf{x}_1$ represents the nodal voltages of the system, and $\mathbf{x}_2$ represents the currents through the type 2 branches. The excitation vector $\mathbf{b}_1$ represents the currents injected into the nodes of the network, and by definition $\mathbf{b}_2$ is zero because the branch voltages of the type 2 elements cannot be externally excited. For simplicity, the time independent matrix, G, will be referred to as the conductance matrix even though the type 2 conductance matrix, $\mathbf{G}_2$, has units of impedance, and the type 1 to type 2 connecting matrix, $\mathbf{G}_3$, is unitless. In the same way, the time dependent matrix, C, is referred to as the susceptance matrix.

Each element of the network can be represented as a simple matrix, as is shown in Fig. 3.1. If one of the branch nodes is 0 (the common node) then the corresponding row and column is eliminated from the matrix. The conductance matrix, G, is formed by the sum of the individual conductance matrices, $\tilde{\mathbf{G}}$, and the susceptance matrix, C, is formed by the sum of the individual susceptance matrices, $\tilde{\mathbf{C}}$. It is easy to see that $\mathbf{G}_1$ is formed solely by the individual type 1 resistance matrices (Fig. 3.1.a), and, because each is symmetric nonnegative definite (i.e. none of the eigenvalues are less than zero), $\mathbf{G}_1$ is symmetric nonnegative definite. In the same way, $\mathbf{C}_1$, which is formed solely by the individual capacitance matrices (Fig. 3.1.b), is also symmetric nonnegative definite. The type 2 susceptance matrix, $\mathbf{C}_2$, which is formed from the sum of the inductors (Fig. 3.1.c) and coupled inductors (Fig. 3.1.d) is symmetric nonpositive definite (no eigenvalues are greater than zero) because each of the individual element matrices has the same property. The type 2 conductance matrix, $\mathbf{G}_2$, is diagonal with zeros (or negative values if some resistors are stamped as type 2 as is shown if Fig. 3.1.e) on the diagonal. The definiteness of the partitions of the net-

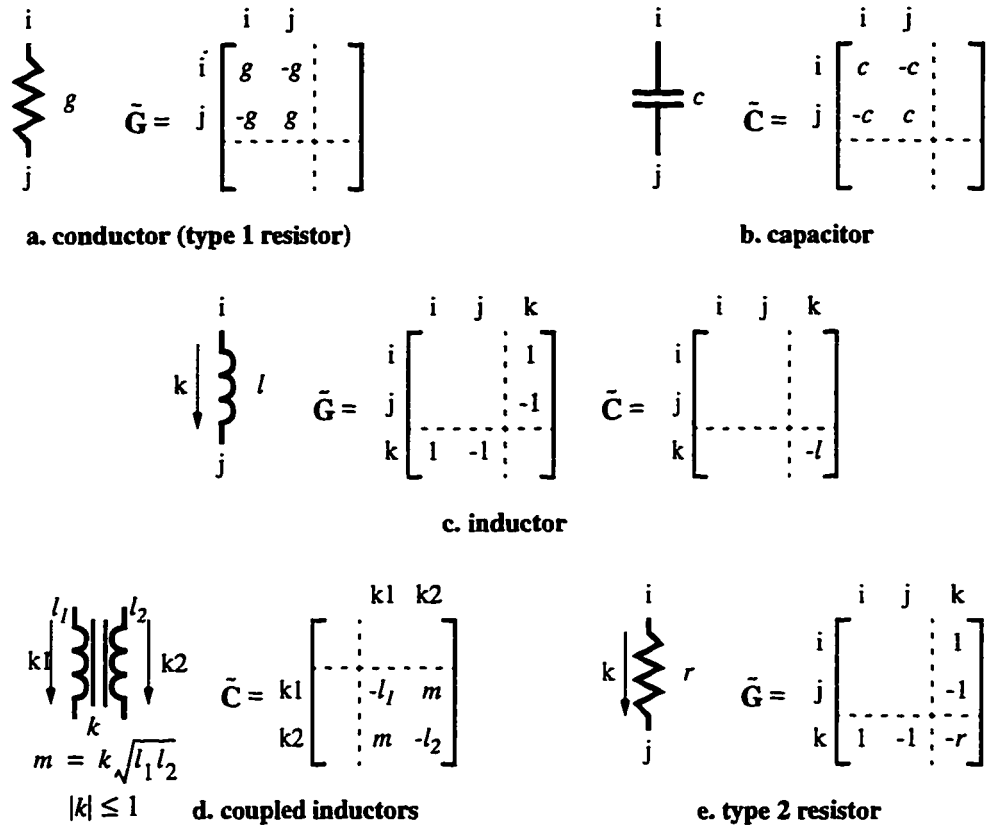

Figure 3.1. Formation of individual RLC elements into matrices using MNA. Each matrix is zero except where shown. The indices i and j represent voltage nodes, and k is the index to the type 2 branch currents. The dotted lines separate the type 1 (upper left) from the type 2 (lower right) portions of the matrices. The conductance matrix for (d) stamps as two individual inductors as shown in (c).

works assumes that all element values are positive with the exception of the inductance coupling coefficients (k) whose absolute values must be less than or equal to 1. *The symmetry and definiteness of the network matrix partitions are key to the derivations of passivity which are shown in Chapters 5 and 6.*

3.2 Formulation of Multiport Admittance

Given a network, which is represented using MNA by the matrices in (3.2), with m ports, n internal voltage nodes, and l type 2 elements, the multiport admittance can by found by partitioning the network into port nodes and internal nodes. The type 1 (voltage) nodes are ordered so that the common port node is 0, the remaining port nodes are in the first m rows, and the n internal voltage nodes are in the next n rows. The type 1 matrices are then partitioned as

$$\left(\begin{bmatrix} \mathbf{G_P} & \mathbf{G_{C1}^T} & \mathbf{G_{C2}^T} \\ \mathbf{G_{C1}} & \mathbf{G_{I1}} & \mathbf{G_{I3}^T} \\ \mathbf{G_{C2}} & \mathbf{G_{I3}} & \mathbf{G_2} \end{bmatrix} + s \begin{bmatrix} \mathbf{C_P} & \mathbf{C_{C1}^T} & \mathbf{0} \\ \mathbf{C_{C1}} & \mathbf{C_{I1}} & \mathbf{0} \\ \mathbf{0} & \mathbf{0} & \mathbf{C_2} \end{bmatrix} \right) \begin{bmatrix} \mathbf{x_P} \\ \mathbf{x_{I1}} \\ \mathbf{x_2} \end{bmatrix} = \begin{bmatrix} \mathbf{b_P} \\ \mathbf{0} \\ \mathbf{0} \end{bmatrix}. \tag{3.3}$$

The m port node voltages are represented by $\mathbf{x_p}$, the n internal node voltages are represented by $\mathbf{x_{I1}}$, and the l branch currents are represented by $\mathbf{x_2}$. The currents injected into the m ports are given by $\mathbf{b_p}$. The type 1 internal excitation vector is zero because no current can be injected into an internal node, and the type 2 excitation vector is zero by definition. The $m \times m$ port conductance and susceptance matrices are given by $\mathbf{G_P}$ and $\mathbf{C_P}$ respectively, and the $(l+n) \times m$ connection conductance and susceptance matrices are given by

$$\mathbf{G_C} = \begin{bmatrix} \mathbf{G_{C1}} \\ \mathbf{G_{C2}} \end{bmatrix} \text{ and } \mathbf{C_C} = \begin{bmatrix} \mathbf{C_{C1}} \\ \mathbf{0} \end{bmatrix}. \tag{3.4}$$

Finally, the $(l+n) \times (l+n)$ internal conductance and susceptance matrices are

$$\mathbf{G_I} = \begin{bmatrix} \mathbf{G_{I1}} & \mathbf{G_{I3}^T} \\ \mathbf{G_{I3}} & \mathbf{G_2} \end{bmatrix} \text{ and } \mathbf{C_I} = \begin{bmatrix} \mathbf{C_{I1}} & \mathbf{0} \\ \mathbf{0} & \mathbf{C_2} \end{bmatrix}. \tag{3.5}$$

To formulate the multiport admittance, $\mathbf{Y}(s)$, (3.3) is simplified by using the identities given in (3.4) and (3.5).

$$\left(\begin{bmatrix} \mathbf{G_P} & \mathbf{G_C^T} \\ \mathbf{G_C} & \mathbf{G_I} \end{bmatrix} + s \begin{bmatrix} \mathbf{C_P} & \mathbf{C_C^T} \\ \mathbf{C_C} & \mathbf{C_I} \end{bmatrix} \right) \begin{bmatrix} \mathbf{x_P} \\ \mathbf{x_I} \end{bmatrix} = \begin{bmatrix} \mathbf{b_P} \\ \mathbf{0} \end{bmatrix} \tag{3.6}$$

Equation (3.6) provides two equations with two unknowns, $\mathbf{x_P}$ and $\mathbf{x_I}$. Using the definition of admittance,

$$\mathbf{Y}(s)\,\mathbf{x_P}(s) = \mathbf{b_P}(s), \tag{3.7}$$

and eliminating $\mathbf{x_I}$ gives

$$\mathbf{Y}(s) = \mathbf{G_P} + s\mathbf{C_P} - (\mathbf{G_C} + s\mathbf{C_C})^{\mathrm{T}} (\mathbf{G_I} + s\mathbf{C_I})^{-1} (\mathbf{G_C} + s\mathbf{C_C}). \tag{3.8}$$

The poles of $\mathbf{Y}(s)$ occur where $(\mathbf{G_I}+s\mathbf{C_I})$ is singular, and these are found from the solution to the generalized eigenvalue problem

$$\mathbf{G_I x} = \lambda \mathbf{C_I x} \tag{3.9}$$

where $s = -\lambda$ is a pole of the system.

It is desirable to simplify (3.8) by zeroing either $\mathbf{G_C}$ or $\mathbf{C_C}$, and to reduce the size of the network while preserving some behavior of $\mathbf{Y}(s)$. Both of these operations are performed by transforming the network using specific congruence transforms which are presented in the next chapter, and the formulation of those transforms is based on that which is presented here.

Chapter 4
Network Reduction Using Congruence Transformations

In this chapter, congruence transforms are used to reduce the size of RLC networks by decreasing the size of the internal matrices, $\mathbf{G_I}$ and $\mathbf{C_I}$, in the derivation of the multiport admittance, $\mathbf{Y}(s)$, given by (3.8). A congruence transformation of a square matrix $\mathbf{A}$ is defined as the transformation $\mathbf{B} = \mathbf{X}^T\mathbf{A}\mathbf{X}$ (note that $\mathbf{A}$ and $\mathbf{B}$ are not those which were defined in Chapter 2). $\mathbf{X}$ is referred to as a *congruence transform*. An important property of these transforms is that they preserve symmetry and definiteness as is shown in Theorem 4.1. This property is used in Chapters 5 and 6 to show how passivity can be preserved. *Application of a transform with fewer columns than rows to the conductance and susceptance matrices of (3.1) reduces the size of the network by decreasing the number of rows (and thus network nodes).* In general, nonsquare transforms cause information to be lost so that the network behavior is not preserved (Section 4.4 shows one exception), but some can be formulated which retain desired behavior such as an admittance poles or moments.

This chapter is written using a "cookbook" approach in the sense that several transforms are independently presented which are needed in subsequent chapters. Theses transforms are used to zero the conductance or susceptance connection matrices without changing the network behavior (Section 4.1), and to match a selected set of poles (Section 4.2) or moments (Section 4.3) of the multiport admittance while reducing network size. Section 4.4 shows how to eliminate singularities caused by current loops or floating nodes without affecting the network behavior.

Theorem 4.1. If $\mathbf{A}$ *is a symmetric nonnegative definite matrix, then* $\mathbf{B} = \mathbf{X}^T\mathbf{A}\mathbf{X}$ *is also a symmetric nonnegative definite matrix, where* $\mathbf{X}$ *is any real matrix with the appropriate number of rows.*

Proof: Because $\mathbf{A}$ is symmetric nonnegative definite, it can be written as

$$\mathbf{A} = \mathbf{U}\Lambda\mathbf{U}^T \tag{4.1}$$

where **U** is the real, orthonormal matrix containing the eigenvectors of **A**, and Λ is the diagonal matrix containing the real nonnegative eigenvalues of **A**. Since each element of Λ is greater than or equal to zero, **A** can be written as

$$\mathbf{A} = \mathbf{W}\mathbf{W}^{\mathrm{T}} \text{ where } \mathbf{W} = \mathbf{U}\Lambda^{1/2}. \tag{4.2}$$

Because the product of a real matrix and its transpose is symmetric and nonnegative definite,

$$\mathbf{B} = \mathbf{X}^{\mathrm{T}}\mathbf{A}\mathbf{X} = \left(\mathbf{W}^{\mathrm{T}}\mathbf{X}\right)^{\mathrm{T}}\left(\mathbf{W}^{\mathrm{T}}\mathbf{X}\right) \tag{4.3}$$

is symmetric and nonnegative definite.

QED.

4.1 Transformation to Zero Connection Matrices

It is possible to apply a transformation to the network given by (3.6) which will cause *either* the connection susceptance *or* the connection conductance matrix to be zero while preserving the port behavior. Given the transform

$$\mathbf{X} = \begin{bmatrix} \mathbf{I} & \mathbf{0} \\ \mathbf{V} & \mathbf{I} \end{bmatrix}, \tag{4.4}$$

the transformation of the network matrices in (3.6) is

$$\tilde{\mathbf{G}} = \mathbf{X}^{\mathrm{T}}\mathbf{G}\mathbf{X} = \begin{bmatrix} \mathbf{G}_{\mathbf{P}} + \mathbf{V}^{\mathrm{T}}\mathbf{G}_{\mathbf{C}} + \mathbf{G}_{\mathbf{C}}^{\mathrm{T}}\mathbf{V} + \mathbf{V}^{\mathrm{T}}\mathbf{G}_{\mathbf{I}}\mathbf{V} & \mathbf{G}_{\mathbf{C}}^{\mathrm{T}} + \mathbf{V}^{\mathrm{T}}\mathbf{G}_{\mathbf{I}} \\ \mathbf{G}_{\mathbf{C}} + \mathbf{G}_{\mathbf{I}}\mathbf{V} & \mathbf{G}_{\mathbf{I}} \end{bmatrix} = \begin{bmatrix} \tilde{\mathbf{G}}_{\mathbf{P}} & \tilde{\mathbf{G}}_{\mathbf{C}}^{\mathrm{T}} \\ \tilde{\mathbf{G}}_{\mathbf{C}} & \tilde{\mathbf{G}}_{\mathbf{I}} \end{bmatrix} \tag{4.5}$$

and

$$\tilde{\mathbf{C}} = \mathbf{X}^{\mathrm{T}}\mathbf{C}\mathbf{X} = \begin{bmatrix} \mathbf{C}_{\mathbf{P}} + \mathbf{V}^{\mathrm{T}}\mathbf{C}_{\mathbf{C}} + \mathbf{C}_{\mathbf{C}}^{\mathrm{T}}\mathbf{V} + \mathbf{V}^{\mathrm{T}}\mathbf{C}_{\mathbf{I}}\mathbf{V} & \mathbf{C}_{\mathbf{C}}^{\mathrm{T}} + \mathbf{V}^{\mathrm{T}}\mathbf{C}_{\mathbf{I}} \\ \mathbf{C}_{\mathbf{C}} + \mathbf{C}_{\mathbf{I}}\mathbf{V} & \mathbf{C}_{\mathbf{I}} \end{bmatrix} = \begin{bmatrix} \tilde{\mathbf{C}}_{\mathbf{P}} & \tilde{\mathbf{C}}_{\mathbf{C}}^{\mathrm{T}} \\ \tilde{\mathbf{C}}_{\mathbf{C}} & \tilde{\mathbf{C}}_{\mathbf{I}} \end{bmatrix}. \tag{4.6}$$

A straightforward substitution of the partitions of $\tilde{\mathbf{G}}$ and $\tilde{\mathbf{C}}$ into (3.8) shows that the multiport admittance, $\mathbf{Y}(s)$, is unchanged.

If

$$\mathbf{V} = -\mathbf{G}_{\mathbf{I}}^{-1}\mathbf{G}_{\mathbf{C}} \tag{4.7}$$

then (4.5) simplifies to

$$\tilde{\mathbf{G}} = \begin{bmatrix} \mathbf{G_P} - \mathbf{G_C^T G_I^{-1} G_C} & \mathbf{0} \\ \mathbf{0} & \mathbf{G_I} \end{bmatrix}, \tag{4.8}$$

and the connection conductance is zeroed. Likewise, if the transform uses

$$\mathbf{V} = -\mathbf{C_I^{-1} C_C}, \tag{4.9}$$

then (4.6) simplifies to

$$\tilde{\mathbf{C}} = \begin{bmatrix} \mathbf{C_P} - \mathbf{C_C^T C_I^{-1} C_C} & \mathbf{0} \\ \mathbf{0} & \mathbf{C_I} \end{bmatrix}, \tag{4.10}$$

and the connection susceptance is zeroed. It is not always possible to use **V** given in (4.7) unless some assurance can be made that the internal conductance matrix is nonsingular. On the other hand, Theorem 4.2 shows that, if the network capacitors are positive, it is always possible to zero the connection susceptance matrix.

Theorem 4.2. If all of the elements of an RLC network are positive, then **V** *can always be formulated such that*

$$\mathbf{C_C} + \mathbf{C_I V} = \mathbf{0}, \tag{4.11}$$

where $\mathbf{C_C}$ *and* $\mathbf{C_I}$ *are the partitions of the network matrices defined in (3.6).*

Proof: As shown by (3.4) and (3.5), $\mathbf{C_I}$ is block diagonal with type 1 and 2 blocks, and the type 2 connection susceptance matrix is zero. Therefore, (4.11) is satisfied for the type 2 rows if the corresponding rows of **V** are zero. If the type 1 block of $\mathbf{C_I}$ is permuted so that it is block diagonal, then each block is by definition irreducible (this is the mathematical definition, and should not to be confused with "network not able to be reduced"). As can be seen from Fig. 3.1.b, each diagonal element is greater than or equal to the absolute sum of the off diagonals if all of the capacitors are positive, and diagonals are greater than the sums at locations for which the corresponding rows of $\mathbf{C_C}$ are nonzero. From the corollary of Theorem 1.8 in [22], each block of the type 1 partition of $\mathbf{C_I}$ is nonsingular if there is a nonzero in at least one of the corresponding rows of $\mathbf{C_C}$, and thus a solution to (4.9) exists for these blocks. The remaining singular blocks of $\mathbf{C_I}$ have zeros in the corresponding rows of $\mathbf{C_C}$, so (4.11) is satisfied for these rows by setting the corresponding rows of **V** to zero.

QED.

4.2 Preservation of Admittance Poles

If a congruence transform of the form

$$\mathbf{X} = \begin{bmatrix} \mathbf{I} & \mathbf{0} \\ \mathbf{0} & \mathbf{V} \end{bmatrix} \tag{4.12}$$

is applied to the network represented by (3.6), the multiport admittance of transformed network is given by

$$\tilde{\mathbf{Y}}(s) = \mathbf{G_P} + s\mathbf{C_P} - (\mathbf{G_C} + s\mathbf{C_C})^{\mathrm{T}}\mathbf{V}\left(\mathbf{V}^{\mathrm{T}}\mathbf{G_I}\mathbf{V} + s\mathbf{V}^{\mathrm{T}}\mathbf{C_I}\mathbf{V}\right)^{-1}\mathbf{V}^{\mathrm{T}}(\mathbf{G_C} + s\mathbf{C_C}) \tag{4.13}$$

It is easy to show that if **V** is square and of full rank then the multiport admittance of the network is unchanged. If **V** has fewer columns than rows, then the size of the network is reduced, but the multiport admittance of the network is not preserved because **V** is not invertible. Theorem 4.3 shows that even if **V** is not square or is less than full rank, if the columns of **V** span an eigenvector, **x**, which is given by (3.9) and which is associated with a pole of the system, then the multiport admittance of the reduced network also contains that pole. If **V** spans **x** then **x** is equal to some linear combination of the columns of **V**. Theorem 4.3 is useful if a selected set of poles need to be retained.

Theorem 4.3. A congruence transformation of a symmetric network of the form

$$\begin{bmatrix} \mathbf{I} & \mathbf{0} \\ \mathbf{0} & \mathbf{V}^{\mathrm{T}} \end{bmatrix}\left(\begin{bmatrix} \mathbf{G_P} & \mathbf{G_C}^{\mathrm{T}} \\ \mathbf{G_C} & \mathbf{G_I} \end{bmatrix} + s\begin{bmatrix} \mathbf{C_P} & \mathbf{C_C}^{\mathrm{T}} \\ \mathbf{C_C} & \mathbf{C_I} \end{bmatrix}\right)\begin{bmatrix} \mathbf{I} & \mathbf{0} \\ \mathbf{0} & \mathbf{V} \end{bmatrix} \tag{4.14}$$

where $\mathbf{G_P}$ *and* $\mathbf{C_P} \in \Re^{m\times m}$, $\mathbf{G_I}$ *and* $\mathbf{C_I} \in \Re^{n\times n}$, $\mathbf{G_C} \in \Re^{n\times m}$, *and* $\mathbf{V} \in \Re^{n\times k}$, *preserves the* i*th pole of the multiport admittance of the network as defined by (3.6) and (3.8) if the columns of* **V** *are linearly independent,* $\mathbf{G_I}$ *and* $\mathbf{C_I}$ *are symmetric, and*

$$\mathrm{span}(\mathbf{x}_i) \subseteq \mathrm{span}(\mathbf{V}) \tag{4.15}$$

where $\mathbf{x}_i$ *is the complex eigenvector associated with the* i*th solution of the generalized symmetric eigenvalue problem given by*

$$\mathbf{G_I}\mathbf{x}_i = \lambda_i\mathbf{C_I}\mathbf{x}_i. \tag{4.16}$$

Proof: The poles of the multiport admittance given in (3.8) are equal to $-\lambda$ where λ comes from (4.16), and preserving λ_i preserves the ith pole of the multiport admittance. Let **X** be a complex square matrix whose n columns are the n eigenvalues, $\mathbf{x}_i$, from (4.16). Because the two matri-

ces in (4.16) are symmetric

$$\mathbf{X}^{\mathrm{T}}(\mathbf{G}_{\mathrm{I}}-\lambda\mathbf{C}_{\mathrm{I}})\mathbf{X} = \mathrm{diag}(g_1 \ldots g_n) - \lambda \cdot \mathrm{diag}(c_1 \ldots c_n) \text{ and } \lambda_i = \frac{g_i}{c_i}. \tag{4.17}$$

Because $\mathbf{V}$ is full rank and spans $\mathbf{x}_i$, from (4.17) there exists a nonsingular square complex matrix β and a complex rectangular matrix $\tilde{\mathbf{X}}$ such that

$$\widehat{\mathbf{X}} = \left[\mathbf{x}_i \; \tilde{\mathbf{X}}\right] = \mathbf{V}\beta \text{ and } \mathbf{x}_i^{\mathrm{T}}\mathbf{C}_{\mathrm{I}}\tilde{\mathbf{X}} = \mathbf{x}_i^{\mathrm{T}}\mathbf{G}_{\mathrm{I}}\tilde{\mathbf{X}} = \mathbf{0}. \tag{4.18}$$

One of the eigenvalues of

$$\det\left(\widehat{\mathbf{X}}^{\mathrm{T}}(\mathbf{G}_{\mathrm{I}}-\lambda\mathbf{C}_{\mathrm{I}})\widehat{\mathbf{X}}\right) = \det\left(\begin{bmatrix} g_i & \mathbf{0} \\ \mathbf{0} & \tilde{\mathbf{X}}^{\mathrm{T}}\mathbf{C}_{\mathrm{I}}\tilde{\mathbf{X}} \end{bmatrix} - \lambda\begin{bmatrix} c_i & \mathbf{0} \\ \mathbf{0} & \tilde{\mathbf{X}}^{\mathrm{T}}\mathbf{G}_{\mathrm{I}}\tilde{\mathbf{X}} \end{bmatrix}\right) = 0 \tag{4.19}$$

is λ_i. Because congruence transforms preserve eigenvalues of the generalized eigenvalue problem,

$$\det\left(\beta^{-\mathrm{T}}\widehat{\mathbf{X}}^{\mathrm{T}}(\mathbf{G}_{\mathrm{I}}-\lambda\mathbf{C}_{\mathrm{I}})\widehat{\mathbf{X}}\beta^{-1}\right) = \det\left(\mathbf{V}^{\mathrm{T}}(\mathbf{G}_{\mathrm{I}}-\lambda\mathbf{C}_{\mathrm{I}})\mathbf{V}\right) = 0, \tag{4.20}$$

also preserves λ_i, and (4.14) preserves the ith pole of the admittance.

QED.

4.3 Preservation of Admittance Moments

When reducing networks, it is often desirable to preserve a selected set of the moments of $\mathbf{Y}(s)$ as defined in (4.29). Because it is always possible to zero out the connection susceptance as is shown by Theorem 4.2, $\mathbf{C}_{\mathrm{C}}$ is assumed to be zero so that the derivation of Theorem 4.4 is simpler. This theorem shows that to match $2q$ moments of the multiport admittance expanded about $s = s_0$, the span requirements for $\mathbf{V}$ in the transform given by (4.12) form a Krylov subspace

$$\mathbf{K}_q\left(\mathbf{A}^{-1}\mathbf{C}_{\mathrm{I}}, \mathbf{A}^{-1}\mathbf{G}_{\mathrm{C}}\right) = \mathrm{span}\left[\mathbf{A}^{-1}\mathbf{G}_{\mathrm{C}}, \mathbf{A}^{-1}\mathbf{C}_{\mathrm{I}}\mathbf{A}^{-1}\mathbf{G}_{\mathrm{C}}, \ldots, \left(\mathbf{A}^{-1}\mathbf{C}_{\mathrm{I}}\right)^{q-1}\mathbf{A}^{-1}\mathbf{G}_{\mathrm{C}}\right] \subseteq \mathbf{V} \tag{4.21}$$

where

$$\mathbf{A} = \mathbf{G}_{\mathrm{I}} + s_0\mathbf{C}_{\mathrm{I}}. \tag{4.22}$$

This span requirement is similar to that derived for MPVL and the Arnoldi based methods. One difference, however, is that since both the Arnoldi and Lanczos methods form a matrix $\mathbf{V}$ with the span requirements given by (4.21), *either* method can be used to generate a transform which preserves $2q$ moments. In contrast, the Arnoldi-based method reviewed in Section 2.5 only preserves

half as many moments. The difference results because the algorithms presented in Chapter 2 are nonsymmetric, whereas congruence transformations are symmetric.

Theorem 4.4. A congruence transformation of a symmetric network of the form

$$\begin{bmatrix} \mathbf{I} & \mathbf{0} \\ \mathbf{0} & \mathbf{V}^{\mathrm{T}} \end{bmatrix} \left(\begin{bmatrix} \mathbf{G_P} & \mathbf{G_C^T} \\ \mathbf{G_C} & \mathbf{G_I} \end{bmatrix} + s \begin{bmatrix} \mathbf{C_P} & \mathbf{0} \\ \mathbf{0} & \mathbf{C_I} \end{bmatrix} \right) \begin{bmatrix} \mathbf{I} & \mathbf{0} \\ \mathbf{0} & \mathbf{V} \end{bmatrix} \tag{4.23}$$

where $\mathbf{G_P}$ *and* $\mathbf{C_P} \in \Re^{m \times m}$, $\mathbf{G_I}$ *and* $\mathbf{C_I} \in \Re^{n \times n}$, $\mathbf{G_C} \in \Re^{n \times m}$, $V \in \Re^{n \times k}$, *and* $\mathbf{A} = \mathbf{G_I} + s_0 \mathbf{C_I}$, *preserves the first 2p moments expanded at* $s = s_0$ *of the multiport admittance of the network as defined by (3.6) and (3.8) if* $\mathbf{A}$ *is nonsingular, the columns of* $\mathbf{V}$ *are linearly independent,* $\mathbf{G_I}$ *and* $\mathbf{C_I}$ *are symmetric, and*

$$\operatorname{span}\left[\left(\mathbf{A}^{-1}\mathbf{C_I}\right)^i \mathbf{A}^{-1}\mathbf{G_C}\right] \subseteq \operatorname{span}(\mathbf{V}),\ (i \in \{0, 1, \ldots, p-1\}) . \tag{4.24}$$

Proof: Equation (4.24) implies that

$$\text{there exists } \left(\alpha_i \in \Re^{k \times m}\right) \text{ such that } \left(\mathbf{A}^{-1}\mathbf{C_I}\right)^i \mathbf{A}^{-1}\mathbf{G_C} = \mathbf{V}\alpha_i,\ (i \in \{0, 1, \ldots, p-1\}) . \tag{4.25}$$

Because $\mathbf{A}$ is nonsingular, it follows that

$$\left(\mathbf{C_I}\mathbf{A}^{-1}\right)^i \mathbf{G_C} = \mathbf{A}\mathbf{V}\alpha_i . \tag{4.26}$$

Therefore, because the columns of $\mathbf{V}$ are linearly independent and $\mathbf{A}$ is nonsingular,

$$\begin{aligned} \mathbf{V}\left(\mathbf{V}^{\mathrm{T}}\mathbf{A}\mathbf{V}\right)^{-1}\mathbf{V}^{\mathrm{T}}\left(\mathbf{C_I}\mathbf{A}^{-1}\right)^i \mathbf{G_C} &= \mathbf{V}\left(\mathbf{V}^{\mathrm{T}}\mathbf{A}\mathbf{V}\right)^{-1}\left(\mathbf{V}^{\mathrm{T}}\mathbf{A}\mathbf{V}\right)\alpha_i \\ = \mathbf{V}\alpha_i = \left(\mathbf{A}^{-1}\mathbf{C_I}\right)^i \mathbf{A}^{-1}\mathbf{G_C}, &\qquad (i \in \{0, 1, \ldots, p-1\} \end{aligned} \tag{4.27}$$

From (3.8),

$$\mathbf{Y}(s + s_0) = (\mathbf{G_P} + s_0\mathbf{C_P}) + s\mathbf{C_P} - \mathbf{G_C^T}(\mathbf{A} + s\mathbf{C_I})^{-1}\mathbf{G_C}, \tag{4.28}$$

and the Taylor series expansion at $s = s_0$ is

$$\begin{aligned} \mathbf{Y}(s + s_0) &= (\mathbf{G_P} + s_0\mathbf{C_P}) + s\mathbf{C_P} - \mathbf{Y}_0 - s\mathbf{Y}_1 - \ldots \\ \mathbf{Y}_i &= \mathbf{G_C^T}\left(-\mathbf{A}^{-1}\mathbf{C_I}\right)^i \mathbf{A}^{-1}\mathbf{G_C} \end{aligned} \tag{4.29}$$

Substitution of the partitions of the transformed network from (4.23) into (4.29) gives

$$\tilde{\mathbf{Y}}(s+s_0) = (\mathbf{G_P}+s_0\mathbf{C_P}) + s\mathbf{C_P} - \tilde{\mathbf{Y}}_0 - s\tilde{\mathbf{Y}}_1 - \ldots$$
$$\tilde{\mathbf{Y}}_i = \mathbf{G_C^T V}\left[-\left(\mathbf{V^T A V}\right)^{-1}\mathbf{V^T C_I V}\right]^i\left(\mathbf{V^T A V}\right)^{-1}\mathbf{V^T G_C} \quad , \tag{4.30}$$

and a straightforward recursion using the equality given in (4.27) as well as its transpose (which is allowed because $\mathbf{G_I}$ and $\mathbf{C_I}$ are symmetric) shows

$$\tilde{\mathbf{Y}}_i = \mathbf{Y}_i (i \in \{0, 1, \ldots, 2p-1\}) , \tag{4.31}$$

and the first $2p$ moments of the multiport admittance at $s = s_0$ are matched.

QED.

In some cases, it is desirable to zero the connection conductance matrix instead of the susceptance. This is done for both RC networks in Chapter 5 and LC networks in Chapter 7. Theorem 4.5 is similar to the previous theorem except that it shows the span requirements to preserve moments when $\mathbf{G_I} = \mathbf{0}$ at $s_0 = 0$.

Theorem 4.5. A congruence transformation of a symmetric network of the form

$$\begin{bmatrix}\mathbf{I} & \mathbf{0}\\ \mathbf{0} & \mathbf{V^T}\end{bmatrix}\left(\begin{bmatrix}\mathbf{G_P} & \mathbf{0}\\ \mathbf{0} & \mathbf{G_I}\end{bmatrix} + s\begin{bmatrix}\mathbf{C_P} & \mathbf{C_C^T}\\ \mathbf{C_C} & \mathbf{C_I}\end{bmatrix}\right)\begin{bmatrix}\mathbf{I} & \mathbf{0}\\ \mathbf{0} & \mathbf{V}\end{bmatrix} \tag{4.32}$$

where $\mathbf{G_P}$ *and* $\mathbf{C_P} \in \Re^{m\times m}$, $\mathbf{G_I}$ *and* $\mathbf{C_I} \in \Re^{n\times n}$, $\mathbf{C_C} \in \Re^{n\times m}$, *and* $V \in \Re^{n\times k}$, *preserves the first 2p+2 moments expanded at* $s = 0$ *of the multiport admittance of the network as defined by (3.6) and (3.8) if* $\mathbf{G_I}$ *is nonsingular, the columns of* $\mathbf{V}$ *are linearly independent,* $\mathbf{G_I}$ *and* $\mathbf{C_I}$ *are symmetric, and*

$$\text{span}\left[\left(\mathbf{G_I}^{-1}\mathbf{C_I}\right)^i\mathbf{G_I}^{-1}\mathbf{C_C}\right] \subseteq \text{span}(\mathbf{V}), \ (i \in \{0, 1, \ldots, p-1\}) . \tag{4.33}$$

Proof: Equation (4.33) implies that

$$\text{there exists } \left(\alpha_i \in \Re^{k\times m}\right) \text{ such that } \left(\mathbf{G_I}^{-1}\mathbf{C_I}\right)^i\mathbf{G_I}^{-1}\mathbf{C_C} = \mathbf{V}\alpha_i, \ (i \in \{0, 1, \ldots, p-1\}) . \tag{4.34}$$

Because $\mathbf{G_I}$ is nonsingular, it follows that

$$\left(\mathbf{C_I}\mathbf{G_I}^{-1}\right)^i\mathbf{C_C} = \mathbf{G_I}\mathbf{V}\alpha_i . \tag{4.35}$$

Therefore, because $\mathbf{V}$ is linearly independent and $\mathbf{G_I}$ is nonsingular,

$$\mathbf{V}\left(\mathbf{V^T G_I V}\right)^{-1}\mathbf{V^T}\left(\mathbf{C_I}\mathbf{G_I}^{-1}\right)^i\mathbf{C_C} = \mathbf{V}\left(\mathbf{V^T G_I V}\right)^{-1}\left(\mathbf{V^T G_I V}\right)\alpha_i \quad . \tag{4.36}$$
$$= \mathbf{V}\alpha_i = \left(\mathbf{G_I}^{-1}\mathbf{C_I}\right)^i\mathbf{G_I}^{-1}\mathbf{C_C}, \qquad (i \in \{0, 1, \ldots, p-1\})$$

From (3.8),

$$\mathbf{Y}(s) = \mathbf{G_P} + s\mathbf{C_P} - s^2\mathbf{C_C}^{\mathbf{T}}(\mathbf{G_I} + s\mathbf{C_I})^{-1}\mathbf{C_C}, \tag{4.37}$$

and the Taylor series expansion at $s = 0$ is

$$\begin{aligned} \mathbf{Y}(s) &= \mathbf{G_P} + s\mathbf{C_P} - s^2\mathbf{Y}_2 - s^3\mathbf{Y}_3 - \ldots \\ \mathbf{Y}_i &= \mathbf{C_C}^{\mathbf{T}}\left(-\mathbf{G_I}^{-1}\mathbf{C_I}\right)^{i-2}\mathbf{G_I}^{-1}\mathbf{C_C},\ (i \geq 2) \end{aligned} \tag{4.38}$$

Substitution of the partitions of the transformed network from (4.32) into (4.38) gives

$$\begin{aligned} \tilde{\mathbf{Y}}(s) &= \mathbf{G_P} + s\mathbf{C_P} - s^2\tilde{\mathbf{Y}}_2 - s^3\tilde{\mathbf{Y}}_3 - \ldots \\ \tilde{\mathbf{Y}}_i &= \mathbf{C_C}^{\mathbf{T}}\mathbf{V}\left[-\left(\mathbf{V}^{\mathbf{T}}\mathbf{G_I}\mathbf{V}\right)^{-1}\mathbf{V}^{\mathbf{T}}\mathbf{C_I}\mathbf{V}\right]^{i}\left(\mathbf{V}^{\mathbf{T}}\mathbf{G_I}\mathbf{V}\right)^{-1}\mathbf{V}^{\mathbf{T}}\mathbf{C_C},\ (i \geq 2) \end{aligned} \tag{4.39}$$

Inspection of (4.39) shows that the first two moments are always preserved, and a straightforward recursion using the equality given in (4.36) as well as its transpose (which is allowed because $\mathbf{G_I}$ and $\mathbf{C_I}$ are symmetric) shows

$$\tilde{\mathbf{Y}}_i = \mathbf{Y}_i (i \in \{2, 3, \ldots, 2p+1\}), \tag{4.40}$$

and the first $2p$+2 moments of the multiport admittance at $s = 0$ are matched.

QED.

4.4 Elimination of Singular Current Loops and Floating Voltage Nodes

A network which has floating nodes or current loops has a valid solution to the multiport admittance at the ports, but the internal conductance matrix is singular. Floating nodes cause singularities because there is no DC path to these nodes, so that they can support nonzero voltages even when the input currents are zero. When inductors form a loop, a singularity is created because a DC current can be sustained through the loop even when all voltages are zero.

Most singularities can be removed from a network without affecting the port behavior as is demonstrated for two simple networks in Fig. 4.1. Singularities which cannot be removed correspond to inductor loops which are formed when the port nodes are shorted together. For example, the one-port network formed by a single inductor has the MNA conductance matrix

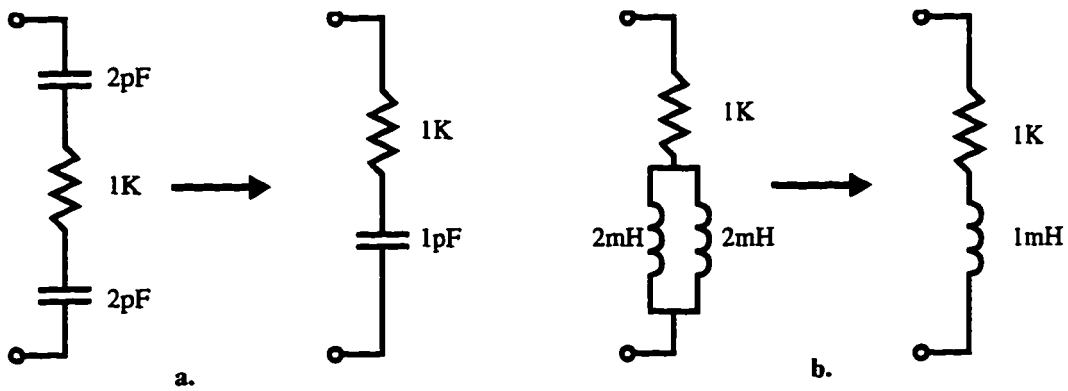

Figure 4.1. Simple examples of network reduction which eliminate DC singularities due to (a) floating nodes, and (b) current loops.

$$\mathbf{G} = \begin{bmatrix} \mathbf{G_P} & \mathbf{G_C}^T \\ \mathbf{G_C} & \mathbf{G_I} \end{bmatrix} = \begin{bmatrix} 0 & 1 \\ 1 & 0 \end{bmatrix}, \tag{4.41}$$

and the internal matrix, $\mathbf{G_I} = 0$, is singular. The singularity exists because the inductor forms a loop when its two terminals are shorted. As a result, current can flow into the port even when the port voltage is zero, and by definition, the network has an admittance pole at $s = 0$.

A general technique for the elimination of singularities without changing network behavior uses the null and spanning spaces of the internal conductance matrix $\mathbf{G_I}$. Let $\mathbf{X_N}$ be an orthonormal basis for the null space of $\mathbf{G_I}$ such that

$$\mathbf{G_I X_N} = \mathbf{0} \text{ and } \mathbf{X_N^T X_N} = \mathbf{I}, \tag{4.42}$$

and let $\mathbf{X_S}$ be an orthonormal basis for the spanning space of $\mathbf{G_I}$ such that

$$\text{span}\,(\mathbf{G_I}) = \text{span}\,(\mathbf{X_S}),\ \mathbf{X_S^T X_S} = \mathbf{I}, \text{ and } \mathbf{X_N^T X_S} = \mathbf{0}. \tag{4.43}$$

The total number of columns in $\mathbf{X_N}$ and $\mathbf{X_S}$ is equal to the number of rows in $\mathbf{G_I}$. Application of the full rank square transform

$$\mathbf{X} = \begin{bmatrix} \mathbf{I} & \mathbf{0} & \mathbf{0} \\ \mathbf{0} & \mathbf{X_S} & \mathbf{X_N} \end{bmatrix} \tag{4.44}$$

to the network in (3.6) gives

$$\tilde{G} = X^T G X = \begin{bmatrix} G_P & G_C^T X_S & G_C^T X_N \\ X_S^T G_C & X_S^T G_I X_S & 0 \\ X_N^T G_C & 0 & 0 \end{bmatrix} = \begin{bmatrix} G_P & G_{CS}^T & G_{CN}^T \\ G_{CS} & G_{ISS} & 0 \\ G_{CN} & 0 & 0 \end{bmatrix} \tag{4.45}$$

and

$$\tilde{C} = X^T C X = \begin{bmatrix} C_P & C_C^T X_S & C_C^T X_N \\ X_S^T C_C & X_S^T C_I X_S & X_S^T C_I X_N \\ X_N^T C_C & X_N^T C_I X_S & X_N^T C_I X_N \end{bmatrix} = \begin{bmatrix} C_P & C_{CS}^T & C_{CN}^T \\ C_{CS} & C_{ISS} & C_{ISN} \\ C_{CN} & C_{INS} & C_{INN} \end{bmatrix}. \tag{4.46}$$

This transformation does not affect the port behavior of the network.

Now that the internal matrices of $\tilde{G}$ are zero in the bottom and right columns and rows, isolation of the bottom right block of $\tilde{C}$ allows the nodes corresponding to that block to be removed from the network. The isolation is achieved by zeroing the off-diagonal blocks on the bottom and right sides of the susceptance matrix. For simplicity, the following derivation assumes that C_{INN} is nonsingular. This is a reasonable assumption if all inductances are greater than zero. Because the third row and column matrices of $\tilde{G}$ are zero, it is easy to show that the transform

$$X = \begin{bmatrix} I & 0 & 0 \\ 0 & I & 0 \\ -C_{INN}^{-1} C_{CN} & -C_{INN}^{-1} C_{INS} & I \end{bmatrix} \tag{4.47}$$

results in a network of the form

$$\bar{G} = X^T \tilde{G} X = \begin{bmatrix} \bar{G}_P & \bar{G}_{CS}^T & \bar{G}_{CN}^T \\ \bar{G}_{CS} & G_{ISS} & 0 \\ \bar{G}_{CN} & 0 & 0 \end{bmatrix} \tag{4.48}$$

and

$$\bar{C} = X^T \tilde{C} X = \begin{bmatrix} \bar{C}_P & \bar{C}_{CS}^T & 0 \\ \bar{C}_{CS} & \bar{C}_{ISS} & 0 \\ 0 & 0 & C_{INN} \end{bmatrix} \tag{4.49}$$

without changing the port behavior of the system. Even if C_{INN} is singular, a transform exists

which zeros the off-diagonal susceptance matrices for reasons related to those given in Theorem 4.2.

Once the lower right diagonal block is isolated from the other network internal nodes, the network can be split into two separate networks which are added in parallel at the ports. These are

$$G' = \begin{bmatrix} \bar{G}_P & \bar{G}_{CS}^T \\ \bar{G}_{CS} & G_{ISS} \end{bmatrix} \text{ and } C' = \begin{bmatrix} \bar{C}_P & \bar{C}_{CS}^T \\ \bar{C}_{CS} & \bar{C}_{ISS} \end{bmatrix}, \tag{4.50}$$

and

$$\hat{G} = \begin{bmatrix} 0 & \bar{G}_{CN}^T \\ \bar{G}_{CN} & 0 \end{bmatrix} \text{ and } \hat{C} = \begin{bmatrix} 0 & 0 \\ 0 & C_{INN} \end{bmatrix}. \tag{4.51}$$

The network in (4.50) contains no DC singularities. The network in (4.51) contains all of the DC singularities of the system, and $\bar{G}_{CN}$ is nonzero if the network has any poles at DC which are observable through the ports. These poles must be extracted from (4.51) and included in the reduced network if the DC behavior of the network is to be preserved.

The transforms presented in the previous sections can be used to reduce any RLC networks. DC singularities can be eliminated using the transform in Section 4.4, and one of the connection matrices can be zeroed using that in Section 4.1. The size of the network can then be reduced using a transform which preserve moments and/or poles of the multiport admittance as given in Sections 4.2 and 4.3. The next chapter shows that this set of transforms can be used to passively reduce RC networks, and the following chapter provides modifications which preserve passivity during the reduction of general RLC networks.

Chapter 5
RC Network Reduction Using Pole Analysis via Congruence Transformations (PACT)

The algorithm called "Pole Analysis via Congruence Transformations" (PACT) was created for the reduction of RC substrate networks [23][24][25][26]. Wemple and Yang [5] developed a technique to extract large 3-D mesh RC network models of the substrate from a VLSI layout. These models are used to simulate coupling between digital devices (which inject current into the substrate) and analog devices (which are sensitive to the substrate voltage fluctuations resulting from these currents) on the same chip. The networks are so large that the circuits containing substrate macromodels cannot be simulated by HSPICE [27], and they must be reduced before simulation. The motivation for PACT is that AWE is ill-conditioned, and the number of ports is large enough that MPVL and the Arnoldi technique are inefficient.

PACT places an absolute bound on error (without testing the reduced network against the original) and provides a guarantee of passivity (without synthesizing a reduced network and throwing away all negative elements) for general RC networks. The technique is not a Padé approximation as the low frequency poles of the network are retained rather than the low-order moments. The theorems and examples presented here are taken from [26].

5.1 Formulation

The RC networks are partitioned according to (3.6) as

$$\left(\begin{bmatrix} G_P & G_C^T \\ G_C & G_I \end{bmatrix} + s \begin{bmatrix} C_P & C_C^T \\ C_C & C_I \end{bmatrix} \right) \begin{bmatrix} x_P \\ x_I \end{bmatrix} = \begin{bmatrix} b_P \\ 0 \end{bmatrix}, \tag{5.1}$$

and have m ports and n internal nodes. Because there are no type 2 elements (inductors),

$$\mathbf{G} = \begin{bmatrix} \mathbf{G_P} & \mathbf{G_C}^T \\ \mathbf{G_C} & \mathbf{G_I} \end{bmatrix} = \mathbf{G}_1 \text{ and } \mathbf{C} = \begin{bmatrix} \mathbf{C_P} & \mathbf{C_C}^T \\ \mathbf{C_C} & \mathbf{C_I} \end{bmatrix} = \mathbf{C}_1, \tag{5.2}$$

and the network admittance matrices, as well as the diagonal partitions, are symmetric and nonnegative definite. These properties affect both the passivity and accuracy of the reduction as is shown in the subsequent sections. The matrix $\mathbf{G_I}$ is nonsingular if a DC path exists to all internal nodes, and, because the transforms presented in Section 4.4 can be used to eliminate the singular nodes before the network reduction is performed, it is assumed to be nonsingular. Two separate congruence transforms are used to reduce the size of the network. The first transformation zeros the connection conductance matrix so that the first two moments of $\mathbf{Y}(s)$ (slope and offset) at DC (i.e. expanded at $s = 0$) are preserved regardless of the selection of the poles of the network. The second transformation uses eigenvectors to diagonalize the internal susceptance matrix so that each pole is associated with a single internal node, and unwanted poles are dropped by cutting the corresponding internal nodes.

The first congruence transform, which is based on that presented in Section 4.1, converts the internal conductance matrix, $\mathbf{G_I}$, into the identity matrix and eliminates the connection conductance matrix, $\mathbf{G_C}$. From Theorem 4.2.3 of [7], the Cholesky factorization, $\mathbf{L}\mathbf{L}^T = \mathbf{G_I}$ ($\mathbf{L}$ is a lower triangular matrix and is not that defined in Chapter 2), exists because $\mathbf{G_I}$ is positive definite. The transform based on $\mathbf{L}$ is

$$\mathbf{X} = \begin{bmatrix} \mathbf{I} & \mathbf{0} \\ -\mathbf{G_I}^{-1}\mathbf{G_C} & \mathbf{L}^{-T} \end{bmatrix}, \tag{5.3}$$

and the corresponding transformation of the network is

$$\mathbf{G}' = \mathbf{X}^T\mathbf{G}\mathbf{X} = \begin{bmatrix} \mathbf{G_P} - \mathbf{G_C}^T\mathbf{A} & \mathbf{0} \\ \mathbf{0} & \mathbf{L}^{-1}\mathbf{G_I}\mathbf{L}^{-T} \end{bmatrix} = \begin{bmatrix} \mathbf{G_P}' & \mathbf{0} \\ \mathbf{0} & \mathbf{I} \end{bmatrix} \tag{5.4}$$

and

$$\mathbf{C}' = \mathbf{X}^T\mathbf{C}\mathbf{X} = \begin{bmatrix} \mathbf{C_P} - \mathbf{B}^T\mathbf{A} - \mathbf{A}^T\mathbf{C_C} & \mathbf{B}^T\mathbf{L}^{-T} \\ \mathbf{L}^{-1}\mathbf{B} & \mathbf{L}^{-1}\mathbf{C_I}\mathbf{L}^{-T} \end{bmatrix} = \begin{bmatrix} \mathbf{C_P}' & \mathbf{C_C}'^T \\ \mathbf{C_C}' & \mathbf{C_I}' \end{bmatrix}, \tag{5.5}$$

where $\mathbf{A} = \mathbf{G_I}^{-1}\mathbf{G_C}$ and $\mathbf{B} = \mathbf{C_C} - \mathbf{C_I}\mathbf{A}$, are intermediate variables. Equation (3.8) is rewritten

using the partitions of $\mathbf{G}'$ and $\mathbf{C}'$ as

$$\mathbf{Y}(s) = \mathbf{G_P}' + s\mathbf{C_P}' - s^2\mathbf{C_C}'^{\mathrm{T}}(\mathbf{I} + s\mathbf{C_I}')^{-1}\mathbf{C_C}', \tag{5.6}$$

and a straightforward, but tedious, substitution of variables shows that $\mathbf{Y}(s)$ in (5.6) is identical to that in (3.8). The right-most term in (5.6) contains the poles of the network at $s = -\lambda^{-1}$ where λ is an eigenvalue of $\mathbf{C_I}'$. Because it is multiplied by s^2, this term makes no contribution to the first two moments of $\mathbf{Y}(s)$.

The second transformation, which is based on that presented in Section 4.2, isolates and drops unwanted poles of the network. Since these poles occur where $(\mathbf{I}+s\mathbf{C_I}')$ is singular, they can be isolated by diagonalizing $\mathbf{C_I}'$ using the symmetric eigendecomposition, $\mathbf{C_I}' = \mathbf{U}\Lambda\mathbf{U}^{\mathrm{T}}$. The diagonal matrix, Λ, contains the eigenvalues of $\mathbf{C_I}'$, and $\mathbf{U}$ is the square matrix whose columns are the corresponding eigenvectors. The matrix $\mathbf{U}$ is orthonormal, meaning $\mathbf{U}^{\mathrm{T}}\mathbf{U} = \mathbf{I}$. The eigenvectors diagonalize $\mathbf{C_I}'$ through the transformations

$$\mathbf{G}'' = \begin{bmatrix} \mathbf{I} & \mathbf{0} \\ \mathbf{0} & \mathbf{U}^{\mathrm{T}} \end{bmatrix} \begin{bmatrix} \mathbf{G_P}' & \mathbf{0} \\ \mathbf{0} & \mathbf{I} \end{bmatrix} \begin{bmatrix} \mathbf{I} & \mathbf{0} \\ \mathbf{0} & \mathbf{U} \end{bmatrix} = \begin{bmatrix} \mathbf{G_P}' & \mathbf{0} \\ \mathbf{0} & \mathbf{U}^{\mathrm{T}}\mathbf{I}\mathbf{U} \end{bmatrix} = \begin{bmatrix} \mathbf{G_P}' & \mathbf{0} \\ \mathbf{0} & \mathbf{I} \end{bmatrix} \tag{5.7}$$

and

$$\mathbf{C}'' = \begin{bmatrix} \mathbf{I} & \mathbf{0} \\ \mathbf{0} & \mathbf{U}^{\mathrm{T}} \end{bmatrix} \begin{bmatrix} \mathbf{C_P}' & \mathbf{C_C}'^{\mathrm{T}} \\ \mathbf{C_C}' & \mathbf{C_I}' \end{bmatrix} \begin{bmatrix} \mathbf{I} & \mathbf{0} \\ \mathbf{0} & \mathbf{U} \end{bmatrix} = \begin{bmatrix} \mathbf{C_P}' & \mathbf{C_C}'^{\mathrm{T}}\mathbf{U} \\ \mathbf{U}^{\mathrm{T}}\mathbf{C_C}' & \mathbf{U}^{\mathrm{T}}\mathbf{C_I}'\mathbf{U} \end{bmatrix} = \begin{bmatrix} \mathbf{C_P}' & \mathbf{C_C}''^{\mathrm{T}} \\ \mathbf{C_C}'' & \mathbf{C_I}'' \end{bmatrix}, \tag{5.8}$$

so that $\mathbf{C_I}'' = \Lambda$ is the diagonal matrix containing the eigenvalues of $\mathbf{C_I}'$. The admittance $\mathbf{Y}(s)$ is preserved if $\mathbf{U}$ is square and nonsingular, and this is true when $\mathbf{U}$ contains the complete set of eigenvectors. Now that both internal matrices are diagonal, (5.6) can be written as

$$\mathbf{Y}(s) = \mathbf{G_P}' + s\mathbf{C_P}' - \frac{s^2\mathbf{r}_1^{\mathrm{T}}\mathbf{r}_1}{1+s\lambda_1} - \ldots - \frac{s^2\mathbf{r}_n^{\mathrm{T}}\mathbf{r}_n}{1+s\lambda_n}, \tag{5.9}$$

where $\mathbf{r}_i$ is the ith row of $\mathbf{C_C}''$ and λ_i is the ith diagonal of $\mathbf{C_I}''$.

The size of the network is reduced by dropping terms from (5.9) for which λ_i is less than some cutoff value, λ_c (Section 5.3 shows how an appropriate value for λ_c is selected to preserve the desired accuracy). Terms are dropped by eliminating rows and columns of $\mathbf{G}''$ and $\mathbf{C}''$, and these are removed by deleting the corresponding eigenvectors (columns) in $\mathbf{U}$ before the transformation given by (5.7) and (5.8) is performed. The benefit here is that a full eigendecomposition of $\mathbf{C_I}'$ is

not required — the eigendecomposition routine needs only to find those eigenvalues (and associated eigenvectors) greater than λ_c. When n is small, $\mathbf{C_I}'$ can be decomposed efficiently with standard symmetric real eigendecomposition techniques such as those provided by EISPACK [28]. When n is large, $\mathbf{C_I}'$ should be left as the product of sparse matrices $\mathbf{L^{-1}C_IL^{-T}}$, and a sparse eigenvalue technique, such as those reviewed in [7], should be used. PACT can use any algorithm to perform the decomposition because that tool is used as a "black box" which is simply passed the matrix $\mathbf{C_I}'$ and the range of eigenvalues to be found. However, a poor choice could result in an inaccurate or inefficient system.

In this implementation of PACT, the Lanczos Algorithm with Selective Orthogonalization (LASO) [29] is used when n is large. The technique has a simple interface, requires no modification of the matrix being analyzed, returns eigenvectors as well as eigenvalues, and finds only those (large) eigenvalues in a specified range. In addition, the technique avoids loss of orthogonality in the Lanczos vectors which slows convergence of the less dominant eigenvalues and creates "ghosts" of the dominant eigenvalues. Furthermore, LASO allows closely spaced or multiple occurrences of eigenvalues to be found, and it avoids breakdown, which is the failure to identify an eigenvalue because the associated eigenvector is orthogonal to the random seed vector that is used to start the Lanczos iteration.

5.2 Preservation of Passivity

Because the RC network admittance matrices are symmetric nonnegative definite, and PACT uses congruence transformations to reduce the network, the reduced network matrices are also symmetric nonnegative definite as shown by Theorem 4.1. Theorem 5.1, given below, shows that a necessary and sufficient condition for RC networks to be passive is that the conductance and susceptance matrices representing the networks be nonnegative definite. As a result, *any passive RC network which is reduced by congruence transformations remains passive (and thus absolutely stable).*

Theorem 5.1. A necessary and sufficient condition for RC networks to be passive is that the conductance and susceptance matrices representing the networks be nonnegative definite.

Proof: Let the admittance of an arbitrary RC network can be represented by (3.6), and let $s = \sigma + j\omega$ be complex frequency where σ and ω are real, and $j = \sqrt{-1}$. The theorem is proven by

showing that the admittance of the network, $\mathbf{W}(s) = (\mathbf{G} + s\mathbf{C})$, is positive real (and therefore passive) if the admittance matrices are nonnegative definite, and by showing that $\mathbf{W}(s)$ is not positive real if one of the admittance matrices is indefinite. Necessary and sufficient conditions for $\mathbf{W}(s)$ to be positive real are [30]:

1. Each element of $\mathbf{W}(s)$ is analytic (no poles) for $\sigma > 0$.
2. $\mathbf{W}(s^*) = \mathbf{W}^*(s)$ where * is the complex conjugate operator.
3. $\mathbf{W}'(s) = \frac{1}{2}[\mathbf{W}^{\mathrm{T}}(s^*) + \mathbf{W}(s)] = \mathbf{G} + \sigma\mathbf{C}$ is a nonnegative definite matrix for $\sigma > 0$.

Requirements 1 and 2 are always met because $w_{kl}(s) = g_{kl} + sc_{kl}$, and g_{kl} and c_{kl} are real scalars. $\mathbf{W}'(s)$ is equal to the sum of two symmetric nonnegative definite matrices when $\sigma > 0$, and thus requirement 3 is met since such a sum is also symmetric and nonnegative definite. Sufficiency is proven.

Necessity can be shown by letting at least one eigenvalue of $\mathbf{G}$ or $\mathbf{C}$ be negative. If $\mathbf{G}$ contains a negative eigenvalue, then for sufficiently small σ, $\mathbf{W}'(s) \equiv \mathbf{G}$ has a negative eigenvalue, and requirement 3 is violated. In the same way, if $\mathbf{C}$ contains a negative eigenvalue, then $\mathbf{W}'(s)$ has a negative eigenvalue for sufficiently large σ, and requirement 3 is violated.

QED.

5.3 Preservation of Accuracy

Theorem 5.2 shows that if the terms associated with λ_i in (5.9) are dropped when $\lambda_i < \lambda_c$, the relative error of each of the individual elements of $\mathbf{Y}(s)$ is bounded on the imaginary axis for $|\omega| \le \omega_c$ by $\varepsilon \le \varepsilon_c$ if

$$\varepsilon_c = \omega_c\lambda_c + \omega_c^3\lambda_c^3. \tag{5.10}$$

Here, ε is defined as the maximum error in any term of $\mathbf{Y}(j\omega)$ relative to the average of the diagonals of $\mathbf{Y}(j\omega)$ which are in the same row and column (i.e. the error in the lth row and kth column is divided by the average of the lth and kth diagonals). The value of λ_c is determined by inserting the user-specified error, ε_c, and maximum frequency, ω_c, in (5.10). The analysis of the theorem relies on the fact that the conductance and susceptance matrices are nonnegative definite.

Theorem 5.2. If all terms associated with $\lambda_i < \lambda_c$ are dropped from Equation (5.9) to form the reduced multiport admittance $\tilde{\mathbf{Y}}(s)$, the relative error of each of the individual terms of the

admittance is bounded by

$$\varepsilon \le \omega_c \lambda_c + \omega_c^3 \lambda_c^3 \tag{5.11}$$

where the relative error is defined as

$$\varepsilon = \max_{k,\, l = [1 \ldots m],\, \omega = [-\omega_c \ldots \omega_c]} \left(\frac{\left| \mathbf{Y}_{kl}(j\omega) - \tilde{\mathbf{Y}}_{kl}(j\omega) \right|}{\frac{1}{2} \left| \mathbf{Y}_{kk}(j\omega) + \mathbf{Y}_{ll}(j\omega) \right|} \right) \tag{5.12}$$

and where k and l are indices to the individual terms of $\mathbf{Y}(s)$, ω *is frequency on the* $j\omega$ *axis, and* $\omega_c > 0$.

Proof: The theorem can be proven true for two reasons. The first is that the residues associated with dropped poles in (5.9) cannot be arbitrarily large because the susceptance matrix is nonnegative definite, and the second is that all of the diagonal values of conductance and susceptance matrices are greater than or equal to zero.

Because $\mathbf{C}^{\sim}$ given by (5.8) is nonnegative definite, the matrix

$$\mathbf{B} = \mathbf{C_P}' - \sum_{i=1}^{n} \frac{\mathbf{r}_i^{\mathrm{T}} \mathbf{r}_i}{\lambda_i} \tag{5.13}$$

is nonnegative definite where $\mathbf{r}_i$ is the ith row of $\mathbf{C_C}^{\sim}$ and λ_i is the ith diagonal of $\mathbf{C_I}^{\sim}$ (refer to the proof of Theorem 4.2.6 in [7]). It is assumed that the internal nodes are permuted so that $\lambda_i \ge \lambda_{i+1}$. Equation (5.9) can be rewritten by using (5.13) to substitute for $\mathbf{C_P}'$ as

$$\mathbf{Y}(s) = \mathbf{G_P}' + s\mathbf{B} + s \sum_{i=1}^{n} \mathbf{r}_i^{\mathrm{T}} \mathbf{r}_i \left(\frac{1}{\lambda_i} - \frac{s}{1 + s\lambda_i} \right), \tag{5.14}$$

and the reduced response is given by

$$\tilde{\mathbf{Y}}(s) = \mathbf{G_P}' + s\mathbf{B} + s \sum_{i=1}^{n'} \mathbf{r}_i^{\mathrm{T}} \mathbf{r}_i \left(\frac{1}{\lambda_i} - \frac{s}{1 + s\lambda_i} \right) + s \sum_{i=n'+1}^{n} \mathbf{r}_i^{\mathrm{T}} \mathbf{r}_i \cdot \frac{1}{\lambda_i} \tag{5.15}$$

where $\lambda_i > \lambda_c$ for $i = 1 \ldots n'$ and $\lambda_i \le \lambda_c$ for $i = n'+1 \ldots n$.

Using (5.14) and (5.15), the numerator of (5.12) is

$$\left| \mathbf{Y}_{kl}(j\omega) - \tilde{\mathbf{Y}}_{kl}(j\omega) \right| = \omega^2 \left| \sum_{i=n'+1}^{n} r_{ik} r_{il} \cdot \frac{1}{1 + j\omega\lambda_i} \right|, \tag{5.16}$$

where r_{ik} is the kth column of $\mathbf{r}_i$, and therefore

$$\left|\mathbf{Y}_{kl}(j\omega) - \tilde{\mathbf{Y}}_{kl}(j\omega)\right| \le \omega^2 \sum_{i=n'+1}^{n} \left|r_{ik}r_{il}\right| \cdot \left|\frac{1}{1+j\omega\lambda_i}\right|. \tag{5.17}$$

The right most term in (5.17) is less than or equal to one so that

$$\left|\mathbf{Y}_{kl}(j\omega) - \tilde{\mathbf{Y}}_{kl}(j\omega)\right| \le \omega^2 \sum_{i=n'+1}^{n} \left|r_{ik}r_{il}\right|. \tag{5.18}$$

Using (5.14), the denominator of (5.12) is

$$\frac{1}{2}\left|\mathbf{Y}_{kk}(j\omega) + \mathbf{Y}_{ll}(j\omega)\right| = \frac{1}{2}\left|g_{kk} + g_{ll} + j\omega\,(b_{kk} + b_{ll}) + \sum_{i=1}^{n}\left(r_{ik}^2 + r_{il}^2\right)\frac{\omega^2\lambda_i + j\omega}{\lambda_i\left(1+\omega^2\lambda_i^2\right)}\right|. \tag{5.19}$$

Because the matrices in (5.7), (5.8) and (5.13) are nonnegative definite, the scalars g_{kk}, g_{ll}, b_{kk}, b_{ll}, and λ_i are nonnegative so that

$$\frac{1}{2}\left|\mathbf{Y}_{kk}(j\omega) + \mathbf{Y}_{ll}(j\omega)\right| \ge \frac{1}{2}\left|\sum_{i=n'+1}^{n}\left(r_{ik}^2 + r_{il}^2\right)\frac{\omega^2\lambda_i + j\omega}{\lambda_i\left(1+\omega^2\lambda_i^2\right)}\right|. \tag{5.20}$$

Dropping the real term in the numerator further decreases the size of the right side of the equation to give

$$\frac{1}{2}\left|\mathbf{Y}_{kk}(j\omega) + \mathbf{Y}_{ll}(j\omega)\right| \ge \frac{1}{2}\left|\sum_{i=n'+1}^{n}\left(r_{ik}^2 + r_{il}^2\right)\frac{|\omega|}{\lambda_i\left(1+\omega^2\lambda_i^2\right)}\right|, \tag{5.21}$$

and because $\lambda_i \le \lambda_c$, λ_i can be replaced by λ_c to give

$$\frac{1}{2}\left|\mathbf{Y}_{kk}(j\omega) + \mathbf{Y}_{ll}(j\omega)\right| \ge \frac{1}{2}\left|\sum_{i=n'+1}^{n}\left(r_{ik}^2 + r_{il}^2\right)\right| \cdot \frac{|\omega|}{\lambda_c\left(1+\omega^2\lambda_c^2\right)}. \tag{5.22}$$

Equations (5.18) and (5.22) are substituted back into (5.12) to show the bound

$$\varepsilon \le \frac{2\sum_{i=n'+1}^{n}\left|r_{ik}r_{il}\right|}{\left|\sum_{i=n'+1}^{n}\left(r_{ik}^2 + r_{il}^2\right)\right|} \cdot |\omega|\lambda_c\left(1+\omega^2\lambda_c^2\right). \tag{5.23}$$

Because

$$r_{ik}^2 + r_{il}^2 \ge 2\left|r_{ik}r_{il}\right|, \tag{5.24}$$

the ratio of the two summations is less than one, and (5.23) reduces to

$$\varepsilon \le |\omega|\lambda_c + |\omega^3|\lambda_c^3. \tag{5.25}$$

Finally, the right hand side of (5.25) is a monotonically increasing function of the frequency, so that (5.11) is true for any $|\omega| \le \omega_c$.

QED.

5.4 Substrate Mesh Reduction Example

This example shows the reduction of a 3-D RC mesh used to simulate voltage fluctuations in the substrate which result from current injected by switching activity in a nearby CMOS one-bit full adder. The adder contains 22 MOSFETs, and each body terminal node is a port of the substrate macromodel. Two port nodes are also used for the Vdd and Vss well and substrate contacts, and an additional node is included to monitor the substrate voltage at a point near the adder. Therefore, the total number of port nodes is 25. The total number of transistors in the circuit is 28 as the three inputs to the adder are driven by separate CMOS inverters.

Fig. 5.1 shows the results of an HSPICE transient simulation of the one-bit full adder circuit. Substrate voltage fluctuations are compared for simulations with the original substrate mesh and with the reduced mesh using $\omega_c^{-1} = 1$ ns and $\varepsilon_c = 5\%$. As can be seen, the reduced network gives a very good approximation to the behavior of the original network. Table 5.1 provides statistics on

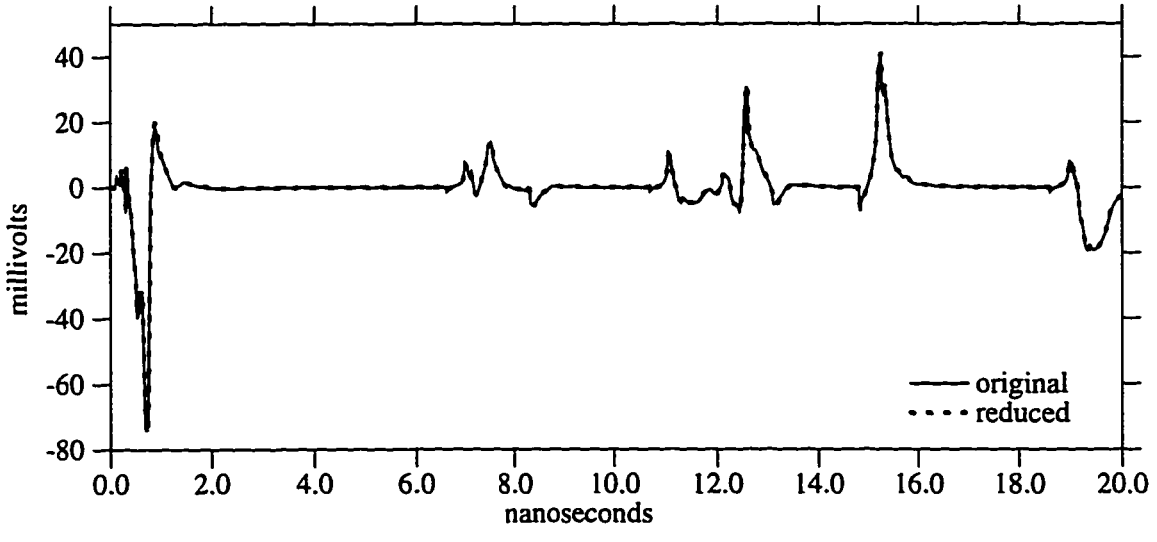

Figure 5.1. Simulation of substrate voltage fluctuations resulting from activity in a one-bit full adder.

Table 5.1. Reduction and transient simulation statistics of the one-bit full adder circuit.

Substrate Network	Total Nodes	Total Elements	RCFIT Reduction		HSPICE Simulation	
			Time (sec)	Memory (Mb)	Time (sec)	Memory (Mb)
original	1540	5256	—	—	12511.6	44.9
reduced, 1 ns	41	431	6.2	1.4	40.0	0.4

the reduction and simulation of the network, and shows that use of the reduced network speeds the simulation by a factor exceeding 300 while reducing the memory required by two orders of magnitude.

Chapter 6
Preservation of Passivity Using Split Congruence Transformations

Congruence transformations preserve passivity in RC networks, as is shown in Section 5.2, because the network admittance matrices, **G** and **C**, are symmetric and nonnegative definite. Unfortunately, the introduction of type 2 elements (inductors) causes a loss of definiteness, because the type 2 blocks are nonpositive definite as is shown in Section 3.1. As a result, congruence transformations do not generally preserve passivity, or even asymptotic stability. This chapter provides a class of congruence transformations call "Split Congruence Transformations" (SCT's) which preserve passivity, by preserving the "passive form" of the network. Split versions of the transforms given in Chapter 4 are provided which zero the connection matrices, preserve moments and poles, and eliminate DC singularities. It is shown that the transforms used in the previous chapter for RC networks are a special case of SCT's. Examples of network reduction using the SCT's provided in this chapter are given in the Chapter 7.

6.1 The Passive Form of an RLC Network

RC networks (with positive elements) can be shown to be passive because the network matrices are symmetric nonnegative definite as is shown in Theorem 5.1. This theorem does not apply to RLC networks, because these contain type 2 elements which form a nonpositive definite type 2 block. If it is assumed that only the type 1 nodes of the network can be externally excited (which is consistent with MNA), then an alternate set of conditions can be used which are sufficient, but not necessary, for passivity through the ports. A network is said to be in *passive form* when it meets the conditions given in Theorem 6.1. As is shown in Section 3.1, *all RLC networks which contain only positive elements and inductive coupling coefficients of magnitude less than or equal to 1, meet the conditions of Theorem 6.1, and thus are in passive form.*

Theorem 6.1. Conditions sufficient for a network to be passive are:

1) The type 1 conductance and susceptance matrices are symmetric nonnegative definite.

2) The type 2 conductance and susceptance matrices are symmetric nonpositive definite.

3) The susceptance matrices which connect type 1 to type 2 elements is zero.

4) The type 2 ports are not excitable.

Proof: A partitioning of the MNA network matrix into type 1 and type 2 elements can be formed as

$$\left(\begin{bmatrix} \mathbf{G}_1 & \mathbf{G}_3^{\mathrm{T}} \\ \mathbf{G}_3 & \mathbf{G}_2 \end{bmatrix} + s \begin{bmatrix} \mathbf{C}_1 & \mathbf{0} \\ \mathbf{0} & \mathbf{C}_2 \end{bmatrix} \right) \begin{bmatrix} \mathbf{x}_1 \\ \mathbf{x}_2 \end{bmatrix} = \begin{bmatrix} \mathbf{b}_1 \\ \mathbf{0} \end{bmatrix} \tag{6.1}$$

as is shown in Section 3.1. Here, $\mathbf{x}_1$ represents the n_1 nodal voltages, and $\mathbf{x}_2$ represents the n_2 branch currents flowing through the type 2 elements. The second partition of $\mathbf{b}$ is zero by definition, as the voltage across inductive elements and resistors comes solely from the current through these elements, and not from outside sources.

Because the second partition of $\mathbf{b}$ is zero, the second row of (6.1) can be multiplied by -1 without changing the voltage-current relationship at the n_1 network nodes to give

$$\left(\underbrace{\begin{bmatrix} \mathbf{G}_1 & \mathbf{G}_3^{\mathrm{T}} \\ -\mathbf{G}_3 & -\mathbf{G}_2 \end{bmatrix}}_{\tilde{\mathbf{G}}} + s \underbrace{\begin{bmatrix} \mathbf{C}_1 & \mathbf{0} \\ \mathbf{0} & -\mathbf{C}_2 \end{bmatrix}}_{\tilde{\mathbf{C}}} \right) \begin{bmatrix} \mathbf{x}_1 \\ \mathbf{x}_2 \end{bmatrix} = \begin{bmatrix} \mathbf{b}_1 \\ \mathbf{0} \end{bmatrix}. \tag{6.2}$$

The conditions from Theorem 5.1 are now applied to $\mathbf{W}(s) = \tilde{\mathbf{G}} + s\tilde{\mathbf{C}}$. Necessary and sufficient conditions for $\mathbf{W}(s)$ to be positive real are [30]:

1. Each element of $\mathbf{W}(s)$ is analytic (no poles) for $\mathrm{Re}(s) > 0$.
2. $\mathbf{W}(s^*) = \mathbf{W}^*(s)$ where * is the complex conjugate operator.
3. $\mathbf{W}'(s) = \frac{1}{2}[\mathbf{W}^{\mathrm{T}}(s^*) + \mathbf{W}(s)]$ is a nonnegative definite matrix for $\mathrm{Re}(s) > 0$.

Requirements 1 and 2 are always met because $w_{kl}(s) = g_{kl} + sc_{kl}$, and g_{kl} and c_{kl} are real scalars. To show requirement 3, let $s = \sigma + j\omega$ be complex frequency where σ and ω are real, and $j = \sqrt{-1}$. Because the diagonal blocks of both matrices are symmetric and the off-diagonal blocks of the susceptance matrix are zero,

$$\mathbf{W}'(s) = \begin{bmatrix} \mathbf{G}_1 & \mathbf{0} \\ \mathbf{0} & -\mathbf{G}_2 \end{bmatrix} + \sigma \begin{bmatrix} \mathbf{C}_1 & \mathbf{0} \\ \mathbf{0} & -\mathbf{C}_2 \end{bmatrix} \tag{6.3}$$

Since the type 1 blocks are nonnegative definite, the type 2 blocks are nonpositive definite, and $\sigma \geq 0$, then $\mathbf{W}'(s)$ is the sum of two symmetric nonnegative definite matrices, and such a sum is also symmetric nonnegative definite. All three requirements are met, and the network is passive. QED.

6.2 Preservation of the Passive Form

The passivity of the reduced networks can be ensured by preserving the passive form during the network reduction transformations, and Theorem 6.2 presents a class of congruence transforms which preserve the passive form. These are referred to as "Split Congruence Transforms" because they are split into type 1 and type 2 diagonal blocks (i.e. there are no nonzero elements in the off-diagonal blocks between the type 1 and type 2 partitions of the transform). The transforms used in Chapter 5 are a special case of SCT's because the dimension of the type 2 partition of RC networks is zero. As a result, all of the transforms are implicitly "split" into type 1 and type 2 parts, since the entire transform is partitioned into a type 1 block. The requirements for splitting the transforms can be combined with the span requirements presented in Chapter 4 in order to provide transformations which perform a number of different types of network reduction operations. Split versions of these transforms are given in the following sections.

Theorem 6.2. If a congruence transform is applied to an RLC network of the form specified by Theorem 6.1, and the transform has zeros in the off-diagonal elements which correspond to connections between the type 1 and type 2 nodes, the resulting network is passive.

Proof: Given a network of the form in (6.1), the corresponding transformation of this system is

$$\mathbf{G}' = \mathbf{X}^{\mathrm{T}}\mathbf{G}\mathbf{X} = \begin{bmatrix} \mathbf{X}_1^{\mathrm{T}} & \mathbf{0} \\ \mathbf{0} & \mathbf{X}_2^{\mathrm{T}} \end{bmatrix} \begin{bmatrix} \mathbf{G}_1 & \mathbf{G}_3^{\mathrm{T}} \\ \mathbf{G}_3 & \mathbf{G}_2 \end{bmatrix} \begin{bmatrix} \mathbf{X}_1 & \mathbf{0} \\ \mathbf{0} & \mathbf{X}_2 \end{bmatrix} = \begin{bmatrix} \mathbf{X}_1^{\mathrm{T}}\mathbf{G}_1\mathbf{X}_1 & \mathbf{X}_2^{\mathrm{T}}\mathbf{G}_3^{\mathrm{T}}\mathbf{X}_1 \\ \mathbf{X}_1^{\mathrm{T}}\mathbf{G}_3\mathbf{X}_2 & \mathbf{X}_2^{\mathrm{T}}\mathbf{G}_2\mathbf{X}_2 \end{bmatrix} \tag{6.4}$$

and

$$C' = X^T C X = \begin{bmatrix} X_1^T & 0 \\ 0 & X_2^T \end{bmatrix} \begin{bmatrix} C_1 & 0 \\ 0 & C_2 \end{bmatrix} \begin{bmatrix} X_1 & 0 \\ 0 & X_2 \end{bmatrix} = \begin{bmatrix} X_1^T C_1 X_1 & 0 \\ 0 & X_2^T C_2 X_2 \end{bmatrix}. \tag{6.5}$$

Because the diagonal type 1 and type 2 blocks are symmetric nonnegative and symmetric nonpositive definite respectively, Theorem 4.1 shows that the corresponding blocks of the reduced network are also symmetric and semidefinite. In addition, the off-diagonal blocks of the transformed susceptance matrix are zero, and from Theorem 6.1, these conditions are sufficient to ensure the passivity of the transformed network.

QED.

6.3 Zeroing Connection Matrices Using Split Congruence Transforms

It can be shown that the transform presented in Section 4.1 to zero the susceptance connection matrix is a split transform. That which zeros the conductance connection matrix is not split for general RLC networks because the type 2 portion of the matrix in (4.7) is not necessarily zero, but it can be shown that it is split for LC networks.

To show that the transform to zero C_C is split, it is noted that the type 2 connection susceptance is zero and the internal susceptance matrix is block diagonal. Therefore, the type 2 portion of the matrix in (4.9) is zero, and (4.4) can be written in split form as

$$X = \left[\begin{array}{cc:c} I & 0 & 0 \\ -C_{I1}^{-1} C_{C1} & I & 0 \\ \hdashline 0 & 0 & I \end{array}\right]. \tag{6.6}$$

The dotted lines separate the type 1 (upper left) and type 2 (low right) portions of the network.

The transform to zero G_C in LC networks is split because there are no resistors. As a result, the diagonal blocks of the internal conductance matrix are zero, and its partition into type 1 and type 2 parts from (3.5) is

$$G_I = \begin{bmatrix} 0 & G_{I3}^T \\ G_{I3} & 0 \end{bmatrix}. \tag{6.7}$$

Likewise the partition of the connection conductance matrix is

$$\mathbf{G_C} = \begin{bmatrix} \mathbf{0} \\ \mathbf{G_{C2}} \end{bmatrix}. \tag{6.8}$$

As a result, (4.4) and (4.7) can be written in split form as

$$\mathbf{X} = \left[\begin{array}{cc:c} \mathbf{I} & \mathbf{0} & \mathbf{0} \\ -\mathbf{G_{I3}^{-1}G_{C2}} & \mathbf{I} & \mathbf{0} \\ \hdashline \mathbf{0} & \mathbf{0} & \mathbf{I} \end{array}\right]. \tag{6.9}$$

6.4 Preservation of Poles and Moments Using Split Congruence Transforms

Selected poles and moments of a general RLC network can be preserved during network reduction by using SCT's. For a general RLC network, the transforms presented in Sections 4.2 and 4.3 can be explicitly split into SCT's. The impact of this splitting is that the resulting transform has more columns than does the non-split transform, and the reduced network is larger. The transforms of LC networks are naturally split so no extra columns need to be added to preserve passivity.

To show how a general RLC transform is split, let the matrix $\mathbf{V}$ contain a span which is sufficient to preserve a desired set of poles and moments of the multiport admittance as is presented in Sections 4.2 and 4.3. This matrix can be partitioned into type 1 and type 2 parts as

$$\mathbf{V} = \begin{bmatrix} \mathbf{V}_1 \\ \mathbf{V}_2 \end{bmatrix}. \tag{6.10}$$

Given the matrix

$$\tilde{\mathbf{V}} = \begin{bmatrix} \tilde{\mathbf{V}}_1 & \mathbf{0} \\ \mathbf{0} & \tilde{\mathbf{V}}_2 \end{bmatrix}, \tag{6.11}$$

if

$$\text{span}\,(\mathbf{V}_1) \subseteq \text{span}\,(\tilde{\mathbf{V}}_1) \text{ and } \text{span}\,(\mathbf{V}_2) \subseteq \text{span}\,(\tilde{\mathbf{V}}_2) \tag{6.12}$$

then

$$\text{span}\,(\mathbf{V}) \subseteq \text{span}\,(\tilde{\mathbf{V}})\,, \tag{6.13}$$

and the split congruence transform

$$\mathbf{X} = \left[\begin{array}{c:c:c} \mathbf{I} & \mathbf{0} & \mathbf{0} \\ \hdashline \mathbf{0} & \tilde{\mathbf{V}}_1 & \mathbf{0} \\ \hdashline \mathbf{0} & \mathbf{0} & \tilde{\mathbf{V}}_2 \end{array}\right] \tag{6.14}$$

preserves the desired set of admittance poles and moments. The matrices, $\tilde{\mathbf{V}}_1$ and $\tilde{\mathbf{V}}_2$, can be built from orthonormal bases of $\mathbf{V}_1$ and $\mathbf{V}_2$ using a technique, such as Gram-Schmidt orthonormalization, that ensures that the matrix columns are linearly independent so that (6.14) is well-conditioned.

The spans necessary to preserve selected poles and moments of LC networks are naturally split. The reason for this is that, because there are no resistors, the internal admittance matrices have the form

$$\mathbf{G}_I = \begin{bmatrix} \mathbf{0} & \mathbf{G}_{I3}^T \\ \mathbf{G}_{I3} & \mathbf{0} \end{bmatrix} \text{ and } \mathbf{C}_I = \begin{bmatrix} \mathbf{C}_{I1} & \mathbf{0} \\ \mathbf{0} & \mathbf{C}_2 \end{bmatrix} \tag{6.15}$$

where $\mathbf{C}_{I1}$ is symmetric nonnegative definite and $\mathbf{C}_2$ is symmetric nonpositive definite. To show that the span to preserve poles is split, Theorem 6.3 proves that the poles of the system are imaginary and occur in conjugate pairs and that the eigenvectors associated with the poles at $s = \pm j\omega$ can be written as the sum

$$\mathbf{x} = \begin{bmatrix} \mathbf{x}_1 \\ \mathbf{0} \end{bmatrix} \pm j \begin{bmatrix} \mathbf{0} \\ \mathbf{x}_2 \end{bmatrix}. \tag{6.16}$$

The vectors $\mathbf{x}_1$ and $\mathbf{x}_2$ are real and correspond to the type 1 and type 2 partitions of the internal matrix. The space which spans the two eigenvectors of the conjugate poles is

$$\begin{bmatrix} \mathbf{x}_1 & \mathbf{0} \\ \mathbf{0} & \mathbf{x}_2 \end{bmatrix}. \tag{6.17}$$

Therefore, the transform which includes this space is naturally split into type 1 and type 2 components. The span preserving the moments is split because the type 1 connection conductance is zero, and internal matrices have the form in (6.15). The inverse of $\mathbf{G}_I$ times $\mathbf{G}_C$ is therefore purely type 1. On following iterations, it is easy to see that the span requirement swaps between having the type 1 and 2 components equal to zero.

Theorem 6.3. Given

$$\begin{bmatrix} 0 & \mathbf{A}^T \\ \mathbf{A} & 0 \end{bmatrix} \begin{bmatrix} \mathbf{x}_1 \\ \mathbf{x}_2 \end{bmatrix} = \lambda \begin{bmatrix} \mathbf{B}_1 & 0 \\ 0 & -\mathbf{B}_2 \end{bmatrix} \begin{bmatrix} \mathbf{x}_1 \\ \mathbf{x}_2 \end{bmatrix} \tag{6.18}$$

where $\mathbf{B}_1$ and $\mathbf{B}_2$ are symmetric nonnegative definite, all solutions are of the form

$$\lambda = \pm j\omega \text{ and } \mathbf{x} = \begin{bmatrix} \mathbf{x}_1 \\ \pm\mathbf{x}_2 \end{bmatrix} \tag{6.19}$$

where ω and $\mathbf{x}_1$ are real, and $\mathbf{x}_2$ is imaginary.

Proof: For simplicity, it is assumed that $\mathbf{B}_2$ is nonsingular. Two separate equations can be written from (6.18)

$$\mathbf{A}^T\mathbf{x}_2 = \lambda\mathbf{B}_1\mathbf{x}_1 \tag{6.20}$$

and

$$\mathbf{A}\mathbf{x}_1 = -\lambda\mathbf{B}_2\mathbf{x}_2 . \tag{6.21}$$

Since $\mathbf{B}_2$ is nonsingular, (6.21) gives

$$\mathbf{x}_2 = -\lambda^{-1}\mathbf{B}_2^{-1}\mathbf{A}\mathbf{x}_1 . \tag{6.22}$$

Substitution of (6.22) into (6.20) gives

$$\mathbf{A}^T\mathbf{B}_2^{-1}\mathbf{A}\mathbf{x}_1 = -\lambda^2\mathbf{B}_1\mathbf{x}_1 . \tag{6.23}$$

Equation (6.23) forms the generalized eigenvalue problem where both matrices are symmetric semidefinite and at least one is nonsingular. From Theorem 8.7.1 of [7], the solution to λ^2 is real and negative, and the vector $\mathbf{x}_1$ is real. From this,

$$\lambda = \pm j\omega . \tag{6.24}$$

Insertion of (6.24) into (6.20) or (6.21) shows that $\mathbf{x}_2$ is imaginary, and its sign depends on the sign of λ. The conditions of (6.19) are satisfied.

If $\mathbf{B}_2$ is singular, then a similar proof can be made which inverts $\mathbf{B}_1$. If this matrix is singular as well, then a more complicated proof can be made by eliminating the singularities in $\mathbf{A}$ in (6.18) via congruence transforms, and inverting the nonsingular matrix which results.

QED.

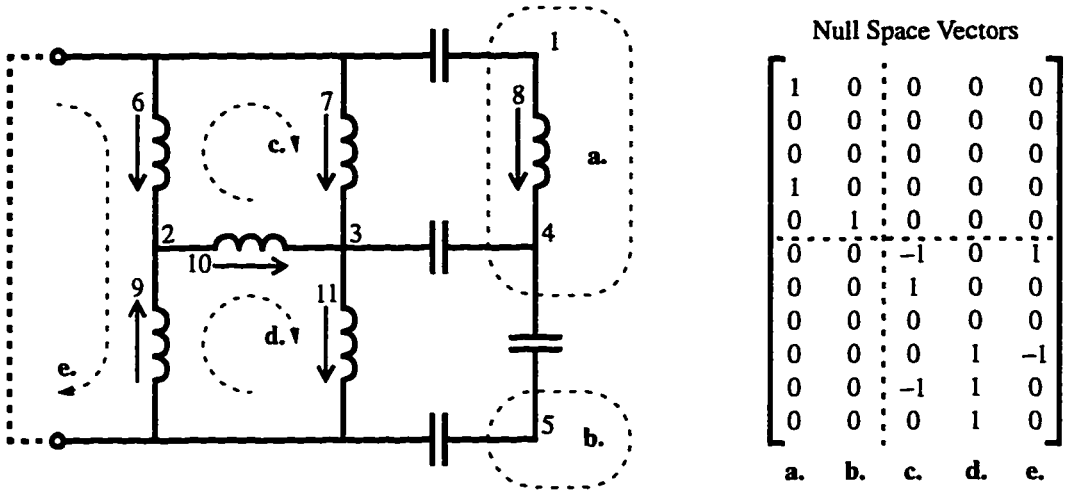

Figure 6.1. Relationship between null space vectors of the internal conductance matrix and the network topology in a simple one-port network. Nodes 1...5 are internal voltage nodes, and 6...11 are inductor branch currents. The solid arrows define the direction of positive current flow through the inductors. Vectors a and b are type 1 vectors which result from internal nodes which are DC isolated from the port nodes. Vectors c, d, and e are type two vectors which result from the three independent singular current loops through the inductors. The dotted lines in the null space vectors separate the type 1 and type 2 variables.

6.5 Elimination of DC Singularities Using Split Congruence Transforms

The transforms presented in Section 4.4 can be split into type 1 and type 2 blocks because the null space of the internal conductance matrix is naturally split. The reason for this is that there is a direct physical relationship between the null space vectors of the internal conductance matrix and the topology of the network. The null space is defined as type 1 or type 2 depending on which set of state variables is singular. A type 1 null space vector exists for each DC-connected group of internal voltage nodes which is DC-isolated from the port nodes (including the common node). These nodes can sustain a nonzero voltage when there are zero inputs to the ports, and by definition, these make the multiport admittance of the network singular. An example of this is shown by vectors a and b of Fig. 6.1. A type 2 null space vector exists for each independent DC current loop formed by the inductors when the port nodes are shorted together. These inductors can sustain a current at DC even when no node of the network has a nonzero voltage, and by definition these make the multiport admittance of the network singular. An example of type 2 null space vectors is given by vectors c, d, and e in Fig. 6.1.

Because the null space vectors can be split, the congruence transform used in (4.44) can be split as

$$\mathbf{X} = \left[\begin{array}{ccc:cc} \mathbf{I} & \mathbf{0} & \mathbf{0} & \mathbf{0} & \mathbf{0} \\ \mathbf{0} & \mathbf{X}_{S1} & \mathbf{X}_{N1} & \mathbf{0} & \mathbf{0} \\ \hdashline \mathbf{0} & \mathbf{0} & \mathbf{0} & \mathbf{X}_{S2} & \mathbf{X}_{N2} \end{array}\right] \tag{6.25}$$

where the subscripts "1" and "2" indicate the type 1 and type 2 partitions from the type 1 and type 2 null and spanning spaces. As a result, the network shown in (4.45) and (4.46) can be written in passive form. The transform used in (4.47) can also be split because the type 1 and type 2 internal susceptance matrices are block diagonal and because the type 2 susceptance connection matrix is zero. Partitioning the internal and connection matrices into type 1 and type 2 blocks results in the split transform

$$\mathbf{X} = \left[\begin{array}{ccc:cc} \mathbf{I} & \mathbf{0} & \mathbf{0} & \mathbf{0} & \mathbf{0} \\ \mathbf{0} & \mathbf{I} & \mathbf{0} & \mathbf{0} & \mathbf{0} \\ -\mathbf{C}_{INN1}^{-1}\mathbf{C}_{CN1} & -\mathbf{C}_{INN1}^{-1}\mathbf{C}_{INS1} & \mathbf{I} & \mathbf{0} & \mathbf{0} \\ \hdashline \mathbf{0} & \mathbf{0} & \mathbf{0} & \mathbf{I} & \mathbf{0} \\ \mathbf{0} & \mathbf{0} & \mathbf{0} & -\mathbf{C}_{INN2}^{-1}\mathbf{C}_{INS2} & \mathbf{I} \end{array}\right] \tag{6.26}$$

which isolates the susceptance blocks which correspond to singular nodes in the conductance matrices. Therefore, the final network shown in (4.50) and (4.51) can be written in passive form.

The SCT's given in this chapter can be used to reduce general RLC networks while preserving passivity. Examples of passive network reduction using these transforms are provided in Chapter 7.

Chapter 7
Examples of Network Reduction Using Split Congruence Transformations

Several examples of examples of RLC network reduction are provided which employ the SCT's introduced in Chapter 6. An LC network is reduced using both moment matching and pole analysis in Section 7.1, and a more general RLC network is reduced in Section 7.2. Section 7.3 shows sparse reduction of an industry network using a prototype reduction tool based on SCT's. All simulations are performed using HSPICE [27] on a SUN SPARC 20 workstation, and network reductions in the first two examples are implemented in MATLAB [31].

7.1 LC Network Reduction Using DC Moment Matching and Pole Analysis

In this example, an ideal 50 Ω lossless transmission line is modeled by the 100 segment LC ladder shown in Fig. 7.1, and the LC network inside of the dotted lines is reduced two separate times. The first reduction uses SCT's based on pole analysis, and second uses those based on moment matching. Because there is an inductive path between the input and output ports, the internal conductance matrix is singular, and the first step of the reduction is to remove the singularity using the transform presented in Section 6.5. Since the singularity is seen by the ports (there is an inductive path between Vin and Vout), it is added back to the reduced network at the end of the process. The transform given in Section 6.3 is used to zero the connection conductance matrix —

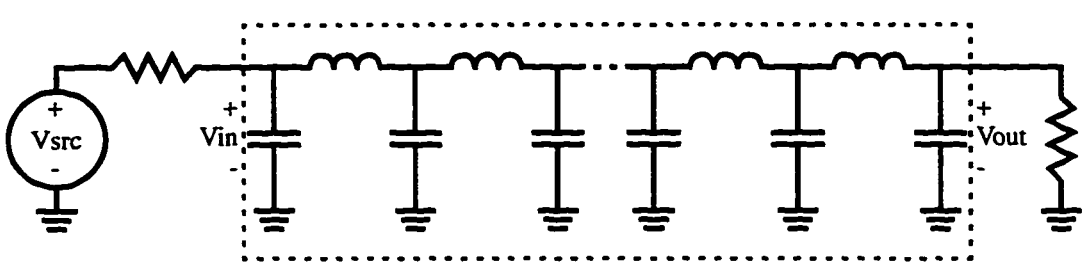

Figure 7.1. Lumped LC model of ideal transmission line using 100 segments. The total capacitance and inductance is 10 pF and 25 nH respectively, and the network is terminated at each end with 50 ohm resistors. The portion of the network inside the dotted lines is reduced.

this is always possible for LC networks.

Two different reductions are then performed. The first reduction finds the eigenvalues associated with the four pole pairs whose frequency is less than 4 GHz, and it creates a transform which spans these eigenvectors in order to preserve the poles according to Theorem 4.3. The second reduction generates a matrix which spans the Krylov subspace specified in Theorem 4.5 by using the Arnoldi process. As is discussed in Section 6.4, both the pole and moment matching transforms are naturally split for LC networks so the moment-matched network is a Padé approximation.

The sizes of the original and reduced networks are given in Table 7.1. The original network has 199 internal nodes (100 are current nodes for the inductors, and 99 are internal voltage nodes). The reduced networks are represented by symmetric admittance matrices, and in order to stamp these matrices into HSPICE, the set of resistors and capacitors is found which has admittance matrices identical to those of the reduced networks. The number of moments matched (10), and the number of pole pairs retained (4) are chosen so that the two reduced networks have the same number of internal nodes, and are thus of comparable accuracy.

The frequency response of the original and reduced networks to a unit input voltage is shown in Fig. 7.2. A properly terminated LC line has a flat frequency response of 0.5 volts for both Vin and Vout, and the reduced networks deviate from this ideal behavior between 3 and 4 GHz. The Padé approximation starts to deviate at a lower frequency, and the pole analysis has a larger deviation at higher frequencies.

The unit step response of the networks is shown in Fig. 7.3. For an ideal transmission line, Vin is a 0.5 volt step, and Vout is a delayed 0.5 volt step. There is some high frequency structure to the response of the original network since it is a lumped approximation and is not ideal. The lower frequency oscillations exhibited by the reduced networks have a dominant frequency component of 3 to 4 GHz which is the frequency at which the reduced networks begin to deviate from ideal.

Table 7.1. Network statistics for LC transmission line and its reduced equivalents.

Network	Ports	Internal Nodes	Network Elements
original	2	199	201
pole analysis (4 pole pairs)	2	9	36
Padé approximation (10 moments)	2	9	42

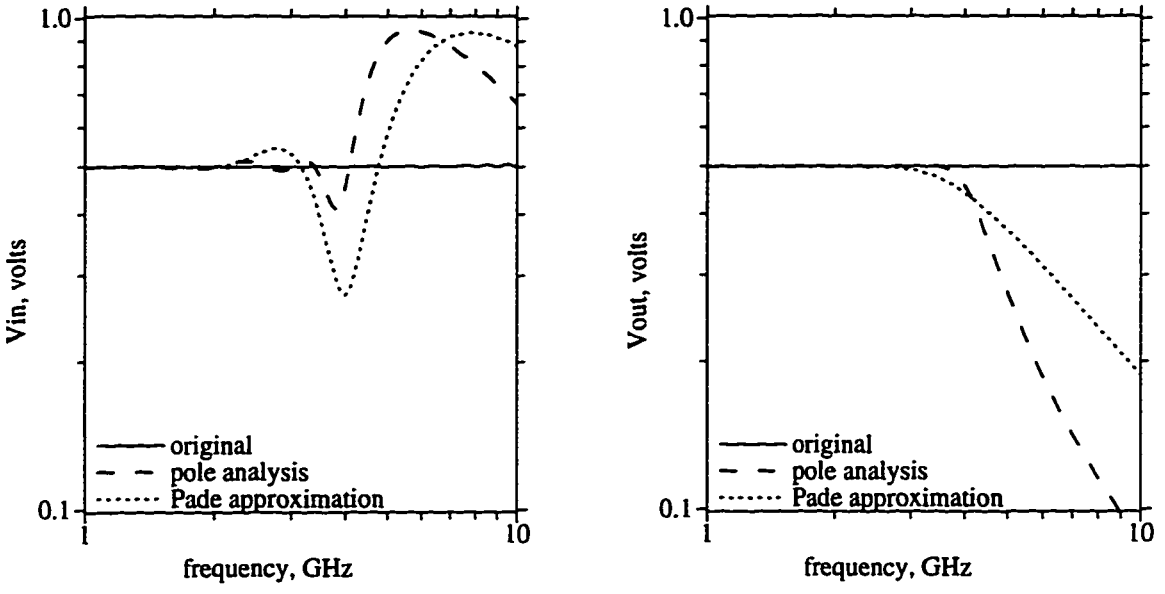

Figure 7.2. Frequency response of the circuit in Fig. 7.1 when Vsrc is a unit input voltage. The LC circuit is replaced by reduced networks based on pole analysis and Padé approximation.

If the input voltage, Vsrc, is limited in frequency (a realistic assumption for circuit simulation), then the reduced networks behave very much like the original. This is demonstrated in Fig. 7.4 which shows the network response when the unit step input is passed through a 3 GHz 4th-order Chebyshev low pass filter with a ripple factor of $\varepsilon = 0.51$ (taken from Example 2.9 in [32]). As can be seen, there is very little deviation between the response of the original and reduced net-

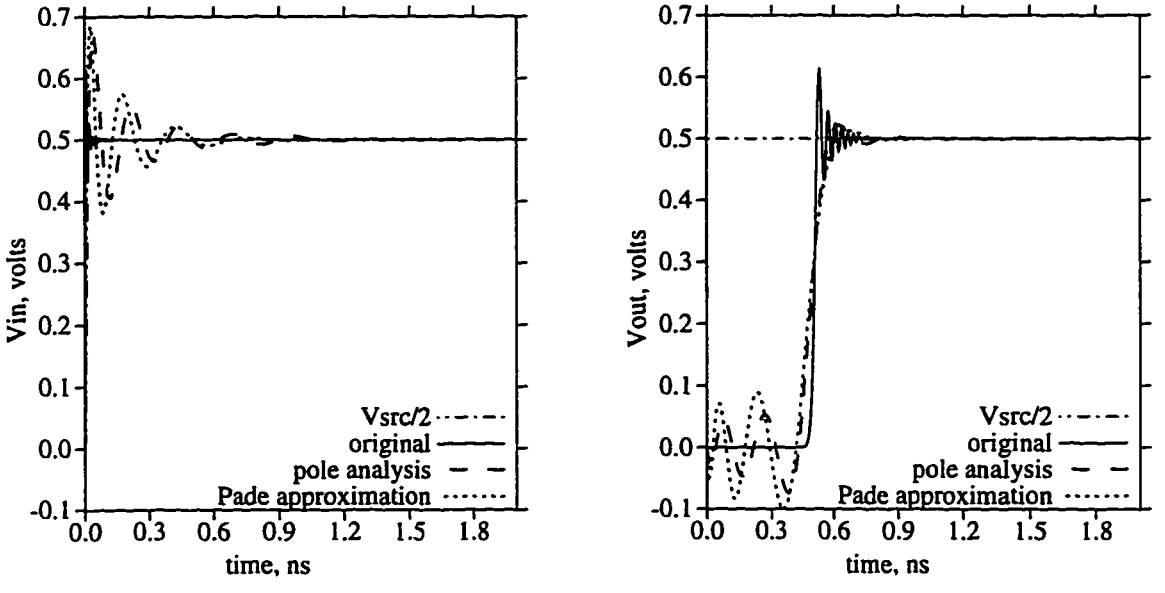

Figure 7.3. Unit step response of the network in Fig. 7.1.

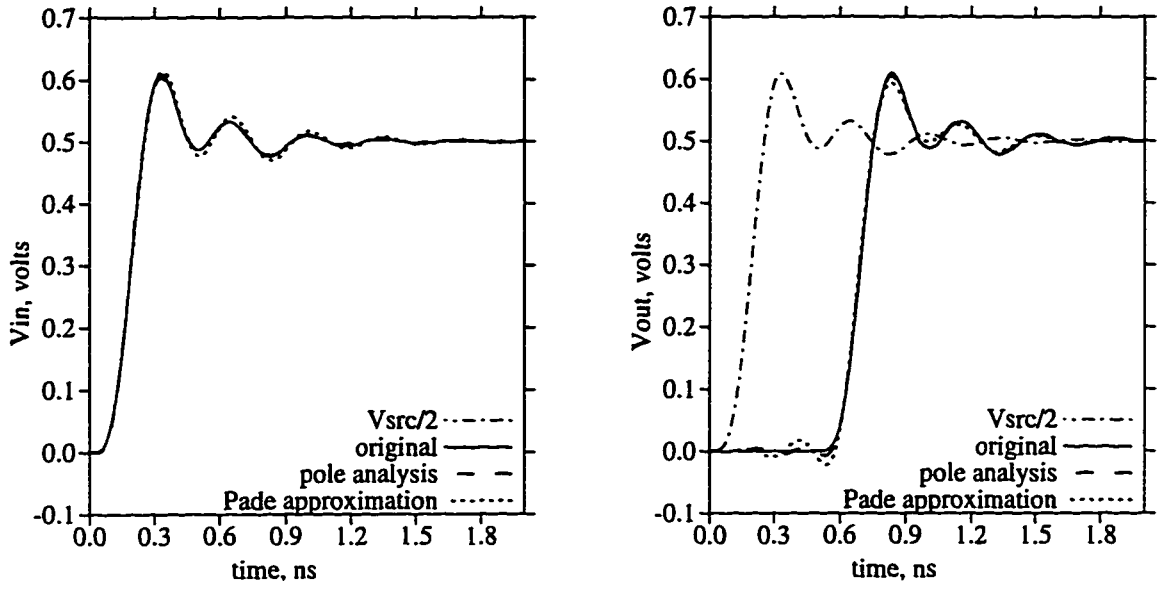

Figure 7.4. Response of the network in Fig. 7.1 to an input step which is passed through a 3 GHz low pass filter.

works. There is no deviation if a filter frequency of 2 GHz is used.

7.2 RLC Network Reduction Using DC Moment Matching

This section shows the reduction of a general RLC network by matching moments at DC, and demonstrates that SCT's preserve absolute stability while providing accuracy which is comparable to the non-split techniques. A random two-port RLC test network is generated which has enough structure in the multiport admittance that the reduce network must match a large number of moments in order to retain accuracy over the entire frequency range. The network is listed in Appendix B, and the number of elements contained in the network is given in Table 7.2. The network has 79 singularities at DC, two of which are seen through the ports. The first step in the reduction is to eliminate the DC singularities as is done for the previous example by using the transform given in Section 6.5. Next, the susceptance connection matrix is zeroed using the transform given in Section 6.3, and the span given by Theorem 4.4 to preserve the DC moments is cal-

Table 7.2. Statistics for RLC test network listed in Appendix B.

Ports	Internal Nodes	Resistors	Capacitors	Inductors	Mutual Inductors
2	159 (41 are voltage)	38	38	118	524

culated using the Arnoldi process.

Two separate reductions are performed. The first uses the transform without splitting to give a reduced network which is a Padé approximation because $2q$ moments are matched when there are qm internal nodes, where $m = 2$ is the number of ports. The second reduction splits the transform so that passivity is preserved, and as a result, only one moment per m internal nodes is preserved. For this example, two of the internal nodes in the reduced networks are required to preserve the DC poles seen through the ports.

Table 7.3 provides the statistics on the reduced networks used in this example. The SCT networks match half as many moments as do the Padé approximations of the same size. On the other hand, SCT reduced networks *never* have unstable poles (i.e. poles whose real part is greater than zero) because asymptotic stability is a requirement of passivity and passivity is *always* preserved. In this example, two of the Padé approximations create unstable poles which make the reduced networks useless for transient circuit simulation unless the poles are dropped (at the expense of accuracy). Once enough moments are preserved that the reduced network behaves like the original over the entire frequency range, these poles disappear (e.g. 60 moments matched in this example).

The number of elements in the reduced network increases as the square of the number of internal nodes because the reduced matrices are dense, and this is shown in the second column from the right in the table. This superlinearity can be eliminated by applying a non-split, well-conditioned square congruence transform which block diagonalizes the internal conductance matrix and diagonalizes the internal susceptance matrix. In the resulting network, the element count increases linearly with the number of nodes, and although it is not in passive form, passivity is preserved because the transform exactly preserves the reduced network's port behavior. The right-most col-

Table 7.3. Statistics for RLC network reduced using SCT's and Padé approximation.

	Moments Matched	Internal Nodes	Unstable Poles	Elements (no diagonalizing)	Elements (diagonalizing)
SCT	10	22	0	330	102
	20	42	0	1145	191
	30	62	0	2460	279
Padé	20	22	2	475	102
	40	42	2	1735	192
	60	62	0	3795	280

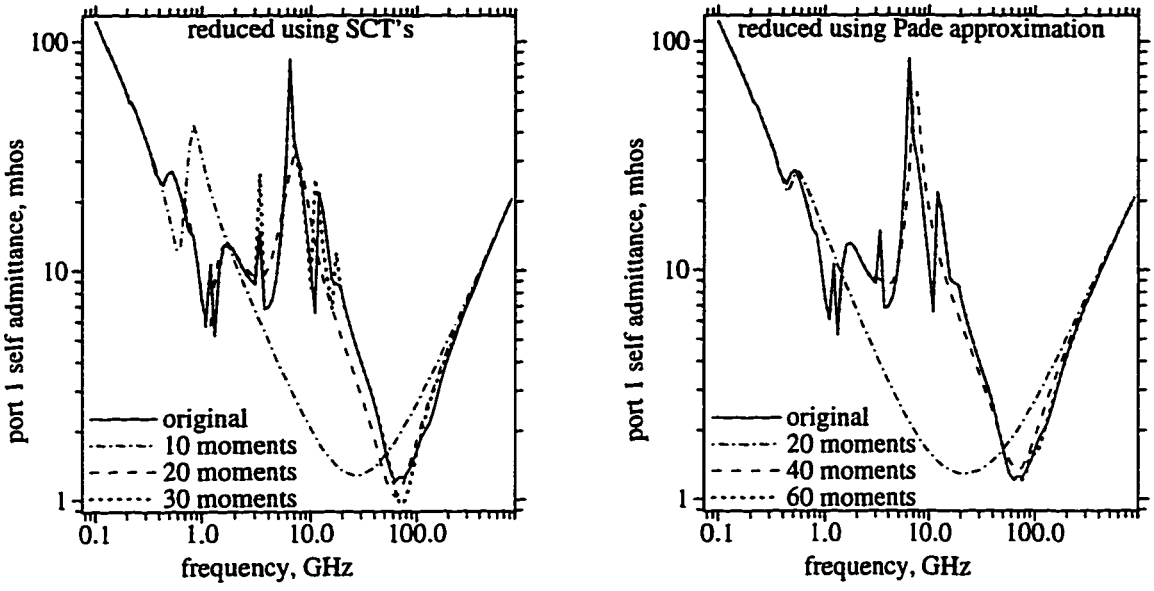

Figure 7.5. Port 1 self admittance of the RLC networks given in Tables 7.2 and 7.3.

umn of the table shows the element count after the networks are block diagonalized.

The accuracy of the reductions can be seen in Fig. 7.5 which shows that the fit improves as the number of matched moments is increased. An ill-conditioned technique such as AWE would not be able to provide accuracy over the entire frequency range shown in the figure without resorting to frequency hopping. The behavior of the network is almost perfectly matched over the entire frequency range when 30 moments are matched using the SCT's or 60 moments are matched using Padé approximations. The Padé approximations are more accurate for the same number of internal nodes since they match more moments, but the increase in accuracy versus network size is at the expense of creating reduced networks which are active.

7.3 Sparse RLC Reduction Using Split Congruence Transformations

This final example demonstrates the sparse implementation of SCT's in a prototype network reduction tool which is passed a network and a frequency range and error tolerance for which accuracy must be preserved. The tool is created solely to demonstrate the use of the different SCT's and is not created with the intent of making a general purpose network reduction tool suitable for industry — to support this point, the tool has not been given a name and is subsequently referred to as "the tool." However, the sparse transforms used by the tool are the same which would be needed by an industry tool. Sparse matrix inversions are performed by Sparse [33], and

dense linear algebra functions such as eigendecomposition and matrix inversion are performed by LAPACK [34].

The basic operation of the tool is as follows. First, a SPICE netlist is parsed, the RLC and K branch elements are extracted, and the port nodes are identified. Graph theory is used to find the null space of the internal conductance network using the concepts illustrated in Fig. 6.1. The null space is stored as a sparse rectangular matrix, and a sparse version of modified Gram-Schmidt orthonormalization is used to make the vectors linearly independent. The transform given by Section 6.5 to eliminate DC singularities is implemented in a sparse manner that does not require the explicit formation of the spanning space of the internal conductance matrix or of the transformed network given in (4.48) and (4.49). Next, poles in the frequency range of interest which lie on the imaginary axis are identified using a technique similar to CFH — this has the same disadvantage of CFH, i.e. multiple complex LU factorizations need to be performed, but it works well for demonstration purposes since it allows different types of span requirements (eigenvectors as well as moments expanded at different frequencies) to be calculated and combined in a single SCT. The eigenvectors associated with complex poles are found and are added to the SCT matrix which is used to reduce the network. The span required to preserve the first two moments at DC is found using Theorem 4.4, and this is split and added to the SCT matrix as well. A series of hops are then taken at frequencies on the imaginary axis, and if the error in the reduced network exceeds the error tolerance at the hop's frequency, then some or all of the span required to match the first two moments at that frequency is added to the SCT matrix. The additional span causes the relative error to drop below the specified error tolerance at that frequency since the slope and offset of the reduced network are identical to the original when the entire span is added to the transform. The process is continued until the error of the reduced network is less than the error tolerance over the entire frequency range. The final step of the reduction is to block diagonalize the reduced network matrix and to form an equivalent RC network as is done in the previous example.

In this example, the network to be reduced is a PEEC model [1], and it has a topology similar to that shown in Fig. 7.6. Two lossless metal plates or lines are floating over a ground plane. The plates are modeled using an inductor mesh containing 42 closed loops (DC singularities), and these are coupled via mutual inductance and capacitance. In addition, the mesh voltage nodes have capacitance to ground. The two-port network is driven by a Thevenin voltage source for simulation, and a 100 MΩ resistor is added between one of the voltage node terminals and ground. The

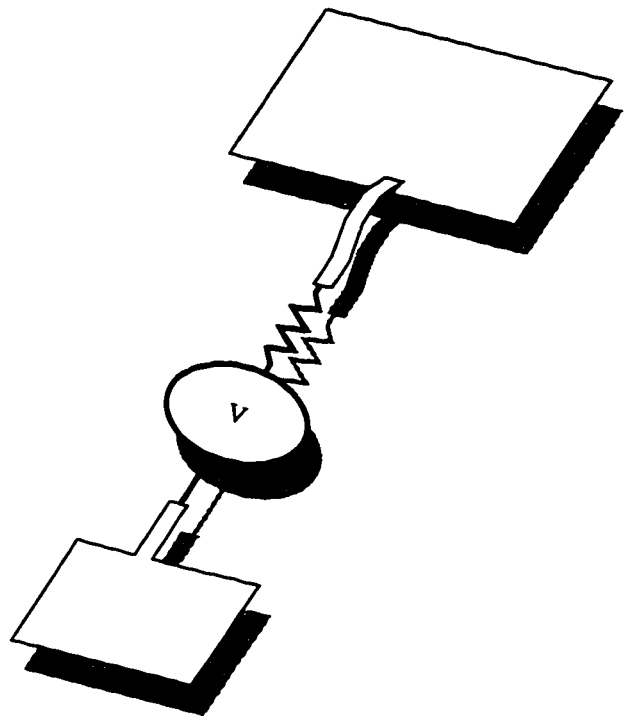

Figure 7.6. Topology of PEEC model and driving circuit.

number of elements in the original model is given in Table 7.4. The inductors are given a resistance of 10^{-15} Ω for the HSPICE simulations so that the simulator does not fail due to singularities encountered during the DC operating point calculation.

The network is reduced four different times. The first two reductions are performed on the LC elements only (LC reduction) with a specified accuracy of 5% between DC and 1 GHz and between DC and 3 GHz respectively. The second two reductions are performed on the network which includes the Thevenin resistance (RLC reduction) for the same two maximum frequencies. The tool uses a pole analysis in the first two cases since the poles are on the complex axis, and it uses moment expansions at multiple frequencies in the second case. The statistics on the network reductions and HSPICE simulations are given in Table 7.5. The reductions take an order of magnitude less time than the simulations and speed the simulations by several orders of magnitude. The

Table 7.4. Network statistics for PEEC model.

Ports	Internal Nodes	Resistors	Capacitors	Inductors	Mutual Inductors
2	302 (130 are voltage)	0	2100	172	6990

Table 7.5. PEEC model reduction and simulation statistics.

Network	Internal Nodes	Elements	Reduction		HSPICE Simulation	
			CPU sec	MBytes	CPU sec	MBytes
original	302	9264	—	—	753.9	10.2
LC, 1 GHz	15	59	93.2	2.8	0.2	0.2
LC, 3 GHz	46	165	211.6	3.0	0.9	0.2
RLC, 1 GHz	14	75	91.7	3.4	0.2	0.2
RLC, 3 GHz	48	586	232.2	4.0	1.9	0.4

HSPICE simulations are AC frequency sweeps of the voltage source, and the output is the current through the voltage source. The results of these simulations are given in Fig. 7.7, and it can be seen that for both cases, the reduced networks are accurate over the specified ranges of frequency.

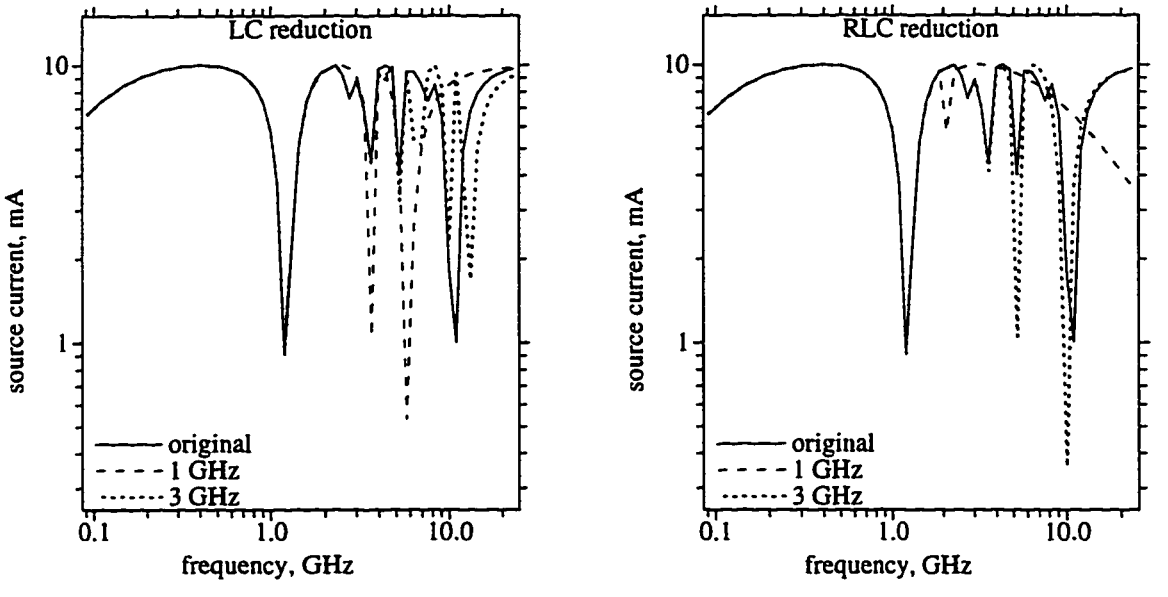

Figure 7.7. AC sweep to measure current through the voltage source as a function of frequency. The plot on the left shows the results using the PEEC model with only the LC elements reduced, and that on the right shows the results when all RLC elements are reduced.

Chapter 8
Concluding Remarks

The main concept presented in this thesis is that the MNA matrices which represent positive RLC networks have a passive form, and network reduction based on split congruence transformations (SCT's) preserves the passive form so that the reduced networks remain passive. It is shown that SCT's can be used to provide well-conditioned admittance-to-admittance transformations of a general RLC network which preserve selected poles and moments of the network multiport admittance while reducing the size of the network. All congruence transforms of RC networks and those which preserve poles and moments of LC networks are naturally split, and therefore always preserve passivity. Several examples of reduction using SCT's demonstrate the stability of the SCT-derived networks and show that a sparse implementation using these transforms can be achieved.

References

[1] A. E. Ruehli. "Equivalent circuit models for three dimensional multiconductor systems," *IEEE Trans. Microwave Theory and Technique*, MTT-22(3), pp. 216-221, March 1974.

[2] H. B. Bakoglu, *Circuits, Interconnects, and Packaging for VLSI*. Reading, MA: Addison-Wesley Pub. Co., 1990.

[3] K. Kamon, M. J. Tsuk, and J. White, "Fasthenry, a multipole-accelerated 3-d inductance extraction program," *Proceedings of the 30th ACM/IEEE Design Automation Conference*, pp. 678-683, June 1993.

[4] S.-S. Lee and D. J. Allstot, "Electrothermal simulation of integrated circuits," *IEEE J. Solid-State Circuits*, vol. 28, pp. 1283-1293, December 1993.

[5] I. L. Wemple and A. T. Yang, "Integrated circuit substrate coupling models based on Voronoi tessellation," *IEEE Trans. Computer-Aided Design*, vol. 14, pp. 1459-1469, December 1995.

[6] C.-W. Ho, A. E. Ruehli and P. A. Brennan, "The modified nodal approach to network analysis," *IEEE Trans. Circuits and Systems.*, vol. CAS-22, pp. 504-509, June 1975.

[7] G. H. Golub and C. F. Van Loan, *Matrix Computations, Second Edition*. Baltimore: Johns Hopkins University Press, 1993.

[8] W. C. Elmore, "The transient response of damped linear networks with particular regard to wide-band amplifiers," *J. Appl. Phys.*, vol. 19, pp. 55-63, January 1948.

[9] L. T. Pillage and R. A. Rohrer, "Asymptotic waveform evaluation for timing analysis," *IEEE Trans. Computer-Aided Design*, vol. 9, pp. 352-366, April 1990.

[10] X. Huang, "Padé approximation of linear(ized) circuit responses," Ph.D. dissertation. Carnegie Mellon Univ., November 1990.

[11] E. Chiprout and M. S. Nakhla, "Analysis of interconnect networks using complex frequency hopping (CFH)," *IEEE Trans. Computer-Aided Design*, vol. 14, pp.186-200, February 1995.

[12] C. Lanczos, "An iteration method for the solution of the eigenvalue problem of linear differential and integral operators," *Journal of Research of the National Bureau of Standards*, vol. 45, pp. 255-282, October 1950.

[13] W. E. Arnoldi, "The principle of minimized iterations in the solution of the matrix eigenvalue problem," *Quart. Appl. Math.*, vol. 9, pp. 17-29, 1951.

[14] C. De Villemagne and R. E. Skelton, "Model reductions using a projection formulation," *Int. J. Control*, vol. 46, pp. 2141-2169, December 1987.

[15] T.-J. Su and R. R. Craig, "Krylov vector methods for model reduction and control of flexible structures," *Control and Dynamic Systems: Advances in Theory*, vol. 54, pp. 449-481, 1992.

[16] K. Gallivan, E. Grimme, and P. Van Dooren, "Asymptotic waveform evaluation via a Lanczos Method," *Appl. Math. Lett.*, vol. 7, pp. 75-80, 1994.

[17] P. Feldmann and R. W. Freund, "Efficient linear circuit analysis by Padé approximation via the Lanczos process," *Proceedings EURO-DAC '94 with EURO-VHDL '94*, pp. 170-175, September 1994.

[18] P. Feldmann and R. W. Freund, "Efficient linear circuit analysis by Padé approximation via the Lanczos process," *IEEE Trans. Computer-Aided Design*, vol. 14, pp. 639-649, May 1995.

[19] P. Feldmann and R. W. Freund, "Reduced-order modeling of large linear subcircuits via a block Lanczos algorithm," *Proceedings of the 32nd ACM/IEEE Design Automation Conference*, pp. 474-479, June 1995.

[20] R. W. Freund, M. H. Gutknecht, and N. M. Nachtigal, "An implementation of the look-ahead Lanczos algorithm for non-Hermitian matrices," *SIAM J. Sci. Comput.*, vol. 14, pp. 137-158, January 1993.

[21] L. M. Silveira, M. Kamon, and J. White, "Efficient reduced-order modeling of frequency-dependent coupling inductances associated with 3-D interconnect structures," *Proceedings of the 32nd ACM/IEEE Design Automation Conference*, pp. 376-380, June 1995.

[22] R. S. Varga, *Matrix Iterative Analysis*. Englewood Cliffs, NJ: Prentice-Hall, Inc., 1962.

[23] K. J. Kerns, I. L. Wemple, and A. T. Yang, "Stable and efficient reduction of substrate model networks using congruence transforms," *IEEE/ACM International Conference on Computer-Aided Design*, pp. 207-214,November 1995.

[24] K. J. Kerns, I. L. Wemple, and A. T. Yang, "Efficient parasitic substrate modelling for monolithic mixed-A/D circuit design and verification," *Analog Integrated Circuits and Signal Processing*, pp.7-21, June/July 1996.

[25] K. J. Kerns and A. T. Yang, "Stable and efficient reduction of large, multiport RC networks by pole analysis via congruence transforms," *Proceedings of the 33rd Design Automation Conference*, pp. 280-285, June 1996.

[26] K. J. Kerns and A. T. Yang, "Stable and efficient reduction of large, multiport RC networks by pole analysis via congruence transforms," to appear *IEEE Trans. Computer-Aided Design*.

[27] HSPICE, Meta-Software, Inc., Version H95.1, Campbell, CA, 1995.

[28] B. T. Smith, *Matrix Eigensystem Routines: EISPACK Guide*, 2nd edition, New York: Springer-Verlag, 1976.

[29] B. N. Parlett and D. S. Scott, "The Lanczos algorithm with selective orthogonalization," *Mathematics of Computation*, vol. 33, pp. 217-238, January 1979.

[30] M. R. Wohlers, *Lumped and Distributed Passive Networks: A Generalized and Advanced Viewpoint*. New York: Academic Press, 1969.

[31] MATLAB, The MathWorks, Inc., Version 4.2, Natick, MA.

[32] W.-K. Chen, *Passive and Active Filters: Theory and Implementations*. New York, NY: John Wiley & Sons, Inc., 1986.

[33] K. S. Kundert and A. Sangiovanni-Vincentelli, *User's Guide for Sparse: A Sparse Linear Equation Solver.* Version 1.3a, Department of EECS, University of California, Berkeley, CA, 1988.

[34] E. Anderson, *et al. LAPACK User's Guide*, 2nd edition, Philadelphia: Society for Industrial and Applied Mathematics, 1995.

Appendix A. RLC SPICE Netlist used for Fig. 2.3

```
.subckt RLC 0 1
R1 29 30 1.433e-01
R2 26 38 1.187e+05
R3 0 21 1.566e-01
R4 16 37 2.225e+02
R5 26 28 2.134e-01
R6 1 9 1.721e-01
R7 3 11 2.398e+03
R8 7 29 8.186e+01
R9 11 18 1.417e+00
R10 12 22 2.561e-01
R11 13 36 5.674e+02
R12 13 14 3.321e+00
R13 6 29 1.642e+05
R14 0 14 2.133e+01
R15 2 3 1.310e+05
R16 6 21 7.981e+03
R17 3 13 5.906e+04
R18 15 16 1.589e+02
R19 5 19 2.038e+01
R20 29 33 9.598e+00
R21 10 12 1.571e+00
R22 26 27 6.199e+03
R23 0 2 3.250e+04
R24 9 35 3.713e-01
R25 21 35 7.246e+00
R26 24 31 4.100e+05
R27 20 21 8.756e-01
R28 9 13 7.570e+03
R29 3 13 5.940e+03
R30 22 34 2.673e+05
R31 2 25 3.320e+01
R32 10 21 2.575e+02
R33 26 37 1.993e+00
R34 7 22 2.984e+04
R35 7 17 1.274e+05
R36 5 26 5.125e+00
R37 20 32 1.199e+05
R38 12 21 2.720e+05
R39 18 24 1.597e+02
R40 0 20 1.482e+00
R41 5 7 2.076e+05
```

```
R42 26 35 8.890e+02
R43 11 28 4.673e+00
R44 31 36 8.754e+01
R45 1 3 2.652e+05
R46 19 39 4.441e+03
R47 12 16 5.865e+02
R48 19 22 5.400e-01
R49 11 32 1.172e+05
R50 2 23 1.481e-01
R51 23 27 1.652e+05
R52 19 23 2.687e+00
R53 20 34 9.662e+01
R54 9 38 4.918e+05
R55 5 32 1.947e+05
R56 3 23 9.011e+00
R57 24 39 1.544e+01
R58 0 4 5.234e+01
R59 32 37 1.127e-01
R60 4 31 4.316e+05
R61 12 30 2.672e-01
R62 13 16 4.940e+05
R63 10 34 1.864e+02
R64 12 23 3.843e+02
R65 12 23 1.051e+05
R66 9 18 4.269e+03
R67 6 7 1.533e-01
R68 5 20 1.557e+04
R69 21 33 4.315e+02
R70 0 30 9.513e+01
R71 24 32 3.648e+03
R72 26 36 1.022e+03
R73 11 35 7.720e-01
R74 14 22 3.444e-01
R75 13 33 5.427e+05
R76 29 39 6.116e+00
R77 33 36 4.084e+00
R78 6 37 9.708e+02
R79 1 31 1.828e+01
R80 14 38 3.006e+01
R81 0 24 1.143e+02
R82 9 10 2.303e+00
R83 7 13 5.683e+05
R84 3 6 1.448e+05
R85 19 20 6.916e+05
R86 7 9 2.197e+01
R87 9 31 3.125e+03
R88 9 27 4.798e+00
R89 2 33 2.695e+05
R90 12 27 7.473e+01
R91 28 38 4.783e+02
R92 34 38 2.039e+04
```

```
R93 32 34 8.906e+03
R94 18 30 3.711e+02
R95 17 32 4.184e+04
R96 30 39 1.015e+02
R97 22 38 2.208e+02
R98 9 29 1.453e+04
R99 3 38 7.959e+03
R100 12 32 1.616e+05
R101 3 7 1.052e+01
R102 24 31 8.282e+05
R103 5 14 2.557e+00
R104 13 16 2.227e+04
R105 4 37 1.169e+02
R106 21 34 4.445e+04
R107 7 27 1.672e-01
R108 2 6 1.259e-01
R109 8 34 8.636e-01
R110 11 14 8.825e+00
R111 21 31 3.362e+02
R112 1 23 1.638e+00
R113 11 23 3.094e+05
R114 9 31 1.441e+03
R115 13 23 7.836e+04
R116 18 37 1.268e+03
R117 7 17 1.765e+04
R118 25 38 4.415e-01
R119 2 19 1.949e+02
R120 7 39 1.745e+00
R121 1 18 1.289e+01
R122 4 5 2.072e-01
R123 3 17 7.322e+05
R124 4 14 1.474e+00
R125 7 38 2.076e+01
R126 21 25 4.310e-01
R127 34 36 7.380e-01
R128 5 13 1.817e+04
R129 29 36 7.423e+01
R130 1 13 4.870e+05
R131 20 29 3.729e+02
R132 21 31 1.347e+05
R133 11 34 3.044e+04
R134 14 32 2.143e+00
R135 9 28 6.924e+05
R136 33 38 5.735e+04
R137 2 18 1.150e+01
R138 22 36 1.756e+04
R139 3 33 2.499e+02
R140 0 31 2.742e+03
R141 18 38 4.501e+05
R142 6 14 1.180e-01
R143 12 36 1.651e-01
```

```
R144 24 33 1.375e+05
R145 1 10 1.808e+05
R146 16 18 6.910e+05
R147 5 32 3.682e+05
R148 13 18 7.313e-01
R149 3 38 5.372e+01
R150 20 26 1.106e+04
R151 30 33 6.204e+01
R152 2 18 5.731e+04
R153 18 38 1.126e+02
R154 14 22 3.283e+02
R155 0 18 3.655e+02
R156 26 32 7.178e+01
R157 7 29 2.293e-01
R158 10 21 4.466e+03
R159 3 9 4.602e+03
R160 11 13 6.327e+03
R161 2 33 7.203e+00
R162 8 38 1.637e+01
R163 12 24 3.091e+00
R164 8 24 2.518e+01
R165 0 27 9.876e+00
R166 2 17 4.101e+05
R167 10 35 1.037e+01
R168 2 13 8.760e+01
R169 17 28 7.411e+01
R170 30 33 1.349e+04
R171 3 20 2.677e+02
R172 0 35 1.642e+02
R173 11 33 3.719e+00
R174 26 39 5.156e+03
R175 20 37 9.890e-01
R176 17 27 1.725e+03
R177 0 5 1.372e+00
R178 11 34 3.053e+01
R179 20 33 1.677e+04
R180 18 26 7.395e+02
R181 4 28 7.535e+00
R182 9 27 3.215e-01
R183 13 36 1.942e+05
R184 2 15 2.787e+04
R185 7 26 6.291e+05
R186 24 28 4.108e+00
R187 0 1 2.337e+01
R188 9 14 8.033e+03
R189 2 10 1.601e+03
R190 32 36 2.181e+00
R191 2 11 4.145e+02
R192 1 23 8.735e+02
R193 17 34 1.589e+05
R194 13 23 9.899e+04
```

```
R195 4 9 6.581e+02
R196 11 28 2.882e+03
*
C1 8 32 1.707e-11
C2 15 33 1.194e-12
C3 17 19 5.780e-10
C4 2 23 2.031e-09
C5 6 35 1.835e-14
C6 15 35 2.264e-09
C7 4 36 9.261e-14
C8 4 34 2.570e-08
C9 27 37 3.064e-09
C10 4 14 1.002e-08
C11 11 28 3.705e-09
C12 2 9 2.405e-09
C13 6 17 1.920e-08
C14 2 18 3.377e-08
C15 0 8 1.449e-13
C16 23 29 1.114e-13
C17 15 26 1.154e-12
C18 27 32 1.273e-10
C19 9 30 2.062e-10
C20 10 31 1.211e-12
C21 24 25 3.233e-13
C22 32 35 2.525e-09
C23 22 39 7.936e-11
C24 10 25 6.207e-09
C25 29 35 2.321e-10
C26 9 32 4.629e-09
C27 7 17 5.709e-13
C28 13 34 3.656e-11
C29 8 24 9.428e-13
C30 33 36 8.005e-08
C31 30 38 9.874e-09
C32 9 14 4.521e-12
C33 19 22 6.870e-08
C34 13 38 1.069e-09
C35 3 23 2.222e-08
C36 12 16 1.162e-09
C37 1 14 1.319e-11
C38 10 24 1.433e-10
C39 33 34 2.141e-14
C40 12 32 6.600e-14
C41 3 21 1.532e-08
C42 6 16 9.897e-12
C43 5 15 7.494e-09
C44 20 38 5.254e-10
C45 18 36 2.221e-12
C46 23 36 1.049e-09
C47 35 37 1.153e-13
C48 6 15 2.044e-11
```

```
C49 10 33 1.403e-09
C50 13 33 3.079e-11
C51 0 33 1.169e-11
C52 5 34 3.975e-12
C53 27 33 3.079e-11
C54 27 34 1.595e-09
C55 5 13 2.300e-08
C56 2 7 2.150e-12
C57 22 23 1.299e-14
C58 6 10 1.388e-10
C59 5 25 3.828e-11
C60 7 33 8.980e-09
C61 18 35 7.554e-13
C62 9 20 3.378e-14
C63 30 37 1.218e-11
C64 0 9 2.053e-10
C65 19 39 1.339e-10
C66 30 32 6.728e-11
C67 0 24 2.599e-12
C68 9 25 3.363e-10
C69 15 27 6.177e-10
C70 1 25 1.270e-10
C71 2 25 2.451e-12
C72 25 26 4.777e-12
C73 17 20 2.347e-14
C74 19 25 3.318e-09
C75 10 19 3.288e-11
C76 23 29 7.432e-14
C77 7 38 3.176e-11
C78 15 17 8.985e-13
C79 7 35 4.719e-13
C80 2 24 1.162e-11
C81 9 32 4.565e-09
C82 28 34 4.417e-13
C83 27 34 3.464e-10
C84 9 30 1.734e-13
C85 7 30 1.057e-09
C86 25 38 1.430e-14
C87 2 38 2.574e-09
C88 15 21 5.858e-11
C89 19 25 1.194e-11
C90 23 27 7.672e-14
C91 0 21 6.963e-11
C92 13 19 6.461e-14
C93 9 25 1.933e-10
C94 24 28 3.233e-11
C95 23 24 3.744e-08
C96 17 24 5.682e-09
C97 17 35 1.170e-14
C98 25 34 4.562e-08
C99 1 14 3.161e-08
```

```
C100 7 17 1.644e-11
C101 21 24 1.012e-11
C102 4 7 7.544e-09
C103 29 37 7.950e-14
C104 7 26 4.722e-12
C105 14 20 3.276e-11
C106 5 32 6.905e-11
C107 4 28 1.955e-12
C108 6 10 5.141e-10
C109 6 10 6.103e-13
C110 1 11 1.898e-14
C111 2 39 1.429e-08
C112 22 35 1.101e-13
C113 7 20 1.358e-11
C114 19 36 8.731e-08
C115 4 16 1.567e-11
C116 21 28 1.737e-12
C117 10 19 3.827e-08
C118 20 31 4.324e-11
C119 7 32 1.592e-11
C120 1 14 3.553e-08
C121 22 35 6.872e-09
C122 20 29 1.072e-11
C123 3 30 9.551e-13
C124 15 18 1.915e-09
C125 34 39 2.409e-12
C126 21 28 7.881e-10
C127 6 29 3.730e-12
C128 8 21 3.329e-11
C129 9 38 1.456e-09
C130 18 20 2.595e-10
C131 13 26 3.694e-14
C132 17 31 1.994e-09
C133 29 34 1.433e-09
C134 4 14 3.030e-14
C135 15 27 9.483e-09
C136 5 26 1.329e-13
C137 14 15 1.698e-13
C138 11 39 9.682e-11
C139 4 14 9.262e-10
C140 11 16 2.436e-08
C141 2 14 4.657e-11
C142 5 39 1.122e-11
C143 0 24 1.191e-08
C144 3 21 1.070e-11
C145 22 33 9.837e-09
C146 14 21 3.480e-10
C147 4 25 3.535e-08
C148 0 37 1.901e-08
C149 29 32 8.783e-14
C150 14 15 1.948e-12
```

```
C151 26 27 1.975e-10
C152 26 34 3.127e-13
C153 0 16 7.704e-09
C154 4 13 4.621e-12
C155 8 31 9.515e-12
C156 24 27 4.615e-09
C157 13 37 7.517e-09
C158 17 39 2.461e-11
C159 23 25 5.510e-11
C160 4 23 8.517e-11
C161 17 19 8.849e-12
C162 2 11 5.839e-09
C163 23 38 5.505e-09
C164 18 37 6.393e-14
C165 12 30 3.242e-09
C166 16 24 1.367e-13
C167 12 27 2.563e-14
C168 17 27 2.570e-11
C169 24 36 4.960e-08
C170 14 17 2.959e-10
C171 5 35 1.260e-13
C172 9 23 9.030e-14
C173 8 34 1.831e-11
C174 0 35 8.333e-11
C175 25 28 1.670e-10
C176 3 15 3.138e-09
C177 21 28 4.125e-11
C178 17 20 9.472e-13
C179 13 25 1.330e-13
C180 22 35 6.800e-14
C181 6 21 3.196e-12
C182 17 27 5.875e-11
C183 15 38 3.585e-12
C184 1 3 4.418e-08
C185 21 37 2.241e-09
C186 0 3 6.091e-12
C187 14 19 2.553e-14
C188 30 38 2.463e-11
C189 0 35 5.795e-11
C190 1 3 8.463e-11
C191 21 31 2.140e-13
C192 7 21 2.558e-09
C193 24 25 3.208e-09
C194 6 9 9.888e-10
C195 20 26 2.467e-14
C196 21 23 1.359e-14
C197 18 33 4.773e-13
C198 24 39 7.800e-08
C199 0 3 2.275e-13
C200 2 11 8.644e-09
C201 6 32 9.180e-14
```

```
C202 4 28 7.106e-13
C203 13 28 1.888e-08
C204 20 21 1.017e-11
C205 35 38 1.874e-09
C206 10 23 2.581e-12
C207 1 29 1.100e-13
C208 5 31 2.844e-09
C209 6 15 2.245e-13
C210 12 22 3.801e-10
C211 12 34 8.413e-08
C212 1 29 3.670e-12
C213 24 27 3.012e-14
C214 6 8 1.441e-08
C215 30 35 2.118e-10
C216 10 27 3.912e-10
C217 22 23 3.029e-10
C218 24 32 1.501e-09
C219 24 26 1.243e-11
C220 5 8 1.406e-13
C221 1 14 1.454e-12
C222 8 14 1.060e-11
C223 8 33 1.122e-10
C224 15 16 4.690e-12
C225 12 32 2.533e-13
C226 5 26 2.285e-14
C227 3 39 1.993e-08
* -> The inductors are lossy: R is the series resistance in Ohms.
L1 19 23 1.900e-10 R=1.127e-1
L2 23 39 1.294e-07 R=1.127e-1
L3 38 20 8.168e-11 R=1.127e-1
L4 8 21 8.949e-09 R=1.127e-1
L5 30 8 7.724e-11 R=1.127e-1
L6 38 25 2.516e-08 R=1.127e-1
L7 29 34 4.602e-09 R=1.127e-1
L8 31 8 4.421e-07 R=1.127e-1
L9 23 26 3.631e-07 R=1.127e-1
L10 18 26 5.606e-09 R=1.127e-1
L11 36 3 3.982e-09 R=1.127e-1
L12 18 14 1.217e-09 R=1.127e-1
L13 5 29 6.967e-12 R=1.127e-1
L14 10 9 6.040e-12 R=1.127e-1
L15 23 34 1.344e-08 R=1.127e-1
L16 19 30 4.128e-08 R=1.127e-1
L17 12 37 4.077e-11 R=1.127e-1
L18 0 31 1.976e-09 R=1.127e-1
L19 8 16 1.527e-09 R=1.127e-1
*
K1 L3 L7 8.124e-01
K2 L4 L16 6.502e-02
K3 L4 L17 -2.898e-01
K4 L6 L14 -3.203e-01
```

```
   K5 L6 L19 -4.183e-01
   K6 L9 L15 2.179e-01
   K7 L9 L16 4.072e-01
   K8 L12 L15 1.100e-01
   K9 L15 L17 -2.171e-01
   K10 L16 L19 -1.026e-01
*
.ends
```

Appendix B. RLC SPICE Netlist Used for Section 7.2

```
.subckt RLC 0 1 2
R1 5 29 3.747e+02
R2 29 36 1.942e-01
R3 3 22 7.752e+03
R4 10 22 4.859e-01
R5 11 25 3.984e-01
R6 26 32 3.014e+04
R7 17 25 2.865e+01
R8 3 9 1.413e+02
R9 31 41 5.969e-01
R10 5 16 1.339e+02
R11 18 29 3.249e+04
R12 30 36 1.135e+05
R13 9 27 7.973e+00
R14 26 41 4.509e+00
R15 6 19 4.417e+03
R16 10 16 2.923e+01
R17 14 36 1.412e+03
R18 25 41 2.964e+01
R19 1 13 7.306e-01
R20 1 32 9.053e+05
R21 34 38 5.440e+03
R22 7 19 8.275e+05
R23 13 36 2.181e-01
R24 11 13 1.503e+02
R25 17 38 1.433e+00
R26 16 21 1.657e+03
R27 18 21 5.334e+02
R28 27 36 7.358e+04
R29 15 39 2.306e+04
R30 7 12 1.257e+03
R31 28 37 2.471e+04
R32 0 33 1.303e+00
R33 11 15 2.130e+02
R34 13 41 4.040e-01
R35 21 30 7.403e+04
R36 4 26 4.069e+01
R37 23 31 1.727e+00
R38 5 7 7.384e+05
*
C1 20 31 3.770e-13
C2 22 27 9.721e-11
```

```
C3 20 34 4.880e-08
C4 3 8 5.784e-13
C5 16 37 2.422e-13
C6 33 35 1.885e-14
C7 0 4 2.029e-09
C8 2 30 2.764e-11
C9 6 37 1.542e-12
C10 5 9 2.717e-08
C11 0 19 5.814e-09
C12 13 41 1.112e-08
C13 9 32 7.958e-09
C14 22 32 1.133e-10
C15 4 26 6.427e-09
C16 12 18 9.027e-13
C17 31 41 4.760e-14
C18 15 25 3.172e-12
C19 19 33 1.893e-11
C20 9 26 2.118e-13
C21 1 15 2.087e-10
C22 19 25 6.357e-11
C23 10 11 2.304e-09
C24 4 38 1.900e-11
C25 1 31 1.108e-12
C26 16 17 3.504e-11
C27 25 35 2.566e-11
C28 24 31 1.812e-08
C29 8 32 8.081e-13
C30 14 40 4.388e-12
C31 14 34 2.038e-14
C32 25 31 6.903e-10
C33 20 21 9.195e-09
C34 30 38 8.105e-10
C35 4 24 3.323e-12
C36 2 40 2.012e-12
C37 2 13 3.045e-14
C38 9 14 8.762e-11
*
L1 24 38 4.161e-11
L2 6 5 6.022e-08
L3 28 31 5.506e-10
L4 11 23 3.285e-06
L5 24 17 3.521e-08
L6 4 23 8.052e-10
L7 38 6 1.073e-12
L8 41 9 8.569e-09
L9 40 4 1.894e-07
L10 2 14 1.301e-09
L11 12 39 1.327e-12
L12 29 1 2.002e-10
L13 0 18 6.433e-12
L14 37 21 4.723e-09
```

```
L15 15 18 4.124e-06
L16 1 12 1.573e-10
L17 22 17 1.820e-11
L18 39 32 7.615e-06
L19 26 16 5.390e-12
L20 7 10 4.560e-11
L21 24 39 2.112e-07
L22 9 7 8.932e-12
L23 3 2 3.326e-08
L24 36 24 4.889e-09
L25 24 28 2.561e-07
L26 29 30 1.328e-06
L27 8 28 4.355e-06
L28 3 19 5.476e-08
L29 28 41 8.666e-08
L30 7 3 8.280e-11
L31 20 15 8.891e-07
L32 36 39 4.291e-09
L33 3 27 3.892e-12
L34 5 41 7.839e-08
L35 15 27 5.006e-12
L36 28 25 4.571e-06
L37 10 17 1.763e-07
L38 38 5 2.905e-12
L39 35 25 1.854e-06
L40 18 6 2.094e-07
L41 29 18 3.422e-06
L42 5 38 4.577e-12
L43 24 3 2.596e-06
L44 28 9 2.161e-12
L45 7 34 2.461e-06
L46 29 40 1.720e-07
L47 23 29 9.528e-12
L48 2 8 4.507e-09
L49 40 33 2.238e-06
L50 30 35 6.918e-10
L51 9 3 5.897e-09
L52 17 22 1.271e-10
L53 25 5 4.883e-09
L54 1 10 2.730e-12
L55 0 3 1.339e-06
L56 35 15 3.053e-09
L57 14 35 1.349e-10
L58 5 6 2.073e-11
L59 26 32 3.559e-11
L60 14 19 5.137e-08
L61 4 6 1.436e-08
L62 27 17 2.420e-10
L63 22 17 9.347e-10
L64 32 36 6.839e-10
L65 11 24 2.504e-12
```

```
L66 3 27 2.617e-10
L67 18 40 1.750e-09
L68 3 9 4.422e-12
L69 34 15 1.179e-06
L70 27 16 3.079e-09
L71 4 21 1.698e-10
L72 28 35 2.220e-09
L73 20 34 5.995e-10
L74 38 41 7.733e-09
L75 24 25 2.186e-10
L76 13 20 6.319e-11
L77 25 9 1.950e-11
L78 26 13 5.612e-07
L79 6 3 7.654e-11
L80 25 35 1.587e-08
L81 7 19 5.959e-06
L82 23 21 1.392e-12
L83 39 2 4.572e-12
L84 31 21 3.966e-07
L85 9 32 7.401e-11
L86 22 10 2.207e-09
L87 38 24 3.118e-09
L88 29 12 1.517e-12
L89 29 8 3.079e-12
L90 41 9 1.145e-06
L91 33 21 4.764e-11
L92 0 10 9.138e-11
L93 15 37 4.583e-06
L94 41 25 3.539e-06
L95 39 2 3.629e-08
L96 9 3 8.304e-09
L97 17 0 2.431e-11
L98 14 6 3.378e-06
L99 1 36 2.123e-09
L100 29 24 4.974e-06
L101 31 19 1.044e-06
L102 19 5 1.740e-12
L103 32 9 2.833e-07
L104 12 33 3.779e-08
L105 1 37 1.997e-06
L106 32 20 6.328e-07
L107 37 9 6.582e-06
L108 38 21 7.073e-10
L109 39 0 1.270e-11
L110 10 18 1.597e-11
L111 16 13 4.744e-10
L112 7 15 1.291e-12
L113 15 5 4.640e-12
L114 41 26 6.489e-09
L115 37 27 5.376e-06
L116 6 31 1.290e-07
```

```
L117 40 3 2.109e-11
L118 7 41 5.367e-10
*
K1 L1 L3 -1.104e-02
K2 L1 L6 9.052e-04
K3 L1 L8 -5.449e-02
K4 L1 L13 -3.475e-02
K5 L1 L14 3.388e-02
K6 L1 L48 2.227e-02
K7 L1 L68 -9.135e-02
K8 L1 L78 -2.021e-02
K9 L1 L113 6.911e-02
K10 L2 L3 1.341e-02
K11 L2 L7 1.299e-01
K12 L2 L12 1.312e-01
K13 L2 L21 1.321e-02
K14 L2 L33 -3.981e-02
K15 L2 L116 -7.594e-02
K16 L3 L32 -9.705e-03
K17 L3 L39 7.299e-02
K18 L3 L68 1.390e-02
K19 L3 L70 -1.302e-02
K20 L3 L74 -1.042e-01
K21 L3 L102 -8.106e-03
K22 L4 L39 -5.017e-02
K23 L4 L47 1.227e-01
K24 L4 L89 3.645e-02
K25 L4 L103 -5.295e-02
K26 L4 L118 -2.126e-01
K27 L5 L7 7.434e-02
K28 L5 L13 6.374e-02
K29 L5 L21 -6.781e-02
K30 L5 L28 -4.805e-03
K31 L5 L36 2.203e-02
K32 L5 L60 8.318e-02
K33 L5 L81 1.058e-02
K34 L5 L92 6.592e-02
K35 L5 L104 7.226e-02
K36 L5 L105 5.272e-02
K37 L5 L112 -6.609e-02
K38 L6 L7 1.121e-01
K39 L6 L35 -3.771e-02
K40 L6 L50 3.779e-02
K41 L6 L76 -2.849e-02
K42 L6 L98 5.780e-02
K43 L6 L110 -4.629e-02
K44 L6 L118 1.281e-01
K45 L7 L10 1.102e-01
K46 L7 L43 -1.178e-01
K47 L7 L65 -6.341e-02
K48 L7 L70 6.604e-02
```

```
K49 L7 L71 8.861e-02
K50 L7 L89 -1.247e-01
K51 L8 L48 -9.839e-02
K52 L8 L52 7.769e-02
K53 L8 L54 6.239e-02
K54 L8 L55 -2.089e-02
K55 L8 L79 8.390e-02
K56 L8 L102 5.434e-02
K57 L8 L108 -3.036e-03
K58 L8 L109 -9.203e-02
K59 L8 L113 -4.976e-03
K60 L9 L24 -6.479e-02
K61 L9 L27 4.512e-02
K62 L9 L30 -2.635e-02
K63 L9 L50 3.981e-02
K64 L9 L57 4.754e-02
K65 L9 L63 3.817e-02
K66 L9 L93 5.324e-02
K67 L9 L102 -8.162e-02
K68 L9 L104 2.631e-02
K69 L10 L39 5.393e-02
K70 L10 L66 -5.325e-02
K71 L10 L67 -8.531e-02
K72 L10 L68 2.856e-03
K73 L10 L113 2.910e-03
K74 L10 L117 4.140e-02
K75 L11 L23 1.294e-02
K76 L11 L26 2.850e-03
K77 L11 L46 9.808e-02
K78 L11 L55 9.289e-02
K79 L11 L67 -7.104e-02
K80 L11 L69 -2.805e-02
K81 L11 L95 1.139e-03
K82 L11 L104 -8.185e-02
K83 L12 L21 8.055e-02
K84 L12 L35 -2.416e-02
K85 L12 L58 -1.928e-03
K86 L12 L65 7.465e-02
K87 L12 L93 -5.807e-02
K88 L12 L95 -5.832e-02
K89 L12 L116 8.565e-02
K90 L13 L19 -5.344e-02
K91 L13 L24 -6.417e-02
K92 L13 L27 -2.839e-02
K93 L13 L45 7.492e-02
K94 L13 L47 -1.031e-02
K95 L13 L59 1.913e-02
K96 L13 L73 -6.336e-02
K97 L13 L78 7.651e-02
K98 L13 L96 2.442e-02
K99 L13 L102 -4.139e-02
```

```
K100 L13 L103 4.975e-02
K101 L13 L107 -4.683e-02
K102 L14 L32 6.517e-02
K103 L14 L42 8.319e-02
K104 L14 L44 6.373e-02
K105 L14 L59 5.933e-02
K106 L14 L65 -2.075e-02
K107 L14 L69 -1.113e-01
K108 L14 L71 -1.368e-02
K109 L14 L77 2.065e-02
K110 L14 L114 -8.563e-02
K111 L15 L16 -4.573e-02
K112 L15 L21 -8.338e-02
K113 L15 L49 4.041e-02
K114 L15 L66 1.080e-01
K115 L15 L110 1.333e-02
K116 L15 L116 -4.589e-03
K117 L16 L25 4.100e-02
K118 L16 L48 -1.755e-01
K119 L16 L67 5.824e-02
K120 L16 L71 1.251e-02
K121 L16 L77 -9.281e-04
K122 L16 L78 2.469e-03
K123 L16 L91 -2.169e-03
K124 L17 L32 1.174e-01
K125 L17 L58 -8.325e-03
K126 L17 L60 -6.352e-02
K127 L17 L65 7.295e-02
K128 L17 L83 9.046e-02
K129 L17 L101 -1.035e-01
K130 L18 L32 -7.673e-02
K131 L18 L37 1.014e-01
K132 L18 L42 5.300e-02
K133 L18 L44 1.716e-02
K134 L18 L46 -6.764e-02
K135 L18 L52 -5.682e-02
K136 L18 L54 -5.178e-02
K137 L18 L56 2.844e-02
K138 L18 L75 6.328e-02
K139 L18 L97 -2.236e-02
K140 L18 L103 5.187e-02
K141 L19 L20 -2.183e-02
K142 L19 L50 -4.275e-03
K143 L19 L54 -5.095e-03
K144 L19 L55 -6.044e-02
K145 L19 L58 -5.624e-02
K146 L19 L74 6.241e-02
K147 L19 L83 -5.576e-02
K148 L19 L98 -6.061e-02
K149 L20 L32 1.668e-02
K150 L20 L73 -1.071e-02
```

```
K151 L20 L79 -3.949e-02
K152 L20 L97 1.188e-01
K153 L20 L112 6.027e-03
K154 L21 L22 8.368e-03
K155 L21 L44 3.138e-02
K156 L21 L52 -5.748e-02
K157 L21 L54 -1.862e-02
K158 L21 L88 -2.952e-02
K159 L21 L100 3.517e-02
K160 L21 L102 -2.249e-02
K161 L21 L113 -5.358e-02
K162 L22 L41 -9.492e-02
K163 L22 L44 -3.466e-02
K164 L22 L59 -2.749e-03
K165 L22 L83 -2.855e-02
K166 L23 L30 1.489e-02
K167 L23 L52 -6.770e-02
K168 L23 L62 5.906e-02
K169 L23 L63 -8.709e-02
K170 L23 L64 7.431e-02
K171 L23 L73 2.286e-02
K172 L23 L91 -4.472e-02
K173 L23 L95 6.578e-02
K174 L23 L99 -3.001e-03
K175 L23 L114 -4.040e-02
K176 L23 L115 1.503e-02
K177 L24 L25 -7.745e-02
K178 L24 L26 -1.835e-02
K179 L24 L30 -6.247e-04
K180 L24 L42 -2.515e-02
K181 L24 L61 9.840e-02
K182 L24 L110 -3.428e-02
K183 L24 L111 -3.270e-02
K184 L24 L113 5.006e-02
K185 L25 L30 -6.540e-02
K186 L25 L34 5.078e-02
K187 L25 L72 -1.316e-01
K188 L25 L76 1.023e-01
K189 L25 L77 -2.750e-02
K190 L25 L88 6.600e-02
K191 L25 L103 -1.289e-02
K192 L26 L39 2.484e-02
K193 L26 L50 9.401e-02
K194 L26 L64 4.131e-02
K195 L26 L66 -6.600e-02
K196 L26 L68 9.731e-03
K197 L26 L93 -7.309e-02
K198 L27 L30 -6.094e-02
K199 L27 L33 -5.750e-03
K200 L27 L45 1.384e-02
K201 L27 L68 7.919e-02
```

```
K202 L27 L71 7.023e-02
K203 L27 L97 2.406e-02
K204 L27 L100 -2.375e-03
K205 L27 L102 4.460e-02
K206 L27 L109 1.841e-02
K207 L27 L114 2.122e-02
K208 L28 L39 6.925e-03
K209 L28 L44 -9.611e-02
K210 L28 L53 1.018e-01
K211 L28 L69 4.003e-02
K212 L28 L73 -7.290e-02
K213 L28 L101 -8.884e-03
K214 L28 L105 6.486e-02
K215 L28 L112 4.968e-02
K216 L28 L117 9.503e-02
K217 L29 L40 -5.459e-02
K218 L29 L44 9.149e-02
K219 L29 L46 4.714e-02
K220 L29 L51 9.947e-02
K221 L29 L64 -5.487e-03
K222 L29 L81 -8.032e-02
K223 L29 L85 5.454e-02
K224 L29 L102 1.818e-02
K225 L29 L112 -1.667e-02
K226 L30 L37 9.123e-02
K227 L30 L50 1.770e-02
K228 L30 L54 9.845e-03
K229 L30 L68 -4.235e-02
K230 L30 L79 -8.947e-02
K231 L30 L81 -5.660e-02
K232 L30 L86 5.661e-02
K233 L30 L95 5.383e-02
K234 L30 L100 2.985e-02
K235 L30 L101 2.875e-03
K236 L31 L51 -7.549e-02
K237 L31 L56 9.848e-02
K238 L31 L61 -1.061e-01
K239 L31 L73 -2.940e-02
K240 L31 L78 -6.062e-02
K241 L31 L81 -4.240e-02
K242 L31 L92 1.407e-01
K243 L31 L116 -3.152e-02
K244 L32 L39 -6.082e-02
K245 L32 L40 2.026e-02
K246 L32 L49 -7.549e-02
K247 L32 L65 6.860e-02
K248 L32 L106 6.830e-03
K249 L33 L52 -6.808e-02
K250 L33 L57 8.307e-02
K251 L33 L72 -7.621e-03
K252 L34 L39 5.843e-03
```

```
K253 L34 L47 1.083e-01
K254 L34 L78 -1.129e-02
K255 L34 L82 -7.293e-02
K256 L34 L86 -5.085e-02
K257 L34 L97 -1.210e-02
K258 L34 L107 1.974e-02
K259 L34 L109 6.411e-02
K260 L34 L112 4.542e-02
K261 L35 L63 1.246e-01
K262 L35 L81 -9.467e-02
K263 L35 L82 6.068e-02
K264 L35 L102 -4.531e-02
K265 L35 L116 -6.948e-02
K266 L36 L38 -5.947e-02
K267 L36 L50 -9.789e-02
K268 L36 L57 -7.392e-02
K269 L36 L59 3.234e-02
K270 L36 L99 5.942e-02
K271 L36 L104 3.239e-04
K272 L36 L117 -1.095e-01
K273 L37 L39 4.371e-02
K274 L37 L40 6.975e-02
K275 L37 L42 1.873e-03
K276 L37 L74 -3.240e-02
K277 L37 L103 6.114e-02
K278 L37 L111 1.705e-02
K279 L38 L47 -1.036e-01
K280 L38 L59 -4.135e-02
K281 L38 L67 -7.662e-02
K282 L38 L85 -1.105e-01
K283 L38 L91 -9.160e-02
K284 L38 L95 8.242e-02
K285 L38 L114 1.076e-01
K286 L39 L54 3.078e-02
K287 L39 L59 8.415e-03
K288 L39 L67 3.413e-02
K289 L39 L73 1.640e-02
K290 L39 L74 -2.309e-02
K291 L39 L91 -3.537e-02
K292 L39 L95 3.781e-02
K293 L39 L97 -5.520e-02
K294 L39 L98 7.131e-02
K295 L39 L112 -6.898e-02
K296 L40 L54 6.538e-02
K297 L40 L55 1.444e-02
K298 L40 L82 -6.982e-02
K299 L40 L83 1.302e-03
K300 L40 L84 -3.703e-02
K301 L40 L89 7.250e-02
K302 L40 L93 -6.172e-02
K303 L40 L95 3.578e-02
```

```
K304 L40 L96 5.955e-02
K305 L40 L101 2.288e-02
K306 L40 L109 -3.319e-02
K307 L41 L60 -6.454e-02
K308 L41 L83 -1.155e-01
K309 L42 L45 -9.460e-02
K310 L42 L56 6.059e-02
K311 L42 L59 -4.790e-02
K312 L42 L83 -2.386e-02
K313 L42 L114 -4.442e-02
K314 L42 L117 5.646e-02
K315 L43 L82 -1.887e-02
K316 L44 L49 -9.058e-04
K317 L44 L57 -4.535e-02
K318 L44 L115 6.085e-02
K319 L44 L117 8.164e-02
K320 L45 L62 -3.965e-02
K321 L45 L75 -7.702e-02
K322 L45 L76 5.051e-02
K323 L45 L78 9.400e-02
K324 L45 L79 2.122e-02
K325 L45 L102 -4.277e-02
K326 L45 L103 -5.399e-02
K327 L46 L50 -4.579e-02
K328 L46 L52 -5.235e-02
K329 L46 L60 -5.962e-02
K330 L46 L81 -7.681e-02
K331 L46 L82 -4.911e-03
K332 L46 L86 -4.295e-02
K333 L46 L93 -1.086e-01
K334 L47 L57 9.576e-02
K335 L47 L101 -5.962e-02
K336 L47 L108 1.193e-01
K337 L48 L93 6.812e-02
K338 L49 L56 -6.678e-02
K339 L49 L67 7.200e-02
K340 L49 L86 -1.030e-01
K341 L49 L107 4.413e-02
K342 L49 L111 3.747e-02
K343 L50 L58 8.152e-02
K344 L50 L66 6.390e-02
K345 L50 L89 -5.968e-02
K346 L50 L96 3.950e-02
K347 L50 L104 3.857e-02
K348 L51 L58 5.340e-02
K349 L51 L67 -1.237e-02
K350 L51 L70 2.074e-02
K351 L51 L89 1.086e-01
K352 L52 L58 5.184e-02
K353 L52 L60 4.796e-02
K354 L52 L63 -6.885e-02
```

```
K355 L52 L77 -6.126e-02
K356 L52 L87 1.126e-01
K357 L52 L89 -4.255e-02
K358 L52 L101 1.848e-02
K359 L53 L110 -1.189e-01
K360 L53 L113 8.972e-02
K361 L53 L115 5.259e-02
K362 L54 L95 -4.617e-02
K363 L54 L101 3.232e-02
K364 L54 L106 -2.228e-02
K365 L54 L107 -7.462e-02
K366 L55 L58 5.445e-02
K367 L55 L90 -1.203e-01
K368 L55 L92 4.274e-03
K369 L55 L105 -2.118e-02
K370 L55 L108 -1.111e-01
K371 L56 L62 6.766e-02
K372 L56 L69 -1.974e-02
K373 L56 L73 8.190e-02
K374 L56 L94 2.571e-03
K375 L56 L98 4.655e-02
K376 L56 L111 3.175e-02
K377 L56 L115 -1.722e-02
K378 L57 L60 4.648e-02
K379 L57 L72 -1.275e-01
K380 L57 L98 1.157e-01
K381 L58 L59 2.039e-02
K382 L58 L75 -4.377e-03
K383 L58 L85 -8.303e-02
K384 L58 L103 -7.783e-02
K385 L59 L85 -8.116e-02
K386 L59 L95 -7.981e-02
K387 L59 L118 -5.254e-02
K388 L60 L61 6.603e-02
K389 L60 L63 -6.234e-02
K390 L60 L73 -1.833e-02
K391 L60 L77 -4.931e-02
K392 L60 L86 2.497e-02
K393 L60 L91 -8.008e-02
K394 L60 L114 -4.456e-02
K395 L61 L64 7.965e-02
K396 L61 L67 1.553e-02
K397 L61 L74 -1.752e-02
K398 L61 L78 -6.426e-02
K399 L61 L102 8.208e-02
K400 L61 L105 -8.934e-03
K401 L61 L112 2.523e-02
K402 L62 L74 -1.061e-01
K403 L62 L90 -1.271e-01
K404 L62 L100 7.220e-02
K405 L62 L111 -5.460e-02
```

```
K406 L63 L74 2.077e-02
K407 L63 L104 4.931e-02
K408 L63 L108 -3.033e-02
K409 L63 L114 8.602e-02
K410 L64 L75 9.126e-02
K411 L64 L96 2.142e-02
K412 L64 L97 -9.331e-02
K413 L64 L109 -2.946e-02
K414 L65 L66 1.169e-01
K415 L65 L75 6.218e-02
K416 L65 L104 -1.529e-02
K417 L65 L105 -3.470e-02
K418 L66 L89 1.341e-01
K419 L66 L106 9.960e-02
K420 L67 L102 -1.580e-02
K421 L67 L106 2.918e-02
K422 L68 L70 6.876e-02
K423 L68 L75 -8.137e-02
K424 L68 L81 7.568e-02
K425 L68 L94 1.494e-01
K426 L68 L103 -2.548e-02
K427 L69 L92 -1.183e-01
K428 L69 L101 -9.903e-02
K429 L70 L74 4.771e-02
K430 L70 L77 7.488e-02
K431 L70 L86 5.091e-02
K432 L70 L101 5.045e-02
K433 L70 L107 1.992e-02
K434 L70 L108 4.556e-02
K435 L70 L110 -2.022e-02
K436 L70 L111 -3.569e-03
K437 L71 L82 -4.717e-02
K438 L71 L103 -9.579e-02
K439 L71 L106 -6.333e-02
K440 L71 L115 -9.559e-02
K441 L72 L79 1.198e-01
K442 L72 L111 -1.015e-01
K443 L73 L86 4.667e-02
K444 L73 L101 4.050e-02
K445 L73 L112 -2.861e-02
K446 L73 L115 6.581e-02
K447 L74 L96 1.001e-01
K448 L74 L111 -7.519e-02
K449 L74 L115 9.013e-02
K450 L75 L90 3.049e-02
K451 L75 L92 7.807e-02
K452 L75 L98 1.946e-02
K453 L75 L105 -3.734e-03
K454 L75 L107 4.878e-02
K455 L75 L109 3.722e-02
K456 L75 L116 -3.112e-02
```

```
K457 L76 L82 2.183e-02
K458 L76 L85 -6.563e-02
K459 L76 L87 1.151e-01
K460 L76 L101 9.542e-02
K461 L76 L112 1.724e-02
K462 L77 L82 -1.547e-02
K463 L78 L82 2.613e-02
K464 L78 L88 1.135e-01
K465 L78 L90 6.420e-02
K466 L78 L110 -6.466e-02
K467 L79 L84 3.419e-02
K468 L79 L104 -2.891e-02
K469 L79 L105 -3.595e-02
K470 L80 L105 2.049e-01
K471 L81 L88 4.974e-02
K472 L81 L97 -6.344e-02
K473 L81 L101 -7.541e-02
K474 L81 L109 7.971e-02
K475 L81 L110 1.881e-02
K476 L81 L113 6.130e-02
K477 L82 L85 -2.003e-02
K478 L82 L97 4.004e-02
K479 L82 L104 -6.996e-02
K480 L83 L86 3.069e-02
K481 L83 L95 -1.474e-02
K482 L83 L96 -4.829e-02
K483 L83 L105 -3.493e-02
K484 L83 L113 -6.146e-02
K485 L84 L105 5.834e-02
K486 L84 L106 -1.582e-01
K487 L85 L99 4.893e-02
K488 L85 L104 1.802e-03
K489 L85 L110 2.682e-02
K490 L85 L114 3.416e-02
K491 L86 L109 4.869e-03
K492 L87 L93 -1.167e-01
K493 L87 L96 -1.704e-01
K494 L88 L92 9.495e-02
K495 L88 L106 1.322e-01
K496 L88 L112 2.203e-03
K497 L90 L94 -7.823e-02
K498 L90 L97 4.314e-02
K499 L90 L112 -6.494e-02
K500 L91 L111 1.051e-01
K501 L91 L117 9.863e-02
K502 L93 L105 -1.702e-02
K503 L94 L113 -1.477e-01
K504 L95 L98 -4.657e-02
K505 L95 L105 -9.461e-03
K506 L95 L111 -5.695e-02
K507 L97 L110 -1.914e-03
```

```
K508 L97 L115 -5.523e-02
K509 L98 L104 6.539e-02
K510 L99 L104 -5.726e-02
K511 L99 L113 9.723e-02
K512 L101 L103 2.117e-02
K513 L102 L109 -8.753e-02
K514 L102 L117 -1.782e-02
K515 L104 L107 -4.808e-02
K516 L104 L118 1.323e-01
K517 L105 L108 -6.126e-02
K518 L106 L107 -7.924e-02
K519 L107 L116 -5.145e-02
K520 L108 L110 8.817e-02
K521 L113 L115 8.111e-02
K522 L114 L116 -3.657e-02
K523 L115 L116 -9.063e-02
K524 L115 L117 7.306e-02
*
.ends
```

Vita

Kevin J. Kerns received the B. S. degree in physics from the United States Air Force Academy, Colorado Springs, CO in 1988. He served for five years in the U.S. Air Force at the Phillips Laboratory, Hanscom AFB, MA as a space research physicist. He left the Air Force as a captain in 1993, and is currently a Ph.D. candidate in the Department of Electrical Engineering at the University of Washington, Seattle, WA.

Publications

S. D. Corey, K. J. Kerns, and A. T. Yang, "Automatic measurement-based characterization of lossy MCM line using lumped elements," to appear *5th Topical Meeting on Electrical Performance of Electronic Packaging*, October 1996.

K. J. Kerns and A. T. Yang, "Stable and efficient reduction of large, multiport RC networks by pole analysis via congruence transforms," to appear *IEEE Trans. Computer-Aided Design.*

K. J. Kerns and A. T. Yang, "Stable and efficient reduction of large, multiport RC networks by pole analysis via congruence transforms," *Proceedings of the 33rd Design Automation Conference*, pp. 280-285, June 1996.

K. J. Kerns, I. L. Wemple, and A. T. Yang, "Efficient parasitic substrate modelling for monolithic mixed-A/D circuit design and verification," *Analog Integrated Circuits and Signal Processing*, pp.7-21, June/July 1996.

K. J. Kerns, I. L. Wemple, and A. T. Yang, "Stable and efficient reduction of substrate model networks using congruence transforms," *Proceedings of the IEEE/ACM International Conference on Computer-Aided Design*, pp. 207-214, November 1995.

K. J. Kerns, D. A. Hardy, and M. S. Gussenhoven, "Modeling of convection boundaries seen by CRRES in 120-eV to 28-keV particles," *Journal of Geophysical Research*, pp. 2403-2414, February 1994.

A. R. Frederickson, E. G. Mullen, K. J. Kerns, P. A. Robinson, and E. G. Holeman, "The CRRES IDM spacecraft experiment for insulator discharge pulses," *IEEE Trans. Nuclear Science*, pp. 233-241, April 1993.

M. S. Gussenhoven, E. G. Mullen, M. Sperry, K. J. Kerns, and J. B. Blake, "The effect of the March 1991 storm on accumulated dose for selected satellite orbits: CRRES dose models," *IEEE Trans. Nuclear Science*, pp. 1765-1772, December 1992.

A. R. Frederickson, E. G. Mullen, D. H. Brautigam, K. J. Kerns, P. A. Robinson Jr., and E. G. Holeman, "Radiation-induced insulator discharge pulses in the CRRES internal discharge monitor satellite experiment," *IEEE Trans. Nuclear Science*, pp. 1614-1621, December 1991.

K. J. Kerns and M. S. Gussenhoven, "Solar wind conditions for a quiet magnetosphere," *Journal of Geophysical Research*, pp. 20867-20875, December 1990.